

Joonas Pekkarinen

LASER CLADDING WITH SCANNING OPTICS

Thesis for the degree of Doctor of Science (Technology) to be presented with due permission for public examination and criticism in the Auditorium 1382 at Lappeenranta University of Technology, Lappeenranta, Finland on the 21th of August, 2014, at noon.

Supervisors	Docent Veli Kujanpää Lappeenranta University of Technology (Prof. of VTT Technical Research Centre) Finland
	Professor Antti Salminen LUT School of Technology LUT Mechanical Engineering Lappeenranta University of Technology Finland
Reviewers	Professor Milan Brandt School of Aerospace, Mechanical and Manufacturing Engineering RMIT University Australia
	Professor Petri Vuoristo Department of Materials Science Tampere University of Technology Finland
Opponents	Professor Milan Brandt School of Aerospace, Mechanical and Manufacturing Engineering RMIT University Australia
	Professor Petri Vuoristo Department of Materials Science Tampere University of Technology Finland

ISBN 978-952-265-625-4

ISBN 978-952-265-626-1 (PDF)

ISSN-L 1456-4491

ISSN 1456-4491

Lappeenrannan teknillinen yliopisto
Yliopistopaino 2014

ABSTRACT

Joonas Pekkarinen

Laser cladding with scanning optics

Lappeenranta 2014

120 p.

Acta Universitatis Lappeenrantaensis 584

Diss. Lappeenranta University of Technology

ISBN 978-952-265-625-4

ISBN 978-952-265-626-1 (PDF)

ISSN-L 1456-4491

ISSN 1456-4491

Scanning optics create different types of phenomena and limitation to cladding process compared to cladding with static optics. This work concentrates on identifying and explaining the special features of laser cladding with scanning optics.

Scanner optics changes cladding process energy input mechanics. Laser energy is introduced into the process through a relatively small laser spot which moves rapidly back and forth, distributing the energy to a relatively large area. The moving laser spot was noticed to cause dynamic movement in the melt pool. Due to different energy input mechanism scanner optic can make cladding process unstable if parameter selection is not done carefully. Especially laser beam intensity and scanning frequency have significant role in the process stability. The laser beam scanning frequency determines how long the laser beam affects with specific place local specific energy input. It was determined that if the scanning frequency is too low, under 40 Hz, scanned beam can start to vaporize material. The intensity in turn determines on how large package this energy is brought and if the intensity of the laser beam was too high, over 191 kW/cm^2 , laser beam started to vaporize material. If there was vapor formation noticed in the melt pool, the process starts to resample more laser alloying due to deep penetration of laser beam in to the substrate.

Scanner optics enables more flexibility to the process than static optics. The numerical adjustment of scanning amplitude enables clad bead width adjustment. In turn scanner power modulation (where laser power is adjusted according to where the scanner is pointing) enables modification of clad bead cross-section geometry when laser power can be adjusted locally and thus affect how much laser beam melts material in each sector.

Power modulation is also an important factor in terms of process stability. When a linear scanner is used, oscillating the scanning mirror causes a dwell time in scanning amplitude border area, where the scanning mirror changes the direction of movement. This can cause excessive energy input to this area which in turn can cause vaporization and process

instability. This process instability can be avoided by decreasing energy in this region by power modulation.

Powder feeding parameters have a significant role in terms of process stability. It was determined that with certain powder feeding parameter combinations powder cloud behavior became unstable, due to the vaporizing powder material in powder cloud. Mainly this was noticed, when either or both the scanning frequency or powder feeding gas flow was low or steep powder feeding angle was used. When powder material vaporization occurred, it created vapor flow, which prevented powder material to reach the melt pool and thus dilution increased. Also powder material vaporization was noticed to produce emission of light at wavelength range of visible light. This emission intensity was noticed to be correlated with the amount of vaporization in the powder cloud.

Keywords: Fiber laser, Linear scanner, Energy input, Process stability, Dilution, Power modulation, Clad bead, Cross-section, Intensity, Scanning frequency, Powder feeding

UDC 621.793:621.795:621.375.826

ACKNOWLEDGEMENTS

This work has been carried out in Research group of laser processing (LUT Laser) in Lappeenranta University of Technology (LUT) from December 2009 until June 2014. This work has been rewarding and exiting but from time to time exhausting. I am very grateful that I got to have this experience and to learn these new things during this journey.

Firstly I would like to express my gratitude to Finnish Metals and Engineering Competence Clusters (FIMECC) Innovation and Network program, Regional Council of Päijät-Häme, Tekes, and the European Regional Development Fund for enabling this work. These organizations have been funding this research and thus they deserve special thanks for it. I would also like to express my gratitude for OSTP Finland Oy for lending me their ILV DC linear scanner and thus enabling these cladding tests.

I would like to express my gratitude to my supervisors Professor Antti Salminen and Professor Veli Kujanpää. Their valuable instructions, comments and criticism guided me to generate the ideas that are presented in this work scientific section. Professor Kujanpää and Professor Salminen also worked as co-authors of my publications and their valuable comments guided my ideas in more comprehensive and clearer form.

I would also like to express my gratitude to Dr. J. Ilonen, Dr. L. Lensu and Professor H. Kälviäinen from Lappeenranta University of Technology Machine Vision and Pattern Recognition Laboratory (MVPR) who helped me with the fourth publication's powder particle speed calculations.


I would also like to express my gratitude to the preliminary examiners / reviews of the dissertation, Professor Milan Brandt from RMIT University and Professor Petri Vuoristo from Tampere University of Technology. Their valuable comments helped to improve the quality of this thesis.

My colleagues at the Research group of laser processing also deserve my thanks for supporting me and challenging me to reach a higher level at my work. Especially I would like to express my gratitude to Dr. Ilkka Poutiainen and Mr. Pertti Kokko for helping me during the experimental phase of this work. They helped me to build the experimental setups and without their help many of these setups would not have been built.

All my friends also deserve my gratitude. All of you helped me to remember that there is much more than work and when I needed a break from my studies you were there for me. Thank you for the encouragement to pursuit my goals and ambitions.

Finally, I would like to express my special gratitude for my parents: Eija and Erkki Pekkarinen who have supported and encouraged me on my studies. Without their help I

would not be able to finish this project. Their encouragement helped me to continue when I wanted to give in and quit.

A handwritten signature in black ink, appearing to be 'J. Pekkarinen', with a long horizontal stroke extending to the right.

Joonas Pekkarinen

Lappeenranta, August 2014

TABLE OF CONTENT

ABSTRACT.....	3
ACKNOWLEDGEMENTS.....	5
LIST OF PUBLICATIONS.....	9
CONTRIBUTION OF CANDIDATE IN THE PUBLICATIONS.....	10
LIST OF ABBREVIATIONS AND SYMBOLS.....	11
PART I: OVERVIEW OF THE DISSERTATION	13
1. Introduction	15
1.1 Background and motivation of thesis	16
1.2 Scientific contribution of thesis.....	16
2. Laser cladding theoretical background.....	18
2.1 Advantages and weaknesses of laser cladding compared to other coating methods.....	18
2.2 Laser cladding with dynamic powder feeding	19
2.3 Laser cladding equipment	21
2.4 Process parameters.....	25
2.5 Powder feeding parameters and the powder cloud behavior	28
2.5.1 Attenuation.....	28
2.5.2. Powder particle temperature rise	30
2.6 Clad bead geometry	33
2.6.1 Dilution	33
2.6.2 Geometrical requirements of clad bead	36
2.7 Laser cladding with scanning optics.....	38
3. Experimental Investigation	42
3.1 General experimental setup.....	42
3.1.1 Used scanner technology	44
3.2 Specific test circumstances	45
3.2.1 Test series for Publication 1	45
3.2.2 The test series for the Publication 2.....	47
3.2.3 The test series for the Publication 3.....	49
3.2.4 The test series for Publication 4	50
4. Review of publications	55

4.1 Publication 1.....	55
Laser cladding using scanning optics	55
4.2 Publication 2.....	57
Laser cladding with scanning optics: The effect of power adjustment	57
4.3 Publication 3.....	57
Laser cladding with scanning optics: Effect of scanning frequency and laser beam power density on cladding process	57
4.4 Publication 4.....	58
Laser cladding using scanning optics – Effect of the powder feeding angle and gas flow on process stability	58
5. Conclusions and recommendations	60
References.....	63
PART II: THE PUBLICATIONS	71

LIST OF PUBLICATIONS

1. Joonas Pekkarinen, Veli Kujanpää and Antti Salminen, 2012. Laser cladding using scanning optics, Journal of Laser Applications, Volume 24, Issue 5, 9 pp.
2. Joonas Pekkarinen, Veli Kujanpää and Antti Salminen, 2012. Laser cladding with scanning optics: Effect of power adjustment, Journal of Laser Applications, Volume 24, Issue 3, 7 pp.
3. Joonas Pekkarinen, Antti Salminen and Veli Kujanpää. 2014. Laser cladding with scanning optics: Effect of scanning frequency and laser beam power density on cladding process, Journal of Laser Applications, Volume 26, Issue 3, 9 pp.
4. Joonas Pekkarinen, Antti Salminen, Veli Kujanpää, Jarmo Ilonen, Lasse Lensu, Heikki Kälviäinen, 2013. Laser cladding using scanning optics – Effect of the powder feeding angle and gas flow on process stability, Proceedings of The International Congress on Applications of Lasers & Electro-Optics (ICALEO), Oct. 6-10 2013, Miami, FL, USA. 10 pp.

CONTRIBUTION OF CANDIDATE IN THE PUBLICATIONS

The candidate was the corresponding author in all the publications that comprise the second part of this thesis. The ideas, study methodology and conclusions that are presented in this thesis are original work of the candidate. The main co-authors Professor Antti Salminen and Professor Veli Kujanpää mainly helped to guide the ideas into more comprehensible form and revise the papers prior to submission to the journals and conference. The work undertaken by the candidate in preparation of the publications:

Publication 1

Literature study: Responsible for carrying out relevant literature study for the publication.
Experimental investigation: Designed the cladding tests and process analysis methodology, determined cladding parameters for tests and made the analysis of the cladding tests.
Writing the paper: Responsible for writing the article.

Publication 2

Literature study: Responsible for carrying out relevant literature study for the publication.
Experimental investigation: Designed the cladding tests and process analysis methodology, determined cladding parameters for tests and made the analysis of the cladding tests.
Writing the paper: Responsible for writing the article.

Publication 3

Literature study: Responsible for carrying out relevant literature study for the publication.
Experimental investigation: Designed the cladding tests and process analysis methodology, determined cladding parameters for tests and made the analysis of the cladding tests.
Writing the paper: Responsible for writing the article.

Publication 4

Literature study: Responsible for carrying out relevant literature study for the publication.
Experimental investigation: Designed the cladding tests and process analysis methodology, determined cladding parameters for tests and made the analysis of the cladding tests.
Writing the paper: Responsible for writing the article.

Received external assistance

In publication 4 Dr. J. Ilonen, Dr. L. Lensu and Professor H. Kälviäinen from Lappeenranta University of Technology Machine Vision and Pattern Recognition Laboratory (MVPR) made measurements and calculations for powder particles speeds in different powder feeding angles.

LIST OF ABBREVIATIONS AND SYMBOLS

Abbreviation	Explanation
A-F	Austenitic-ferritic solidification mode
BPP	Beam parameter product
CO ₂	Carbon dioxide
Cr/Ni eq.	Chrome-nickel equivalent
CW	Continuous wave
Disk	Disk laser
DMD	Direct metal deposition
EDS	Energy-dispersive x-ray spectroscopy
F-A	Ferritic-austenitic solidification mode
Fiber	Fiber laser
fps	Frames per second
HPDL	High power diode laser
LMIA	Laser beam material interaction area
Nd:YAG	Neodymium-doped yttrium aluminum garnet laser
PAP	Power adjustment profile

Symbol	Unit	Explanation
Δt_i	s	Interaction time
Δt_p	s	Time the particles are under the laser light
α	°	The optics refraction angle to the laser
θ	°	Powder feeding angle
ρ	g/cm ³	Density
a	%	Absorption factor
a _p	%	Power adjustment factor
A	mm	Scanning amplitude
a _p		Power adjustment factor
c _p	J/°Kg	Specific heat factor of the powder material
d ₀	mm	Focal point diameter at the focal level,
D _f	mm	Focal point diameter at the substrate material level
f	Hz	Scanning frequency
h _f	mm	Theoretical focal point levels distance to the substrate
H _c	mm	Clad beads critical height
I	W/mm ²	Intensity
L	J/g	Specific latent heat for melting
m		Total amount of power adjustment points at one sine wave
m _p	g	Powder particle mass
n		Power adjustment points number
p _{fr}	g/s	Powder feed rate
p _{lfr}	g/mm	linear feeding rate
p _{fa}	g/mm ²	Powder federate per surface area of the
P	W	Laser power
Q _{sl}	J/mm ²	Local specific energy input
Q _p	J	Powder particles' received energy

Q_s	J/mm^2	Specific energy input
Q_{su}	J/mm^2	Specific energy usage
r_l	mm	Radius of the laser spot
r_p	mm	Powder particle radius
t	s	Time where scanned beams velocity is calculated
t_{max}	s	Powder particle's maximum travelling time inside the laser beam
ΔT	$^{\circ}K$	Temperature change
T_0	$^{\circ}K$	Initial temperature of powder particle
T_{max}	$^{\circ}K$	Powder particles maximum temperature
T_p	$^{\circ}K$	Powder particles temperature
v	mm/s	Cladding speeds
v_p	mm/s	Powder particles velocity
v_{sb}	mm/s	Scanned beam local velocity
w_{lai}	mm	Width of the laser's area of interaction
x'	mm	Powder particles maximum length under the laser light
\hat{y}	mm	Scanning's peak amplitude

PART I: OVERVIEW OF THE DISSERTATION

1. Introduction

Additive manufacturing, in its many forms, has become a very important topic in recent years, and even president Barack Obama has stated [1] that additive manufacturing has potential to revolutionize manufacturing. As additive manufacturing as a whole has become a new interest of research, in the industrial world, laser cladding has again become more interesting and a current process. However, additive manufacturing using laser is not a new thing, laser cladding which can be considered as an additive manufacturing technique, has been around for more than 30 years [2] and has been used successfully in industry. With laser cladding, there is the possibility to clad new surfaces on top of a substrate, a coating process, or to grow new shapes or forms on top of the workpiece, an additive manufacturing process[2]. This allows laser cladding to be used in a versatile way in several different methods, e.g. coating of less noble surfaces with noble material in order to gain better surface properties, repairing broken parts by building them back up layer by layer, or creating new shapes on top of the part [3]. Thus, the laser cladding process is not limited to manufacturing parts as in typical additive manufacturing process, but it can be used in a more versatile way.

Laser cladding in its simplest form is a process where a laser is used to melt small amount of substrate surface and as much as possible of the additive material. When the melted material is left behind it solidifies forming a clad bead [4,5]. This technique has been known since late 1970's, when D. S. Gnanamuthu [4] developed it at Avco Everett Research Laboratory, Inc.. After this, laser cladding has come a long way from cladding with pre-placed additive material [4] to cladding with pneumatic additive material feeding [5]; a process presented by Weerasinghe and Steen in 1987. The next major progress after pneumatic powder delivery was co-axial powder feeding at end of the 1980's [6], which made laser cladding much easier to control and enabled more freedom of movement in the cladding process. In the 21st century, the main development in terms of laser cladding has been in the development of laser source technology. Higher laser powers, at around 1 micron wavelength range (diode-; fiber- and disc lasers), have enabled better productivity in the process in two ways. Firstly, this wavelength is better suited for cladding because it allows better absorption of metals than CO₂ lasers 10.6 micron wavelength [7]. Secondly, the laser's maximum power level is mainly determined by financial resources of the subscriber. Now days, lasers with 100 kW continuous wave (CW) can be made with fiber laser technology [8]. Mainly, the current restrictive factor for process productivity is the usable optics and additive material feeding technology.

Scanner optics is one viable way to control and shape a high power laser beam for cladding purposes. In fact, a scanner technique has been used as early as the late 1970's [9] and early 1980's[10] in laser cladding studies and even in production in order to modify the laser beam interaction zone to the desired form. However, presently, when both laser technology and optics have evolved considerably from those days, scanner optics usage in laser cladding has again become interesting. Two things advocate scanning optics usability in modern laser

cladding solutions: the scanner's power handling capability is high and the scanning optics enables more flexibility. The scanner's power handling capabilities naturally depend on the scanner structure, but at least mirror based scanners can handle relatively high power levels, at least up to 20 kW [11]. Increased flexibility in turn comes from the numerical adjustment options of the scanner. Modern scanners enable numerical adjustment of scanning amplitude and even the laser power adjustment is possible according to the location of laser beam at the interaction zone [12-14]. These factors enable cladding of different width of clad beads with the same optical setup [13,15] but also with relatively high deposition rates [16,17]. Scanning optics usage offers both in laser cladding and in laser cladding technology based additive manufacturing (or Directed energy deposition) possibilities to increase process deposition efficiency alongside of increase of process flexibility.

However, there is very little information on how a scanned beam changes the process dynamics of the cladding process. Most studies where laser cladding has been done using scanning optics, scanner optics have mainly been only as a tool for modifying the laser interaction area to a desired size and shape [9,10,12,13,16,17]. In these studies, there has been very little consideration as to how a scanned beam affects the cladding process itself. Therefore, this thesis focuses on correcting this matter and discovering how a scanned beam actually affects the laser cladding process dynamics, and the special features of this process.

1.1 Background and motivation of thesis

Motivation for this thesis was inspired by the desire to improve cladding process productivity and process flexibility. To increase process productivity obvious choice was to increase the clad bead width such that larger sections could be clad with fewer clad tracks. The scanner optics seemed to be a viable technology in order to research how much productivity could be increased by cladding wide sections. However, early on in these tests it was discovered that scanner optics created a certain situation where the process was either unstable or the qualitative outcome of the clad bead was poor. This generated the need for further research into the matter in order to clarify how different process parameters affect the process stability, the dilution and clad bead geometry. Since these factors had not previously been systematically reported, this seemed to be a perfect subject for this thesis.

1.2 Scientific contribution of thesis

This work focuses on laser cladding with scanning optics, the process mechanisms behind the process and how different cladding and scanning parameters affect the quality and the geometry of clad bead. This thesis main scientific contributions are:

- Defining how melt pools behaviour and clad beads geometry changes according to cladding and scanning parameters. Three different basic clad beads geometries were

observed and shapes were noted to be mainly dependent on cladding speed and scanning amplitude.

- Clad beads dilution was noted to be highly dependent on cladding speed. When scanned laser beam is used direct contact from the laser to substrate material cause's rapid increases in dilution. Thus it was proved that melt pools covering effect is important factor in dilution control in laser cladding with scanning optics.
- Scanned beams power modulation is important to process stability. Without power modulation scanner mirrors dwell time causes uneven energy input to the process which in turn causes vaporization in melt pool.
- Clad bead's geometry depends on scanned beam's power modulation. It was detected that clad beads geometry could be adjusted using power modulation.
- Determining limit values for scanning frequency / scanned beams local specific energy input and power density for stable cladding process. When scanned beams local specific energy input is 2.46 J/mm^2 or under cladding process was noted to be stable. Respectively power density should be 191 kW/cm^2 or under in order to ensure stable cladding process.
- It was observed that powder material can start to vaporize under the scanned laser beam forming a vapor plume. This behaviour was noticed to be most common with steep powder feeding angle, low powder feeding gas flow and low scanning frequency.
- It was also observed that this vapor plume absorbed energy itself from the laser beam. When this this type of phenomena occurred vapor plume started to emit light, mainly at wavelength range of 450 - 650 nm. Vapor plume emitted light intensity was noticed to have correlation with amount of vapor formation.

These matters are treated and discussed in more depth in Part II: The Publications.

2. Laser cladding theoretical background

In its simplest form laser cladding is a relatively straightforward and simple process. A laser is used to melt small amounts of substrate material and large amounts of additive material. When the laser beam moves forward, the melted material solidifies behind it. This way can be created a clad bead, which has a low dilution level and thus the desired material properties. [4,5] However, in reality laser cladding can be one of the most difficult laser process to master. This is due to the enormous number of parameters and their interaction with each other.

Traditionally, laser cladding has been divided in two groups: cladding with preplaced additive material, and cladding with dynamic additive material feeding. The latter of these methods is currently more commonly used and this thesis focuses on this process. Therefore, this section focuses on explaining the theoretical background of laser cladding with dynamic powder feeding.

2.1 Advantages and weaknesses of laser cladding compared to other coating methods

Laser cladding has some unique features that differ from other coating methods. In table 1, laser cladding has been compared to two other common coating methods: arc welding and thermal spraying. The advantages of laser cladding compared to other coating methods come from its low overall heat input, as well as the fact that energy input laser cladding can be controlled more precisely than that of other coating methods [18,19]. For example, the good bonding strength between clad bead and substrate material comes from the factor that the laser also melts some of the substrate material along with the additive material, creating metallurgical or fusion bond between these layers. This is the same type of bonding that occurs in welding. Good energy controllability of the energy input also enables the dilution level to be kept low alongside with a metallurgical bond between these layers. [4,5,9,10,18] This controllability of energy input mainly separates laser cladding from other coating technologies.

Table 1. Features of coating processes. [3,10,18--21] Laser Cladding is considered as single layer process.

Feature	Laser Cladding	Arc Welding	Thermal spraying
Bonding strength	High	High	Moderate
Dilution (%)	1-5	10-50	Nil
Coating materials	Metals & ceramics	Metals	Metals & ceramics
Coating thickness	50 μ m to 4 mm	1 to several mm	50 μ m to several mm
Repeatability	Moderate to high	Moderate	Moderate
Heat-affected zone	Low	High	High
Controllability	Moderate to high	Low	Moderate
Cost	High	Moderate	Moderate

In turn, the low overall heat input enables microstructural advantages for the coating layer as well as low distortion and residual stress in the coated structure. A laser clad surface typically displays a fine and uniform microstructure, due to the low over all heat inputs, which is enabled by high solidification and cooling rates. Fine and uniform microstructure enables, for example, better corrosion and wear resistance properties. [4,5,18,19,22] In addition, when the overall heat input remains low, less distortions are formed and the residual stresses stay low [18].

The main weaknesses of laser cladding are related to its high investment costs and productivity. Laser cladding equipment's are still expensive compared to conventional welding or thermal spraying equipment's and typically productivity of the cladding process is relatively low, in terms of deposition rates (g/min or kg/h) [21]. Productivity can be improved mainly in two ways: introducing another heat source alongside of the laser, using a hybrid cladding process, [21] or increasing the laser power and thus increasing the melting potential of the laser [17]. As Tuominen et al. [17] show in their study that by using scanner optics with a high power laser (15 kW) high deposition rates of 16-17kg/h can be achieved.

Today, when lasers with 100 kW maximum power can be constructed, the efficiency of laser cladding could be increased significantly. With high laser power it is possible to clad wide clad beads and thus the processing time of large areas could be probably decreased. However, there is no actual experience since this of laser cladding with this laser power level, therefore the actual benefits remain theoretical.

2.2 Laser cladding with dynamic powder feeding

Laser cladding with dynamic powder feeding, or the so called one stage cladding process, is a process where additive material is fed into the process simultaneously with the laser beam, figure 1. The laser's task is to create the melt pool where the additive material is fed. The additive material's feeding task is to feed a sufficient amount of additive material into this melt pool. [3,5,] In this way the laser melts small amounts of the substrate material and as much as possible of the additive material. As the laser with the powder feeding moves on, the melted material solidifies behind the laser beam, forming the clad bead. [4,5,19]

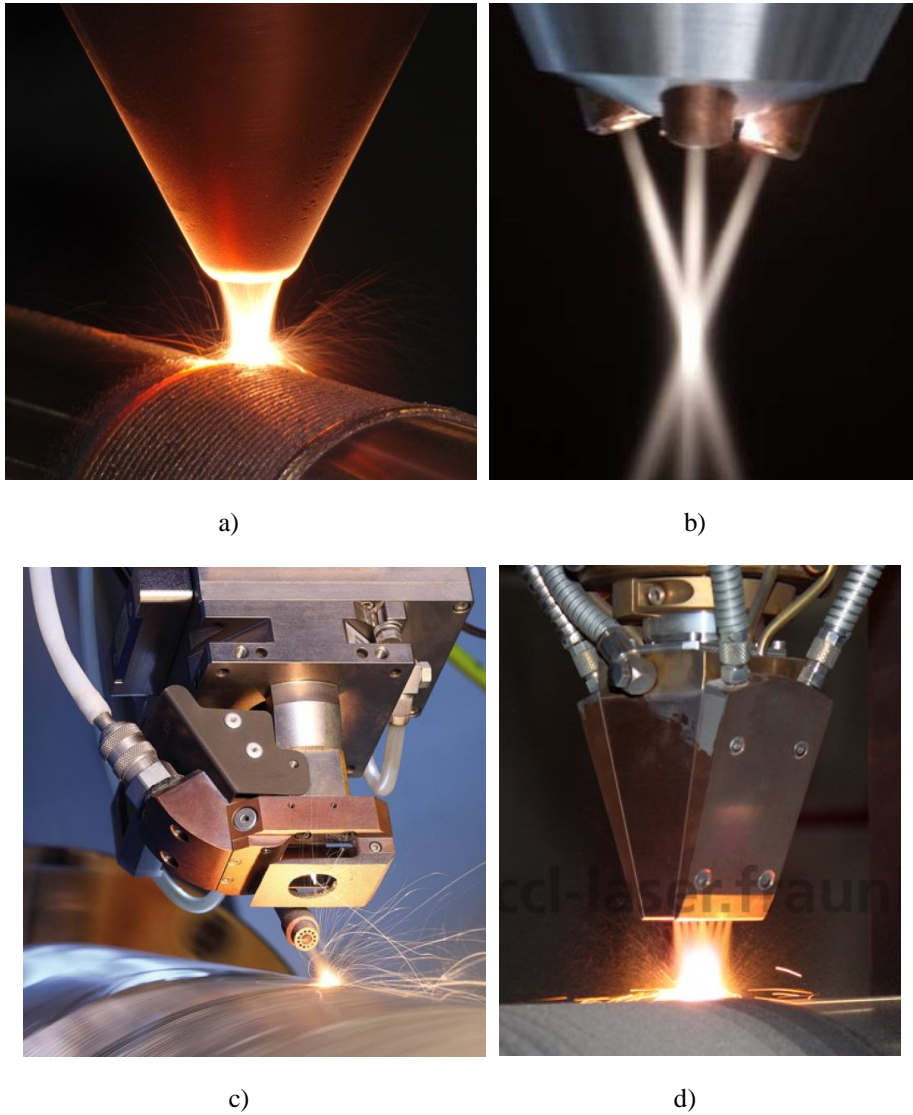


Figure 1. Different kinds of powder feeding methods for laser cladding. a) Co-axial powder feeding [23], b) Co-axial multi nozzle powder feeding [24], c) Off-axial powder feeding [25], d) Symmetrical off-axial powder feeding [26].

Additive material feeding can be performed in two ways, co-axially and off-axially, figure 1. These two methods differ from each other by the direction from which the additive material is fed. In co-axial powder feeding the additive material is fed symmetrically around the laser beam or by multiple nozzles around the laser beam, figure 1a and 1b. Off-axial feeding, in turn, feeds additive material asymmetrically at one side of the laser beam, figure 1c, or symmetrically on both sides of the laser beam, figure 1d. The main difference between co-

and off-axial powder feeding is how wide the clad beads can be made, and the degree of the freedom of movement in the process [3,5,6]. The main advantage of the co-axial cladding is that it enables higher freedom of movement. This is because the additive material is fed around the laser beam symmetrically, and the laser beam can move freely on a 2-dimensional plane, including curved surfaces [6,27,28,29]. Whereas the off-axial powder feeding cladding process can occur only in a one dimensional direction [3,30]. Off-axial powder feeding generally enables cladding of wider clad beads. By using off-axial feeding the additive material can be more easily fed to a wider area than with co-axial, and thus wider clad beads can be made.

2.3 Laser cladding equipment

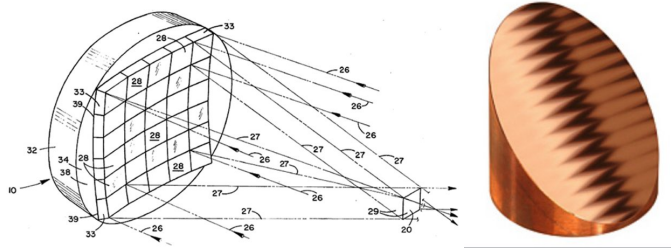
The necessary laser cladding equipment is highly dependent on the cladding method used. When cladding with pre-placed additive material, the required processing equipment places limits mainly on the laser source, the optics, and the melt pool's gas shielding. However, in the case of laser cladding with dynamic powder feeding the number of equipment needed is slightly greater and includes powder feeding nozzles, and powder feeding equipment. This makes the equipment used in cladding with dynamic powder feeding more complex.

The basis of laser cladding, as with all laser processes, is a laser source. Laser claddings requirements for the laser are somewhat different from the needs of other laser processes, e.g. keyhole welding or cutting. Because laser cladding is a surface treatment process it is sensitive to the lasers wavelength. This is due to the materials ability to absorb energy from the laser dependence on lasers wavelength. [3,7] Table 2 summarises the absorption coefficient of different lasers on steel. As previously stated, metallic materials absorb better shorter wavelength of light [7] of around 1 micrometre wavelength light (e.g. HPDL or fiber laser) rather than longer 10 micrometre wavelengths (CO₂ laser), table 2. Because of this absorption coefficient in relation to wavelength, shorter wavelength, high power lasers are more practical for cladding purposes. Another important aspect that restricts usable laser sources is the maximum laser power [3]. J. Ion [20] stated in his book that 2 kW is the minimum laser power level which makes laser cladding sufficiently productive for industrial use. This omits some lasers that work at short wavelength, as excimer lasers, because their maximum CW power is too low.

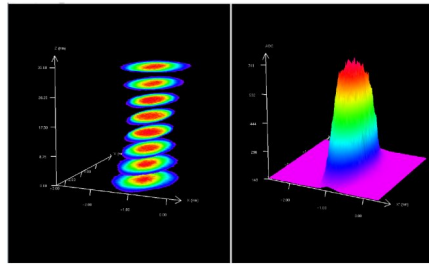
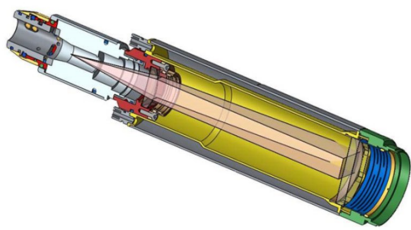
Table 2. The characteristics of different lasers that can be used for laser cladding. [3,8,20,30-42]

Characteristic	CO ₂	Nd:YAG	HPDL	Disk	Fiber
Wavelength [nm]	10 600	1064	808 – 1070	1030	1070-1080
Efficiency [%]	5-10	1-12	30-50	>30 %	30
Available maximum power [kW]	45	5 lamp-pumped 10 diode-pumped	20	16	50 (100) Highest known power
Beam parameter product [mm x mrad]	3,7 - 12	12 - 54	20 - 200	2 - 25	0,33- for 5 kW single mode 10 for 50kW multi-mode
Absorption to Steel [%]	4 – 10	30 - 35	30 – 35	30 - 35	30 – 35
Fiber coupling	No	Yes	Yes	Yes	Yes

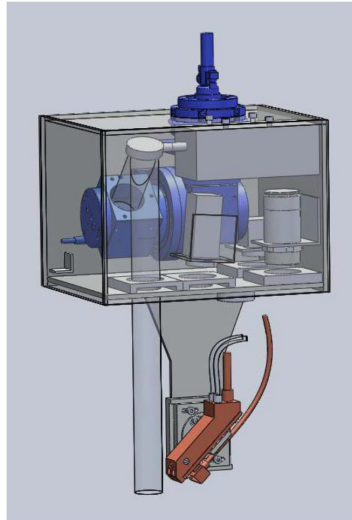
Alongside with the laser source some optics is also required. The task of the optics is, in case of cladding, to spread the laser beam out over the desired area, such that required intensity level is received on the laser spot. The type of optics that can be used is highly dependent on laser source used. For instance, diode lasers need somewhat different kinds of optics than e.g. CO₂ laser because they have different wavelength and higher a beam parameter product. [3,20] The beam parameter product (BPP), defines how much the laser beam diverges itself [3] and affects also suitable type of optics. With a low BPP value laser, the laser beam diverges only lightly so long focal lengths can be used [3]. Long focal length e.g. enables the use of scanner optics, as has been done in this work. Ultimately the suitable optical solutions are somewhat tied to the type of laser that is being used. Some different optical solutions for cladding purposes are presented in figure 2. The laser and the optics together create the intensity pattern on the surface of the workpiece. In figure 3, it is presented some intensity patterns created by different lasers and optics. When the laser spot is moved forward, a heat input pattern is formed, which is related to the spot dimensions and the intensity distribution of the spot, figure 4. Rectangular or line spots give more uniform heat input patterns, figure 4a, [43,44] and scanned beams produce heat input patterns according to the fact how the laser power is adjusted ,figures 3c and 4b [15]. The circular laser spot heat input is more or less centralized, figure 4c [45].



a)

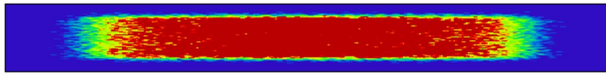


b)

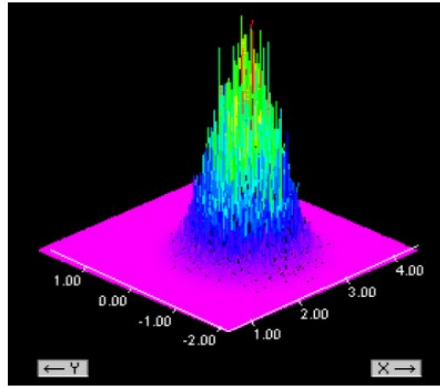
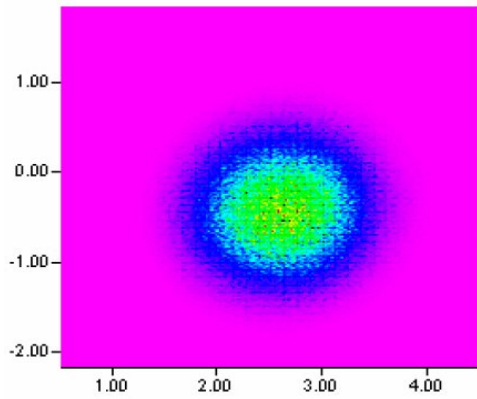


c)

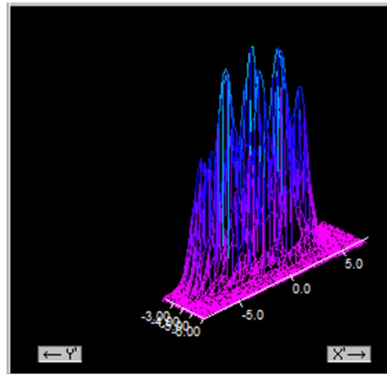
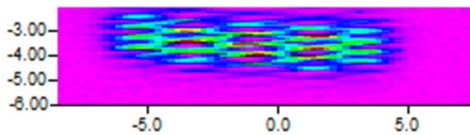
Figure 2. Some specialized optical solutions for cladding purposes. a) Integrating mirrors, left face integrating and right line integrating [46,47] b) Asymmetric cylindrical collimator with square formed fiber [48] c) Scanner optics [49]



a)



b)



c)

Figure 3. Intensity patterns of different laser – optics combinations. a) rectangular spot from a diode laser with 1 to 3 negative lens [44] b) circular spot from an Nd:YAG laser with 600 μm fiber and focusing lens of 200 mm focal length [50] c) A scanned fiber laser beam, with a power adjustment of 200 μm fibers, and a 500 mm focal length focusing lens with workpiece location 60mm of the focal point.

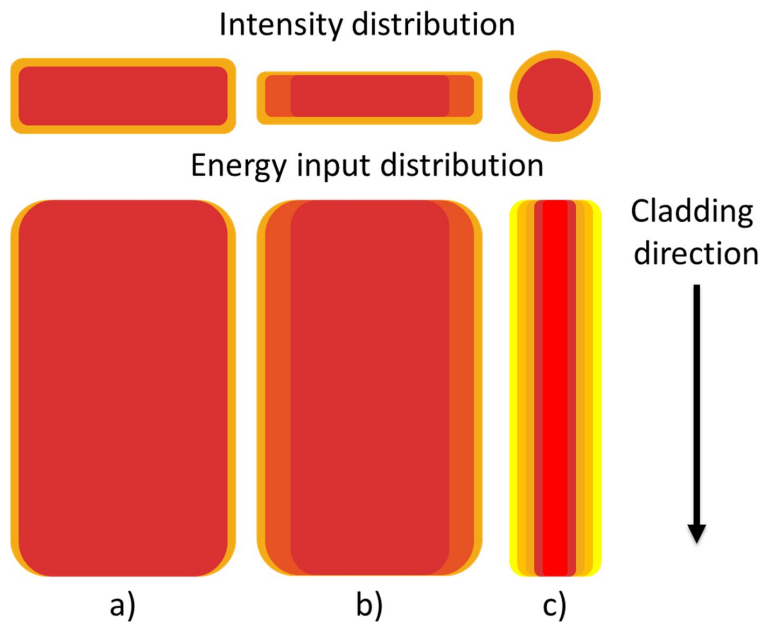


Figure 4. Heat input patterns between different laser spots. Intensity and energy input reduces when the light turns from bright red to yellow. a) rectangle spot with uniform intensity distribution, b) rectangle spot with decreasing intensity distribution from the edges c) round spot with top hat intensity distribution

Additive material dynamical feeding is the key element that makes laser cladding process work. The function of additive material feeding is to ensure that there is constant and sufficient material flow to the process. Constant material feeding flow ensures that the final result of the cladding is uniform. [3,20] Differences in powder feeding rate causes changes in dilution and clad geometry [5,51]. Additive material can be introduced to the process in many forms, e.g. powder, wire, strip, plate or paste, but the most common forms are powder and wire [3,20].

2.4 Process parameters

Laser cladding process parameters can be divided in two categories; energy input side and energy consumptive side, figure 5 and equation 1 and 2, and this separation helps to understand the mass-energy balance, equation 1 and 2. In order for the process be successful there must be balance between the energy input side and the using side [5,10,52-55]. Too high an imbalance towards either side can cause imperfections to the clad bead quality, for example, too high an energy input leads to high dilution rates and in turn if the specific energy usage is too high, the shape of the clad beads can be poor or the clad bead can even suffer a lack of fusion [5,10,54,55].

$$Q_s = \frac{P}{D_f v} \quad (1)$$

$$Q_{su} = p_{fa} c_p \Delta T + p_{fa} L \quad (2)$$

Where Q_s is specific energy input (J/mm^2), P is laser power (W), D_f is laser spots diameter (mm) and v is cladding speed. Q_{su} is specific energy usage that is needed for melting all the powder material per square millimeter (J/mm^2), p_{fa} powder material fed per square millimeter (g/mm^2), c_p powder materials heat capacity, ΔT material temperature rise from initial temperature to melting temperature ($^{\circ}K$) and L specific latent heat for melting (J/g).

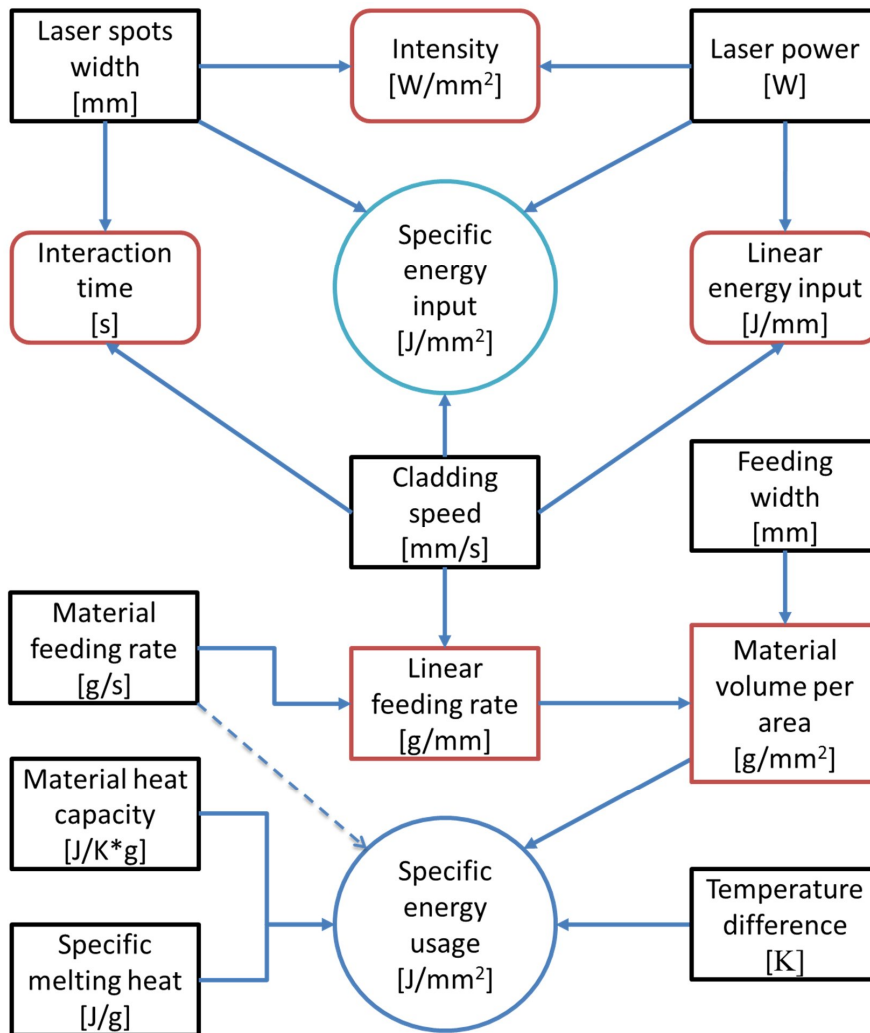


Figure 5. Laser cladding process parameters and their relationship to each other.

Laser power P (W) is the main parameter determining the process energy input. The laser power ultimately defines how much energy is imported into the process. However, laser power alone does not define how the material is going to act under the exposure of laser light, but the laser spot diameter (mm) plays also a great role in this. The spot diameter defines on how large an area the laser power is divided and therefore it defines, together with the laser power, the intensity I , (W/mm^2), figure 5. The intensity determines how the material actually behaves under the laser light; whether the material only warms up, melts or even vaporizes, when it encounters the laser beam [31,56]. Ion [20] and Toyserkani et. al. [3] stated in their books that an intensity of around $100 \text{ W}/\text{mm}^2$ is appropriate for laser cladding. Too high power densities can expose the cladding process to vaporization, and in contrast too low power densities only heat up the material.

The powder feed rate p_{fr} (g/s) ultimately defines how much additive material there is to be melted by the laser beam per time unit. The powder feed rate unambiguously defines the minimum energy that is needed to melt all the additive material and thus it defines the minimum laser power needed [53,55]. Because the feed rate so directly affects the mass-energy balance it has a great importance e.g. to the dilution levels of the clad bead [54,55,57]. Naturally, the actual laser power needs to be larger than the energy required to melt the powder material, due to process losses and the energy needed for melting substrate material, but this approach clarifies the powder feeding and laser power relationship.

The effect of cladding speed v (mm/s) on the cladding process is multifaceted. This is because the cladding speed affects both the energy input and usage sides, figure 5, and thus it is a binding factor between these two sides. The cladding speed defines, how long time laser beam imports energy to a specific location and thus it is also a defining factor on specific energy input Q_s (J/mm^2), figure 5 and equation 1. However, the cladding speed also defines, how long time the powder feeding is in interaction with this same specific point, figure 5. In this way, the cladding speed directly affects how much material is gathered at this specific point, the linear feeding rate p_{lfr} (g/mm), and how much energy there is Q_s (J/mm^2) and thus cladding speed influence on how large melt pool can grow. [55,58,59] The melt pool's size, in turn, affects the forming of the clad bead geometry, and thus the cladding speed directly affects the clad bead geometrical shape [55,57,58,60]. This matter is dressed in details in the following section 2.6.

The cladding speed also defines, together with the spot diameter, how long time the laser beam interacts with a specific point. This interaction time Δt_i is typically in the range of 0.1 s to 1.0 s, as this is a sufficient amount of time to generate metallurgically a uniform clad bead [3,20].

As cladding parameters are related to each other, it must be understood that when one parameter is adjusted this can affect many other factors. This is why the cladding process is more than the sum of its parameters and must be treated and adjusted as a whole.

2.5 Powder feeding parameters and the powder cloud behavior

Other important powder feeding parameters include: the powder feeding angle θ , particle velocity, and particle size. These factors influence how much energy the powder material receives while it is travelling through the laser beam to the melt pool and thus to how high temperature the powder materials can rise [61-66]. As these factors define the rise in the powder material's temperature, they also define at what stage the material will be under the laser beam: solid, liquid, or vapor. As Liu & Lin [64] pointed out in their study, with high laser power and a long exposure time in the laser beam, powder particles can start to vaporize, losing their volume. In the worst case scenario, the powder particle was noticed to lose almost 91 % of its diameter. Parameters that affect the rise in the powder material's temperature are thus important, because they directly affect the powder materials behavior.

2.5.1 Attenuation

Powder feeding creates a powder cloud on top of the melt pool, which causes an attenuation effect. This effect occurs when some of the laser's energy is either absorbed or reflected away by the powder particles during their flight across the beam. Consequently, the laser beam's power level decreases when it passes through the powder cloud. [58,62,63,67,68] Thus, the power levels in the melt pool can be slightly lower than what have left out from the optics.

Powder feeding angles affect both the rise in temperature of the powder particles and the attenuation of laser power. This effect comes from the geometry. Powder feeding angle θ defines how high the powder cloud is in relation to the laser beam, or in other words, how long inside the laser beam the powder particles go, x' in figure 6. As the angle approaches 90° the powder particles time inside the laser beam increases and thus the powder cloud's height in relation to the laser beam increases. [63,66,67] As the powder cloud's height in relation to the laser beam increases, the laser has to go a longer distance and time inside the laser beam, which increases attenuation [62,63,66,67]. This is because of the probability of photons interacting with powder particles will increase together with the height of the powder cloud [55].

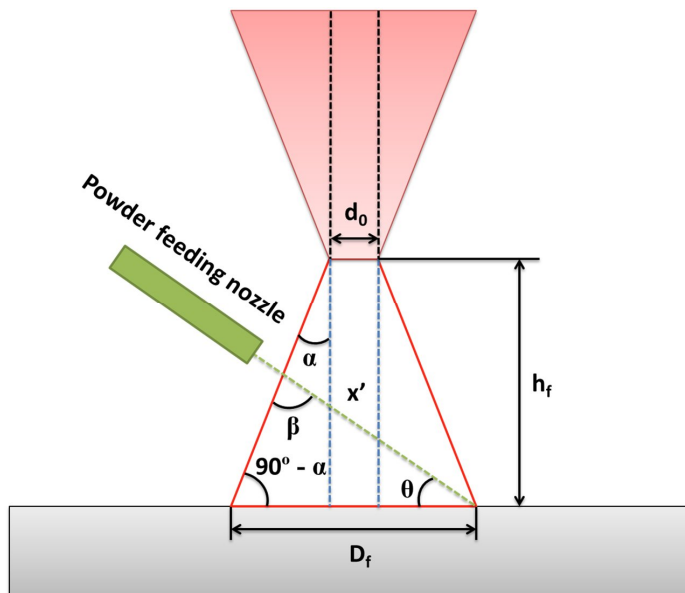


Figure 6. Powder path in the defocused laser beam, x' marks the powder particles longest theoretical path inside the laser beam; h_f is theoretical focal point level distance to the substrate, d_0 is focal point diameter at the focal level, D_f is the focal point diameter at the substrate material level, α is the optics refraction angle to the laser and θ marks the powder feeding angle.

The powder feeding rate has a significant effect to the laser power attenuation. This is due to the mechanism of the number of powder particles flying around inside the laser beam, and the opaqueness of the screen they form [55,60-63,69-72]. As the powder feeding rate determines how much additive material is injected into the cladding process, it therefore also determines, along with particle size, how many powder particles are flying inside the laser beam at any given moment. As the powder feeding volume increases, the number of particles inside the laser beam at a given moment increases. In other words the density of the powder stream increases and therefore the probability of photons interacting with the powder particles is increasing. [55,60-63,70-72] In addition, if the powder particle size is decreased with the same powder feeding rate (g/s), there will be more particles in the powder cloud and this increases the attenuation [55,62,65,72]. When photons interact with powder particles, the laser beam's power attenuates [55,63,70,72].

Pelletier et al. [55], figure 7, divided the powder stream's density effect to attenuation into four groups:

1. Part OA: The powder stream is partly transparent and powder stream's transparency decreases linearly with the powder feeding rate.
2. Part AB: The powder stream's opacity increases significantly with the feed rate. The powder stream is almost opaque as it approaches point B.
3. Part BC: The powder stream's opacity increases linearly with the powder feeding and approaching point C the powder stream is fully opaque.
4. Part CD: The powder stream is now optically fully opaque, and increasing powder feeding does not affect the powder stream's transparency.

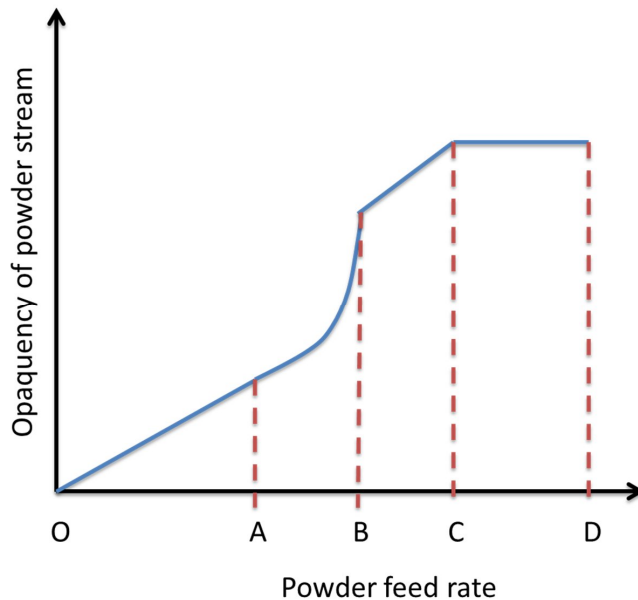


Figure 7. The powder stream's opacity according to the powder feeding rate [55]

2.5.2. Powder particle temperature rise

Powder particle temperature rise inside the laser beam is mainly dependent on the feeding angle, the particle velocity, the particle size, and the laser beam's intensity. The dependence of the temperature rise of the powder particles on the powder feeding angle and particle velocity is related to the time the powder particle is under the laser beam, equation 3 and figure 6. As the powder particle travels a longer distance and/or at a slower velocity through the laser beam, it has more time to absorb energy from the beam, and thus its temperature can rise to higher levels. [61-66,72,73]

From figure 6, the powder particle's maximum travelling time t_{max} inside the laser beam can be geometrically calculated if the particle velocity v_p is known. This calculation uses the following boundary conditions:

1. The powder particle is moving at a constant speed.
2. The powder particle travels through the laser beam from one to opposite corner of the laser spot
3. The gravitation effect on the powder particles' flight path is disregarded
4. The laser beam's power intensity through the laser beam is treated as constant.

The particles' travel time inside the laser beam can be calculated:

$$t_{max} = \frac{D_f \sin(90 - \alpha)}{v_p \sin(90 + \alpha - \theta)} \quad (3)$$

From this it can be seen that the main factors affecting the powder particle time under the laser beam are the spot size, feeding angle and the particles velocity.

The particle size effect on the temperature rise is product of the particles' volume relation to the particles surface area, figure 8, where the r_p is the radius of powder particle. When the absorptive surface area of the powder particle changes in the portion of r_p^2 , the powder particle volume changes in portion of r_p^3 . If the powder particle radius is halved, the powder particle effective absorbing surface area decreases to a quarter of the initial area, but the volume of the particle decreases to an eighth of the initial volume. [55,61,62,64,65,72] The mass for powder particles can be calculated using the equation:

$$m_p = \rho \frac{4\pi r_p^3}{3} \quad (4)$$

, where ρ is density of powder material and r_p is powder particle radius.

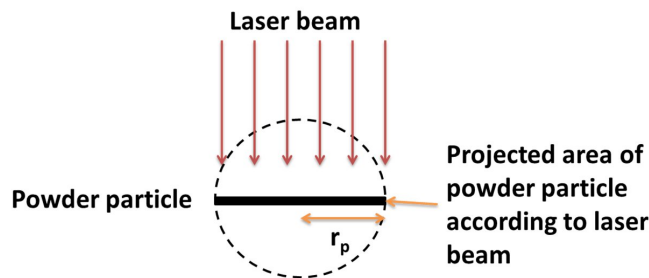


Figure 8. The surface area of the powder particle which absorbs energy from the laser, r_p marks the powder particle radius.

For the single powder particles point of view laser's total power is not important; it is the laser beam's intensity that is crucial as the powder particle can only absorb that part of the

laser radiation with which it is contact [61], equation 5. The energy received by powder particle in time unit depends on the powder particle surface area, laser beam intensity and time which powder particle is under the influence of laser beam. Thus energy can be calculated by using the following equation:

$$Q_p = aI\pi r_p^2 \Delta t_p \quad (5)$$

Where Q_p is the powder particle received energy, a is absorption factor, I is laser the beam's intensity and, r_p is the powder particle radius and Δt_p is the time the particle are under the laser light. However, there are some boundary conditions that must be fulfilled in order for this equation to be true:

1. Reflected photons should not be taken account in this kind of calculation, only the so called primary laser radiation is considered
2. The equation works only for round powder particles
3. The laser beam intensity is constant
4. Absorption is constant

From equation 5, it can be seen that the accumulated energy of the powder particles is the product of intensity, surface area and time. Therefore, when the powder particle has a smaller radius it accumulates less energy. However, because the magnitude of the volume of the powder particle decreases faster than its absorbing area, there is less material to heat with this smaller amount of energy. This is how the powder particle temperature rises to higher temperatures when the particle diameter decreases. [55,61,62,64,65,72]

From equations 6 to 7, it can be concluded, how the different parameters define the temperature rise of the powder particles using following equation:

$$T_p = T_0 + \frac{Q_p}{m_p c_p} \quad (6)$$

where T_0 is the initial temperature of powder particle, Q_p is the absorbed laser energy, m_p is mass of the particle and c_p is the specific heat factor of the powder material ($J/^\circ K g$). In addition, placing equations 3 to 5 to equation 6 the following equation can be obtained, which defines the maximum temperature of powder particle, if there are no changes in material state:

$$T_{max} = T_0 + \frac{aI\pi r_p^2 \frac{D_f \sin(90 - \alpha)}{v_p \sin(90 + \alpha - \theta)}}{\rho \frac{4\pi r_p^3}{3} c_p} \quad (7)$$

In this equation it can be seen that the temperature rise of powder material is highly dependent on spot size, intensity, particle speed, and powder particle size.

2.6 Clad bead geometry

In order for the cladding process to be successful, it has to fulfill some requirements. Firstly, the clad bead should have a low dilution level, figure 9, so that the clad bead obtains the desired material properties such as hardness [5,20,57,75]. Secondly, the clad bead needs to have a proper cross-sectional geometry, such as the clad bead wetting angle [10], sufficient height and width, figure 9 [5,10,51]. These geometrical properties determine e.g. how well the overlapping can be performed [10,51], or how well the different shapes can be formed [76-79]. However, both matters, dilution and the clad bead geometry, are dependent on the cladding parameters, such as the laser power, cladding speed, interaction time, additive material feed rate, power intensity, and spot size etc. [5,10,51,55,56,59,80]. When there is a large number of process parameters (laser power, additive material feed rate, etc.) and they form sub parameters (intensity which is dependent on power and spot size, interaction time which is dependent on spot size and cladding speed, etc.) leads to situation where the process itself and the qualitative outcome of the process can be hard to control. In order to reach the qualitative objective, it is important to understand the effects the different parameters have on the process.

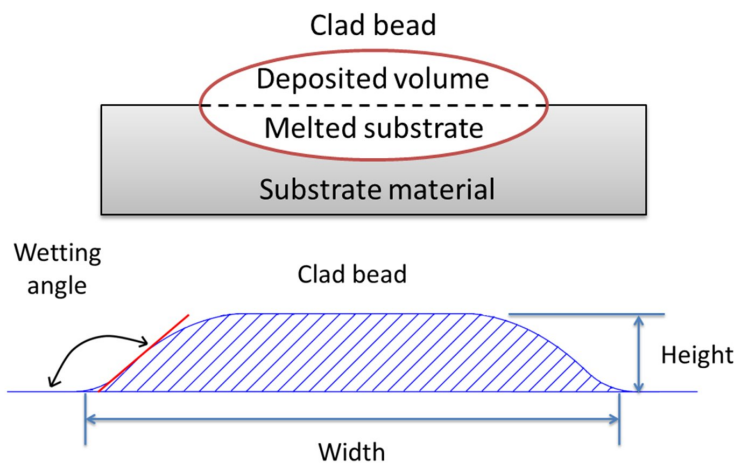


Figure 9. Dilution and geometrical dimensions of the clad beads.

2.6.1 Dilution

Dilution is an important indicator which can be used to evaluate the success of the cladding process. In order for a metallurgical bond to form between the clad bead and the substrate, a small amount of substrate material must be melted alongside the additive material [5,51]. However, this leads to a mixing of the additive material with the substrate material, which dilutes the chemical composition of the additive material; assuming that the additive material

and substrate have different chemical compositions. Because dilution causes change in chemical composition of cladding alloy, it is preferable that melting of substrate is kept minimum. For laser cladding this typically refers to a dilution of under 5 % [20].

Dilution is quite commonly measured by using geometrical dilution. This is measured by comparing melted substrate volume (cross-section area) to overall melted volume (cross-section area), figure 9 and equation 8. It is usually measured as a percentage of the melted substrate in the total clad bead cross-section area, and therefore, the dilution can be calculated in the following way [10,55]:

$$\text{dilution} [\%] = \frac{\text{cross - section area of melted substrate}}{\text{cross - section area of deposit and melted substrate}} \cdot 100\% \quad (8)$$

As mentioned previously, dilution is highly dependent on the process parameters, mainly the laser power, cladding speed, and powder feed rate. However, few studies have been conducted regarding this topic [10,51,54,55,57,59,80-84]. These parameters are the same process parameters that also define much of the mass energy balance. Nevertheless, these different parameters have also some unique features that can affect to the dilution through other mechanisms than the mass-energy balance.

In its simplest form, it can be stated that if there is too much energy compared to the fed additive material, the dilution increases, mass-energy balance. Thus by increasing mass flow rate of additive material to the process, the dilution can be decreased. [10,51,54,55,57,82-84] The effect of laser power (W) on the dilution is quite simple. Laser power ultimately defines, how much energy is inputted into the process. Thus an increase in the laser power increases dilution, if other parameters are held at constant level [10,51,82-84]. This is because amount of energy increases but there is same amount of additive material to melt so excessive energy goes to melting substrate material. The powder feeding rate (g/s) has a converse effect. As the powder feeding rate increases, decreases the dilution, as there is more material to be melted, and therefore there is less energy to melt the substrate material. [10,51,54,57,83]

However, laser beams power intensity and power distribution also affect to the dilution. It was pointed out in the study by de Lange et al. [81] that the laser spot's intensity distribution has an effect on the dilution. They concluded that a typical Gaussian type power distribution, which is normally achieved by using a short focal length lens and defocusing, is less preferable in laser cladding. Gaussian power distribution is more likely to form the burn-in the center of the clad bead than other power distribution shapes. Another way that intensity can cause an increase in the dilution is through vaporization. If the intensity is so high that the material evaporates and some sort of keyhole can be formed, the process resembles more a laser alloying process as Vollertsen et al. [85] showed by demonstrating how a high intensity laser beam can be used in deep penetration laser alloying.

In the literature, there have been evidences of two opposite factors concerning how cladding speed affect the dilution. There have been evidences that the increase of cladding speed can both increase and respectively decrease the dilution. An increase of dilution was concluded in three different studies done by Qian et al.[57], Fathi et al. [80] and de Lange et al. [81]. On the other hand, a decrease in dilution was also concluded in three different studies done by Zhao et al. [84], Huang [83] and. Kim & Peng [82].

The decrease of dilution can be understood via specific energy input. When the cladding speed is increased, the specific energy input is decreased, equation 1. In this way, when the specific energy input decreases there is less energy to melt the substrate material and dilution is decreased [82-84]. For an increase in dilution together with an increase of cladding speed, three possible explanations have been given. Firstly, de Lange et al [81] proposed that this is due to penetration of heat. At high cladding velocity, heat losses to the substrate decrease with an increase of cladding speed and thus this energy proceeds to melting the substrate and thus the dilution increases. Another explanation is given in the study by Qian et al. [57], that when the cladding speed increases, the powder's linear feed rate (g/mm) also decreases. Thus when there is less material fed per length unit (g/mm), the dilution increases when the remaining additive material quantity cannot consume the remaining energy, even though the energy input (W/mm) decreases together with the increase of cladding speed. Another mechanism that could explain the dilution increase with the increase of the cladding speed is melt pool behavior. When the cladding speed is low, the melt pool over-all size increases (height and length) [80,83] and as Hoadley & Rappaz [56] pointed out, the center of the melt pool then moves towards the cladding direction, figure 10b. Thus, the laser beam is largely directly interactional with the large melt pool rather than with the substrate material, figure 10. Thus when cladding speed increases, melt pool pulls back and laser can interact more directly with substrate material increasing dilution, figure 10 a. Thus when laser interacts directly with the substrate material, laser beam energy is used to melt more the substrate material and thus dilution can increase. This type of mechanism was also noticed in the experiments done in this work at publication 1.

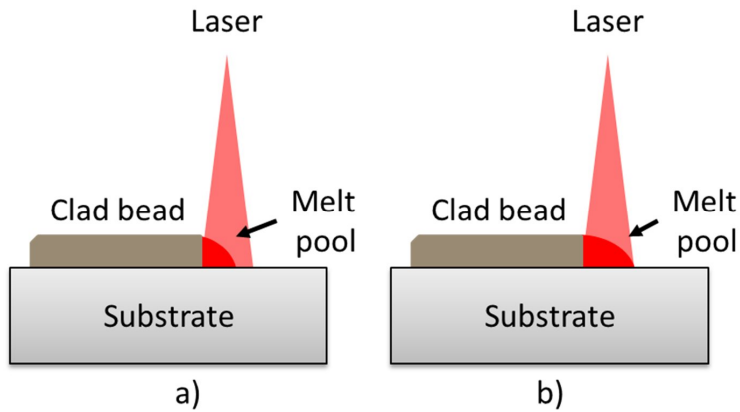


Figure 10. a) When the cladding speed is high the melt pool formed is small and the laser beam has a direct contact with the substrate material. b) By reducing the cladding speed, the melt pool becomes larger and pushes forward. In the latter case the clad bead then “shields” the substrate material against the excessive exposure to the laser beam.

2.6.2 Geometrical requirements of clad bead

Together with the low dilution, the clad bead should fulfill some other geometrical requirements in order the cladding process to be successful. One of the most important of these is the wetting angle of clad bead, which should be 120° or higher so that when the clad beads are overlapped they form a uniform structure. If the side angle is considerably smaller than 120° , the possibility of trapping impurities or the formation of inter-run pores between the clad beads increases significantly. Figure 11 presents the inter-run pores between the clad beads. [5,10]

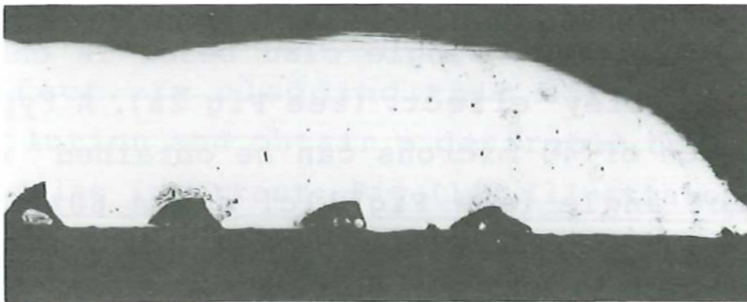


Figure 11. Pore formation between the clad beads when the clad beads side angle has been too close to the straight angle. [5]

Another important geometrical requirement is that the clad bead has width and height. These aspects define, how many clad beads must be done next to each other and/or on top of each other so that the desired area and volume is covered. Both of these variables are highly dependent on process parameters. The width of the clad bead is mainly defined by the laser power, cladding speed, beam diameter, or scanning amplitude of the laser beam [5,10,51,57,58,83,86,87]. Increase in the laser power causes modest widening of the clad bead [51,86], and an increase in the cladding speed modest narrowing of clad bead [5,57,86]. Both of these parameters affect the linear heat input and therefore affect the width of the clad bead through this. As the linear heat input increases, the clad bead width slightly increases and vice versa. The width of the beam radius / laser beam interactional zone, in turn, defines how wide area the laser beam can interact, defining the clad bead width through this mechanism [15,58,87].

The clad bead's height is, in turn, dependent mainly on the clad material mass feed rate, cladding speed, and laser power [5,51,56,57,80,83,86]. Increase in the mass feed rate naturally increases the clad bead height. When there is more material, higher clad bead can be formed [51,83,86]. The cladding speed has the opposite effect. When the cladding speed is increased the clad bead height decreases as less additive material is fed in per unit length (g/mm) [5,51,56,80,83,86]. Increase of the laser power increases the clad bead height [51,56].

Zhang et al [86] stated in their study that for curved shaped clad beads there is maximum height for a single clad bead, figure 12 and equation 9. When the clad bead's height is under this maximum value, the overlapping of the next clad bead should not cause any problems and clad layer top surface should be relatively flat. This critical height equation is the following:

$$h_c < \frac{2}{3}r_1 \quad (9)$$

where h_c is the critical height and r_1 is the radius of the laser spot. The change of the clad bead's side angle is related to the clad bead's height growth. The same parameters that cause increase in the height of the clad bead also cause the decrease of side angle towards a straight angle. [88]

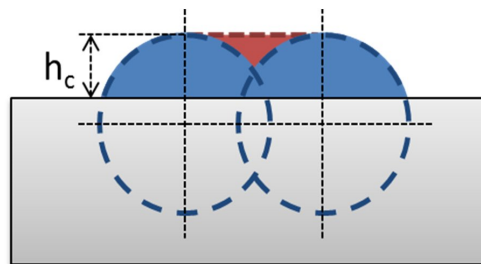


Figure 12. Height and overlapping of the clad beads. The red area is the area of overlapping.

Three different types of shapes have been determined for the clad bead's basic shape. These shapes have been determined by Weerasinghe & Steen [5] in their study, figure 13. If the additive feed rate is too low and/or the intensity is too high excessive dilution occurs, figure 13a. On the other hand, if the additive feed rate is too high and/or the cladding speed is too low the clad bead grows too high which can result during the overlapping in inter-run pores between the clad beads, figure 13c. However, when the laser intensity is correct and the powder feed rate is in balance with the cladding speed a smooth surfaced clad bead with a suitable side angle and low dilution can be achieved, figure 13b. [5]

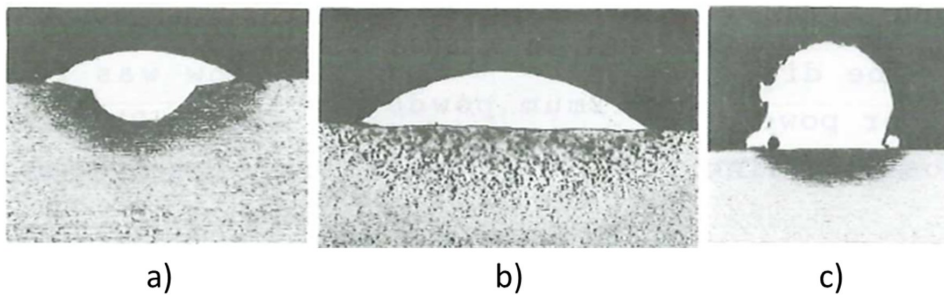


Figure 13. The three basic shapes of clad beads. a) The dilution is high; b) Dilution and side angle are in the correct proportions; c) The dilution is low and the clad beads side angle is too low.[5]

2.7 Laser cladding with scanning optics

Laser cladding using a scanned beam is quite a similar process than laser cladding using static optics. The main difference comes from the manipulation of the laser beam. In laser cladding with scanning optics the laser beam is manipulated with a scanner so that the laser's area of influence can be increased, figure 14 and figure 15. Thus, the laser beam material interaction area is determined by two factors: scanning amplitude and spot size, figure 15 and equation 10. In turn, laser cladding with static optics the size of the interaction areas is determined only by the spot size.

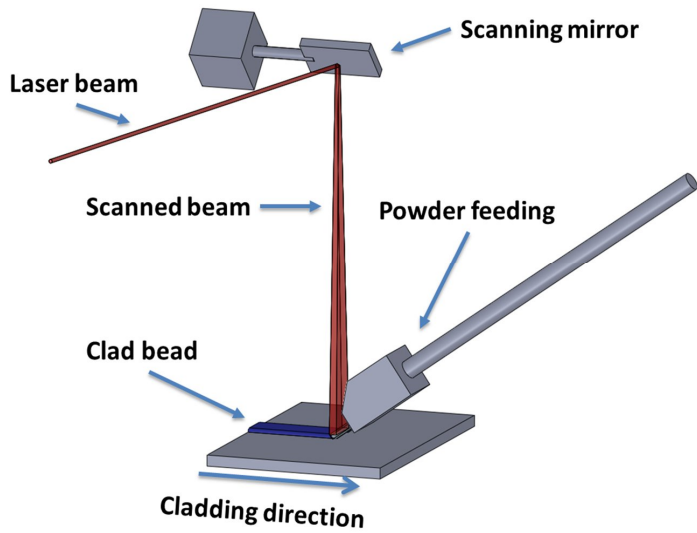


Figure 14. Principal setup of the laser cladding process

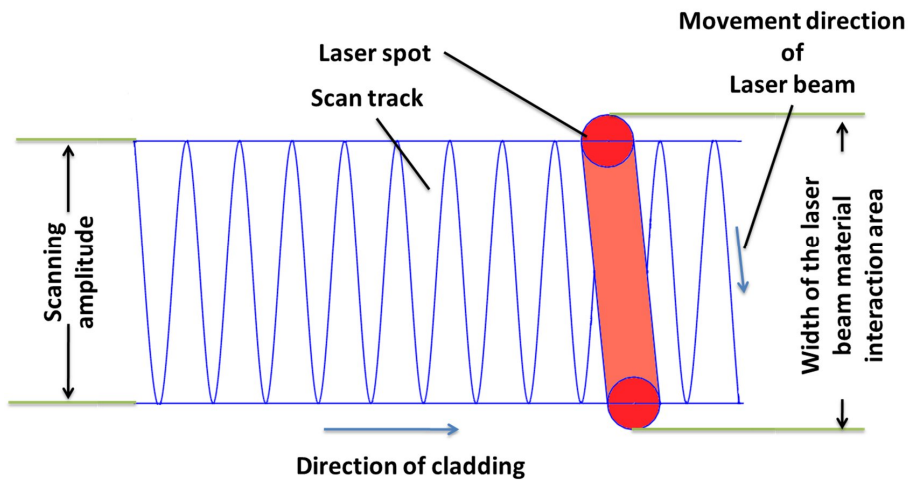
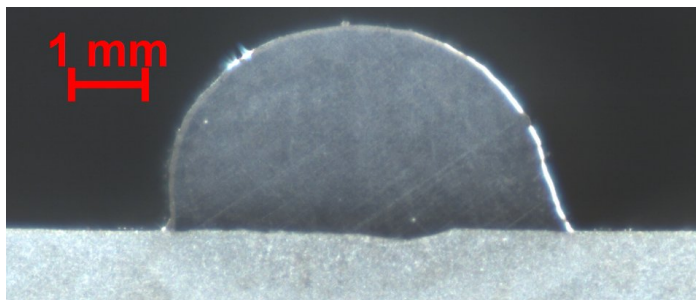


Figure 15. Scanning amplitudes and laser spot relation to the area of laser beam material interaction

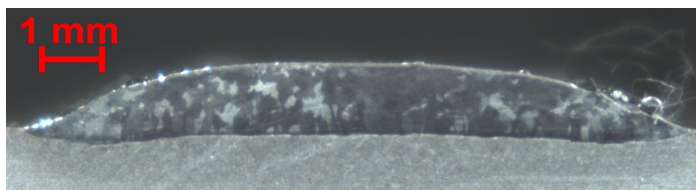
$$W_{lai} = A + D_f \quad (10)$$

Where W_{lai} marks the width of the laser beam material interaction area (LMIA), A marks the scanning amplitudes width and D_f marks the laser spot diameter.

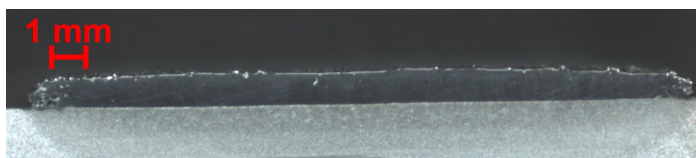
The laser beam material interaction area is defined mainly by the scanning amplitude. As the melt pool width follows the laser beam material interaction area, the clad bead's width can be adjusted through the scanning amplitude. Figure 16 presents three different clad beads that have been clad using the same optical setup. Thus, the adjustment of the scanning amplitude enables considerable flexibility to affect the clad bead's geometry.



a)



b)



c)

Figure 16. Three different clad beads produced with the same optical setup: 500 mm focal length focusing optics, 150 mm collimator and ILV DC scanner, with $f = 100$ Hz scanning frequency, $P = 5$ kW and power adjustment . Only the scanning amplitude and cladding speeds has been modified, a) $A = 3.1$ mm $v = 3.33$ mm/s; b) $A = 9.6$ mm $v = 3.33$ mm/s and c) $A = 17.5$ mm $v = 1.67$ mm/s.

When the laser cladding is done using scanning optics, there is a small difference in energy input mechanism when it is compared to cladding done by using static optics. The energy from the static optics into the process comes through a relatively large spot, which has relatively low laser intensity. However, with scanning optics this energy input takes place

through a relatively small laser spot, which has relatively high power intensity. Thus, local laser energy input is high. However, when this small spot is scanned back and forth rapidly enough over the desired laser beam material interaction area, the average heat input in this area is again relatively low. This dual characteristic of the energy input separates cladding with scanning optics from the cladding with static optics.

One important thing to keep in mind is that when linear scanner with oscillating mirror is used, is that laser beam dwells at the edge region of laser beam material interaction area. This is caused by the scanning mirror deceleration, stopping and acceleration at the scanning amplitude edge where mirror direction of movement changes. This phenomenon is called dwell time and it can cause so called viper tooth energy input pattern, figure 17. Then more energy goes to the edge region of laser beam material interaction area than in the middle. However, this phenomenon can be avoided using scanned beam power adjustment, the matter that is treated at publication 2 of this work.

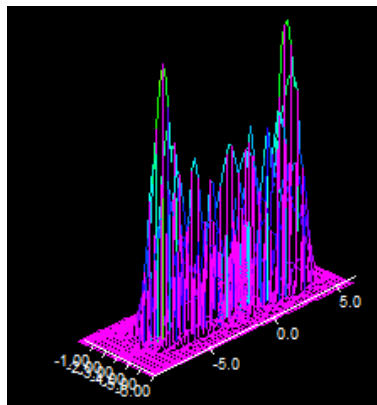


Figure 17. Viper tooth energy input pattern of unadjusted scanned laser beam.

3. Experimental Investigation

The purpose of this study was to determine, how a scanned laser beam changes the process dynamics of the cladding process, and to determine threshold values for the process parameters. In order to study laser cladding with a scanned laser beam, a high power fiber laser was used with a linear scanner. The cladding tests were specifically designed to study the process dynamic of the cladding process, but also to study the possibilities and weaknesses when using scanner optics in laser cladding. The following are the four main research problems which were studied in this work:

- i. The possibility of the scanning amplitude adjustment to adjust the clad bead dimensions. The scanned beam's effect on the melt pool behavior and how the melt pool behavior changes together with the scanning amplitude
- ii. The effect of the scanned beam's dwell times on the stability of the process and how power modulation affect to it. Also the effect of the scanned beam's power modulations on the clad bead's geometry
- iii. The effect of the scanning frequency of the laser beam and power intensity on the cladding process stability and dilution
- iv. Powder cloud behavior under the high power scanned laser beam; the effect of the powder feeding angle and feeding gas flow on the process stability, and how vaporization in the powder cloud can be detected

The results of the experimental study are summarized in the review of publications presented in chapter 4, and reported extensively in the research papers in the second part of this thesis.

3.1 General experimental setup

The experimental system can be divided into four divisions: laser equipment, optical setup, powder feeding, and process monitoring / analyzing equipment. The laser used was a solid-state ytterbium fiber laser manufactured by IPG model YLR-5000-S. The wavelength of the laser was 1070-1080 nm and the maximum laser power 5000 W.

The working fiber diameter used was 150 μm . The focusing optics used was a Precitec YW50 welding head with a collimator lens with a focal length of 150 mm and a focusing lens with a focal length of 500 mm. An ILV DC scanner was mounted between the collimator lens and the focusing lens. A photograph of this setup is presented in figure 18.

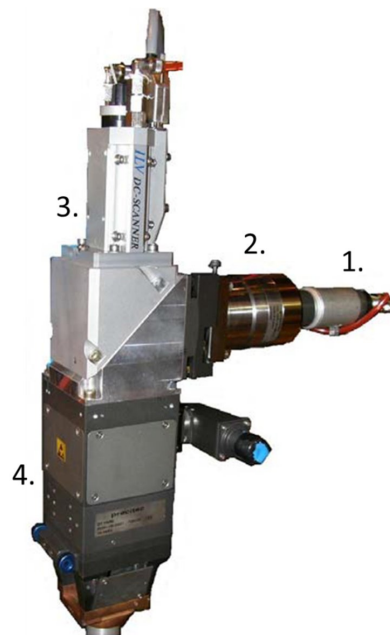


Figure 18. Precitec YW50 welding head and ILV DC scanner, 1. Fiber coupling, 2. Collimator, 3. Scanner and 4. Precitec welding head housing and focusing optics [89]

Powder feeding was implemented using an off-axial pneumatic powder feeding. The powder feeding machine used was a Plasma-Technik Twin-System 10-C powder feeding machine. All the tests were done using argon as a powder carrying gas. The powder feeding width was matched with the scanning amplitude in all the tests using a suitable powder feeding nozzle.

The process analysing equipment consisted of a camera system together with a Cavilux laser illumination system. The Cavilux illumination system illuminates the videoed target at a wavelength of 808 nm. The dichroic window filter, working at this 808 nm wavelength was used to filter other wavelengths away from the cameras sensor. Two different cameras were used in these tests, in test 1 to 3 a normal CCD camera was used, and in test 4 a high-speed camera was used. The CCD camera frame rate was 20–25 fps and the high speed camera's 2000 fps. The focal point size and power distribution in different focal positions was measured using a Primes FocusMonitor. The tests were carried out at focal point positions from ± 0 to +80mm at the laser's full power of 5 kW. In addition, the scanned beam's power distribution was tested using a FocusMonitor.

The feedstock material used in all the test was an AISI 316L stainless steel powder. The particle size of powder material size was between 53 and 150 μm . The substrate material used was standard S355 structural steel plate with a thickness of 6mm, made by the Rautaruukki Corporation. The laser beam was moved by a numerically controlled X-Y portal robot.

The dilution measurements were done by cutting the test clads across in the middle of the clad layer length transverse to clad layer direction, and polishing them mechanically. After this the samples were etched using 5 % Nital etchant. The dilution measurements were done from these samples, measuring the geometrical dilution using an Axivision 4.8 program.

3.1.1 Used scanner technology

The scanner that was used in these tests was an ILV DC linear scanner. This scanner model is based on an oscillating scanning mirror, figure 19. The scanner's mirror oscillates from side to side in the desired frequency and amplitude. Both of these parameters can be adjusted numerically.

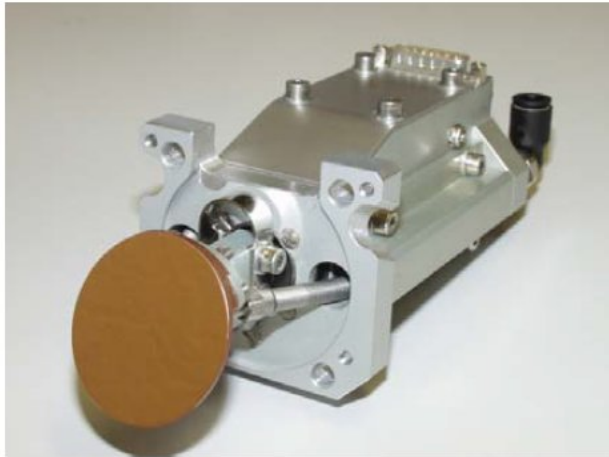


Figure 19. The ILV scanning mirror [90]

This scanner model has one special feature, a power adjustment, which make it quite suitable for laser cladding. The laser power can be adjusted at 32 points according to location where the scanning mirror is directed. Figure 20 presents how these power adjustment points are placed in a sine wave which is formed when scanning mirror movement and process movement are combined. These 32 adjustment points form 17 adjustment lines, figure 20, and from these lines, power adjustment figures can be drawn - where the X- axis presents the adjustment lines and the Y- axis is the power level. An example of the powder adjustment figures is presented in figure 21. Using the power adjustment laser energy input can be adjusted across the laser's area of influence.

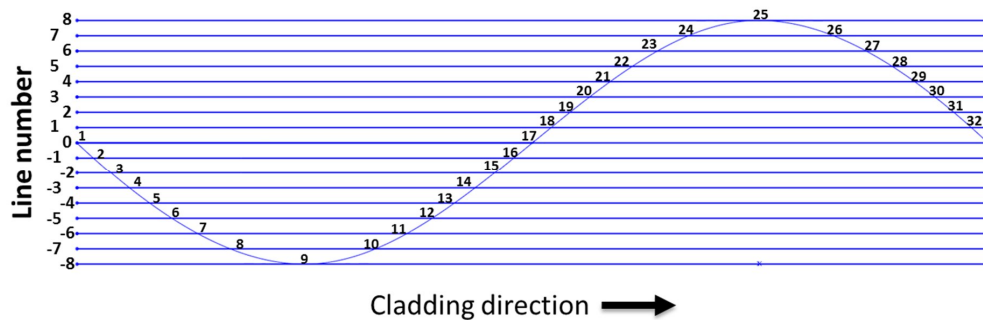


Figure 20. The power adjustment points as a sinus wave

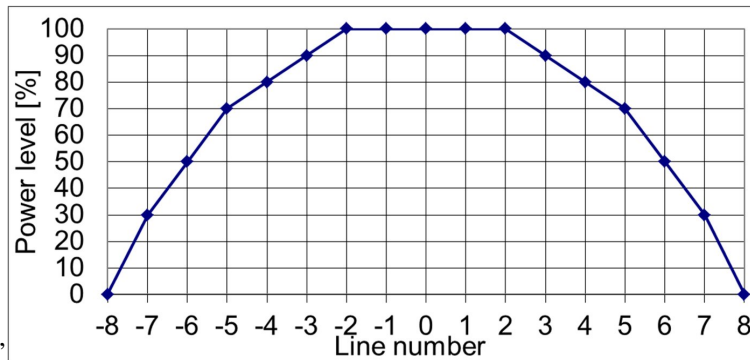


Figure 21. Example of a power adjustment diagram.

This scanner model is a linear scanner that can scan a laser beam in a frequency range from 5 Hz to 800 Hz. For practical reasons, in this work the laser beam was scanned in a frequency range of 5 to 150 Hz. The limit for 150 Hz comes from the laser's power modulation level. The type of laser used can change the laser power level at a frequency of 5000 Hz and with a 150 Hz scanning rate using 32 adjustment points when the laser powder modulation's frequency is 4800 Hz, which is close to the maximum power modulation frequency of the laser.

3.2 Specific test circumstances

3.2.1 Test series for Publication 1

Laser cladding test were conducted using a laser power of 5 kW with the power adjustment presented in figure 21 above. Figure 22 presents the average power distribution of the scanned beam. On average, this power adjustment pattern gave 74% of the maximum power, 3.7 kW, to the scanned area. With this three scanning amplitudes, 3.1, 9.6, and 17.5 mm, were tested at a scanning frequency of 100 Hz. The laser beam was defocused +60 mm, which gave a laser

spot diameter of 2.43 mm on top of the work piece; the average intensity being 369 W/mm^2 , and the local peak intensity inside the laser spot being 1920 W/mm^2 on top of work piece. Figure 22 presents the spot's power distribution.

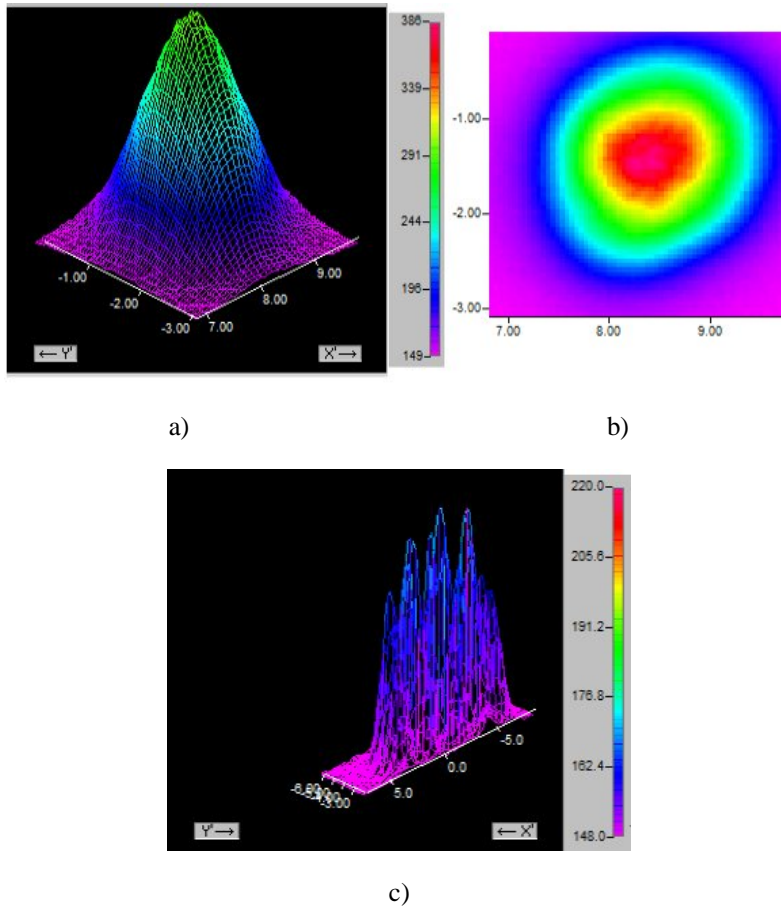
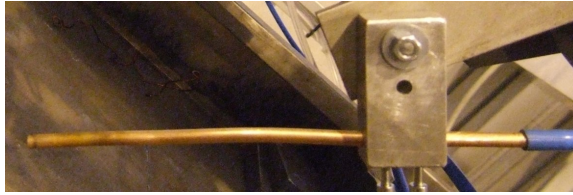


Figure 22. Power distribution of used laser beam: a) and b) The laser spot's power distribution and c) scanned beams average power distribution. Presented power distribution scale is in kw/cm^2 .

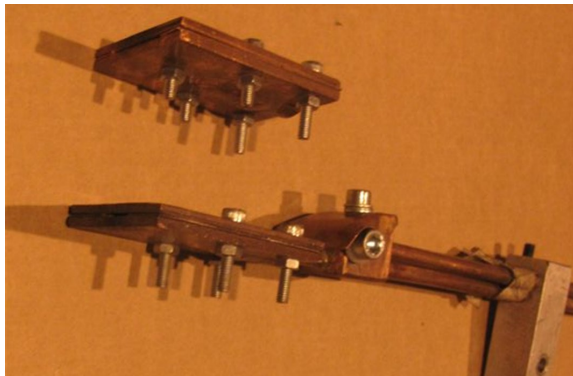
The powder feeding was implemented using three different widths of powder feeding nozzles, figure 23 a-c. These nozzles were made such that the width of the powder flow was equivalent to the laser beam material interaction area. The powder was fed at a 40° angle, at a powder feed rate of 0.5 g/s . The tested cladding speeds varied from 1.67 to 8.30 mm/s . The melt pool behavior was recorded using a CCD camera with a Cavilux illumination system.



a)



b)



c)

Figure 23. Used powder feeding nozzles. a) Pipe nozzle for 3.1 mm scanning amplitude tests. b) Mid wide feeding nozzle for 9.6 mm scanning amplitude tests. c) Powder feeding nozzle with interchangeable nozzle tip. Upper powder feeding nozzle tip was used for 17.5 mm scanning amplitude.

3.2.2 The test series for the Publication 2

Laser cladding tests were done using a laser power of 5 kW with seven different types of power adjustment diagrams. One diagram used was set so that in all the 32 adjustment points the laser power was at 100 % and the other six are presented in figure 24. The scanning amplitude used was 9.6 mm, which gave all together a 12 mm LMIA. The laser beam was defocused +60 mm which gave a laser spot diameter of 2.43 mm on top of the work piece, the

average intensity being 369 W/mm^2 , and the local peak intensity inside the laser spot being 1920 W/mm^2 on top of work piece. The scanning frequency used was 100 Hz.

The powder was fed at a 40° angle with a powder feed rate of 0.5 g/s. The tested cladding speeds varied from 1.67 to 8.30 mm/s. The melt pool behavior was recorded using a CCD camera with a Cavilux illumination system.

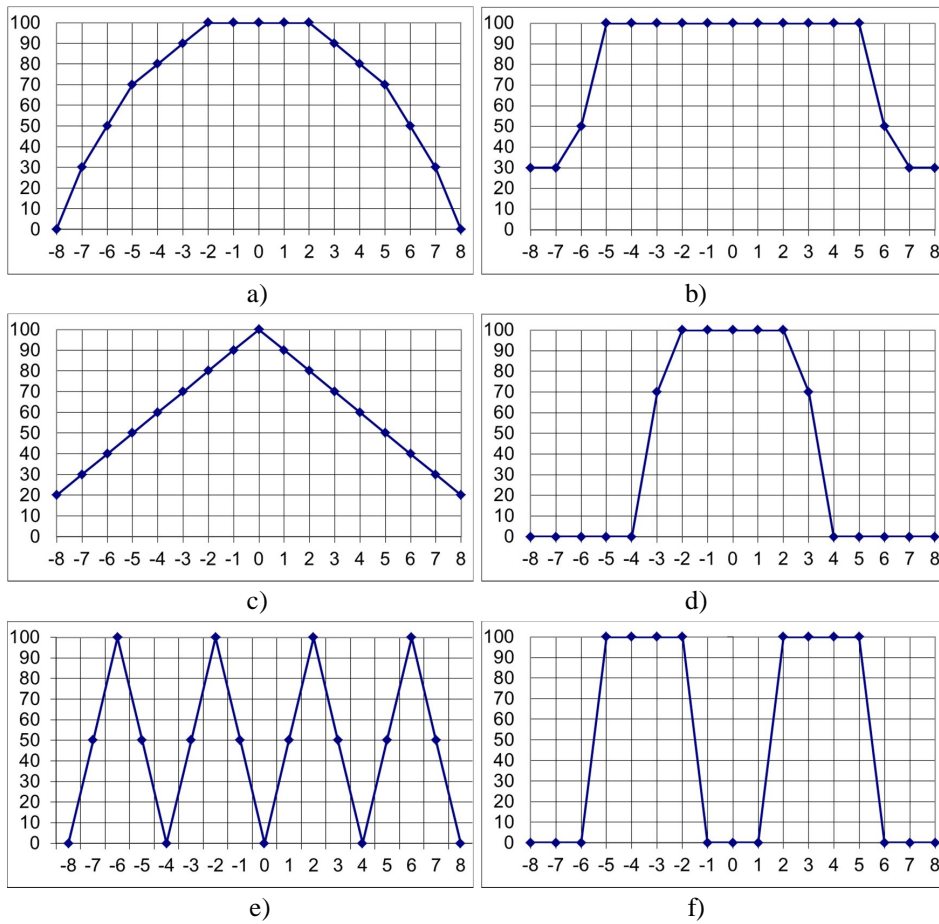


Figure 24. The power adjustment figures used. The power adjustment gives an average of: a) 74 %, b) 83 %, c) 62 %, d) 41 %, e) 52 % and f) 52% from full laser power. The vertical axis is a fraction of maximum laser power in percentage, and the horizontal axis marks the numbers of the adjustment lines.

3.2.3 The test series for the Publication 3

Laser cladding tests were done using 5 kW of laser of power with the power adjustment presented in figure 21. On the average this power adjustment pattern gave 74% of maximum power, 3.7 kW, to the scanned area. The focal point position was +60 mm over the top of the work piece surface in the frequency tests and the scanning amplitude used in all of these tests was 9.7 mm and thus the width of the interaction zone was 12 mm. In the intensity tests five different defocusing distances were used to modify the spot diameters and thus the intensity. In this series focal positions of 0, +20 mm, +40 mm, +60 mm and +80 mm were tested. The scanning amplitude in these tests was 8.7 mm and the corresponding LMIA width was 9.4, 9.9, 10.4, 11.3 and 12.1 mm at 0, +20, +40, +60 and +80 mm at a focal position level, respectively. The laser's peak intensities measured at these different focal positions are presented at table 3 and in figure 25 it is presented measured intensity distributions of these spots.

Table 3. *The measured laser spot's diameters and intensities at the laser's maximum power*

Focal position [mm]	Spot diameter [mm]	Peak intensity at 5 kW power [kW/cm ²]
± 0	0.54	2 836
+20	0.89	1 424
+40	1.73	413
+60	2.56	191
+80	3.44	102

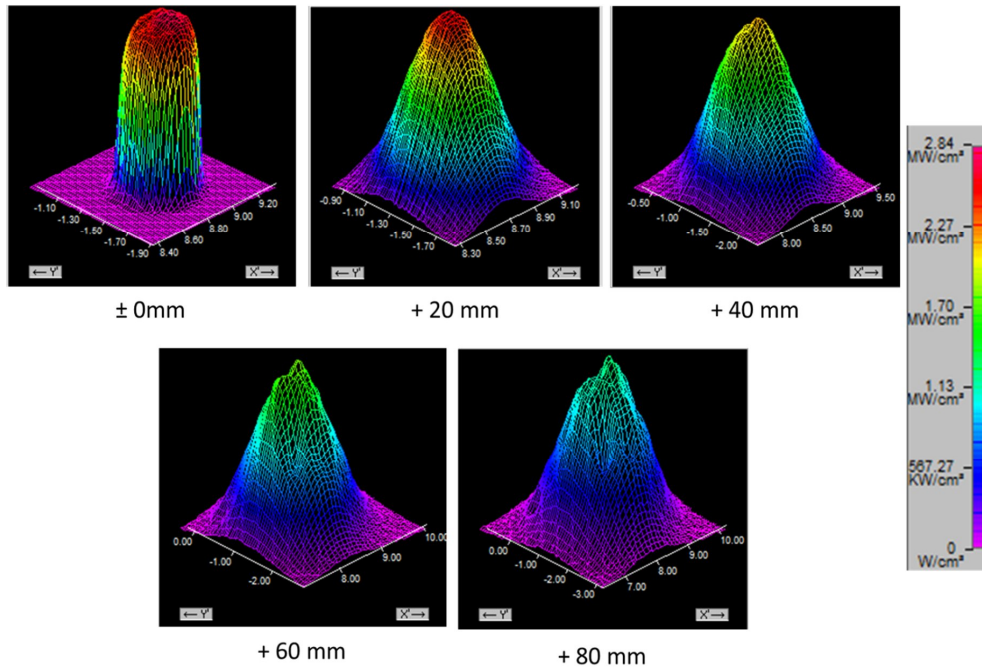


Figure 25. The spot's power distribution at different focal positions.

The powder was fed at a 40° angle with a powder feed rate of 0.5 g/s. Two cladding speeds were used in the scanning frequency tests, 3.33 mm/s and 5.00 mm/s. During the focal point position tests a cladding speed of 5.00 mm/s was used. Melt pool behavior was recorded using a CCD camera with a Cavilux illumination system.

3.2.4 The test series for Publication 4

In these tests the laser power measured after the optics was 4.1 kW and with the power adjustment presented in figure 24b, the average laser power was 3.33 kW. Figure 26 presents the average power distribution of the scanned beam used. These power values were measured with a Primes CPM F-10. With 60 mm defocusing the laser beam diameter on top of the work piece was 2.43 mm, and the local peak intensity was 1920 W/mm² on top of the substrate. The width of the interaction zone was 12.1 mm in these tests. Three different scanning frequencies were used 80, 100 and 150 Hz.

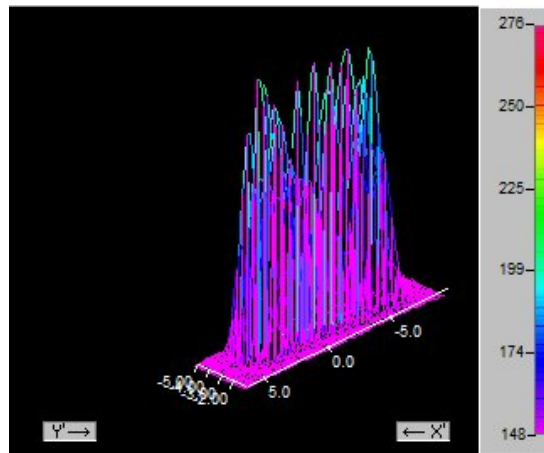


Figure 26. The average power distribution for the power adjustments used. Presented power distribution scale is in kw/cm^2 .

The process analyzing equipment consisted of a spectrometer and a high-speed camera. The spectrometer used was an Ocean Optics HR200+, and it measured the light spectrum within the range of 192 to 652 nm. The spectrometer was used to analyze the light emitted by the powder clouds under the scanned laser beam. The spectrometer was aligned parallel to the substrate surface such that it measured only the radiance emitted from the powder clouds (see Figure 27). A high-speed camera was used with a Cavilux laser illumination system. The camera frame rate used was 2000 fps and the wavelength of the laser illumination system was 808 nm. High-speed imaging was used to study the powder cloud movement during the process.

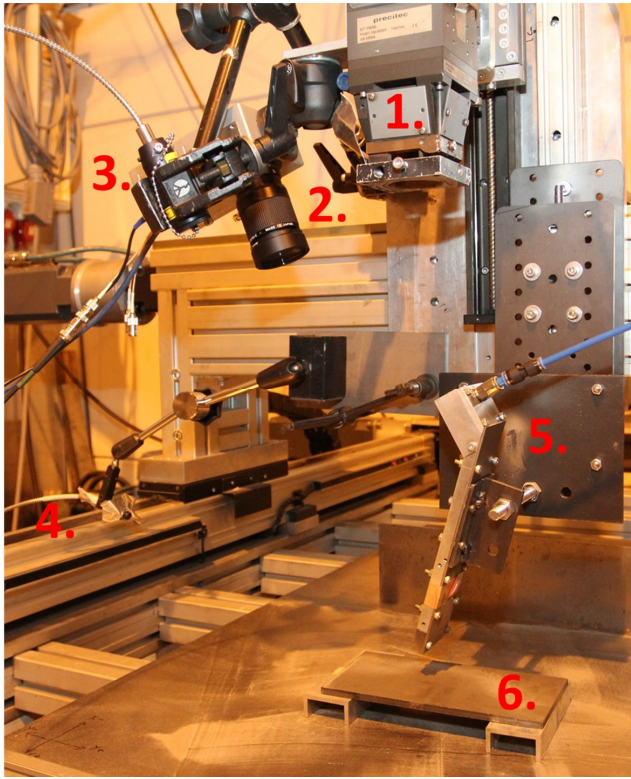


Figure 27. Experimental setup. 1. Precitec welding head. 2. High-speed camera. 3. Illumination system. 4. Spectrometer. 5. Powder feeding nozzle. 6. Workpiece.

The laser beam was moved by a numerically controlled X-Y portal robot. The cladding speed used was 5 mm/s. The powder feeding rate was set at 0.57 g/s and two powder feeding gas flow values were used, 3 l/min and 6 l/min. The gas flow rate was measured between the nozzle entry chamber and the powder feeding tube. Four powder feeding angles used were: 40°, 50°, 60° and 70°. The powder feeding nozzle construction was redesigned for this test series, figure 28. The design was based on experience gained from Publications 1-3.

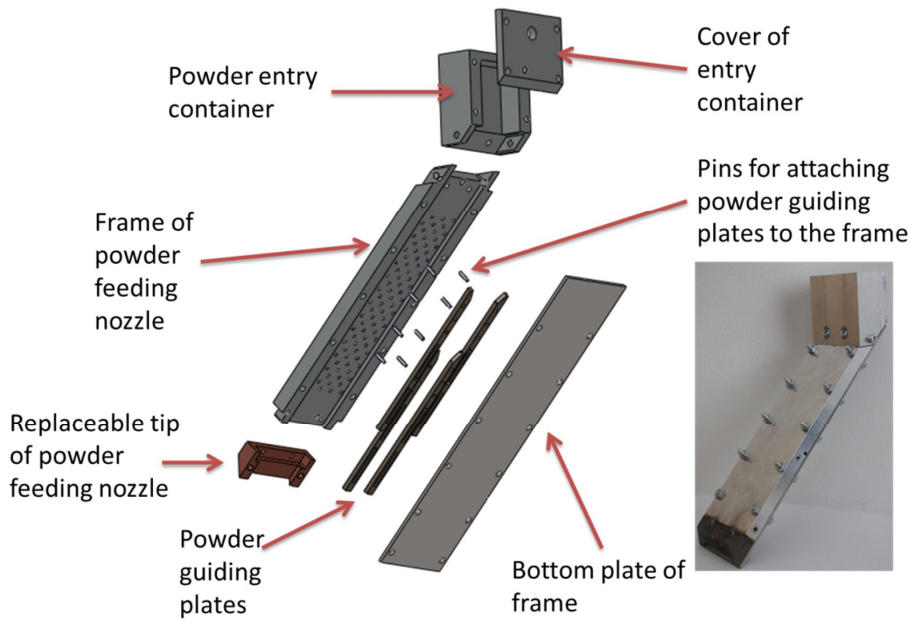


Figure 28. Powder feeding nozzle construction.

The powder particle velocities were estimated from the videos captured with a high-speed camera. The images in the sequences were 400x400 pixel grayscale frames with 256 intensity levels, and the movement of the particles in the image sequences was estimated as follows. The background removal was performed by subtracting the previous frame from the current one and by limiting the values in the resulting image from 0 to 10. The particles were brighter than the background, and thus both bright spots and dark "holes" in the image sequence were created after the background removal, facilitating the following of the motion. The translational motion was determined by using a Fourier transform-based phase correlation optical flow algorithm [91], which is highly resistant to noise. The images were divided into 100x100 pixel sub-windows and the windows were positioned at every 25th pixel, resulting in 13x13 motion vectors for each image. The motion was tracked separately in each sub-window after application of the Hann windowing function to avoid edge effects in the Fourier transform. The resulting motion vectors were not stable between the frames due to the noise in the original images and the difficulty of detecting even single particles reliably. Therefore, a Kalman filter (software) [92] was used to smooth the noisy motion vectors between the different frames. Two consecutive frames from an analyzed video are shown in Figure 29.

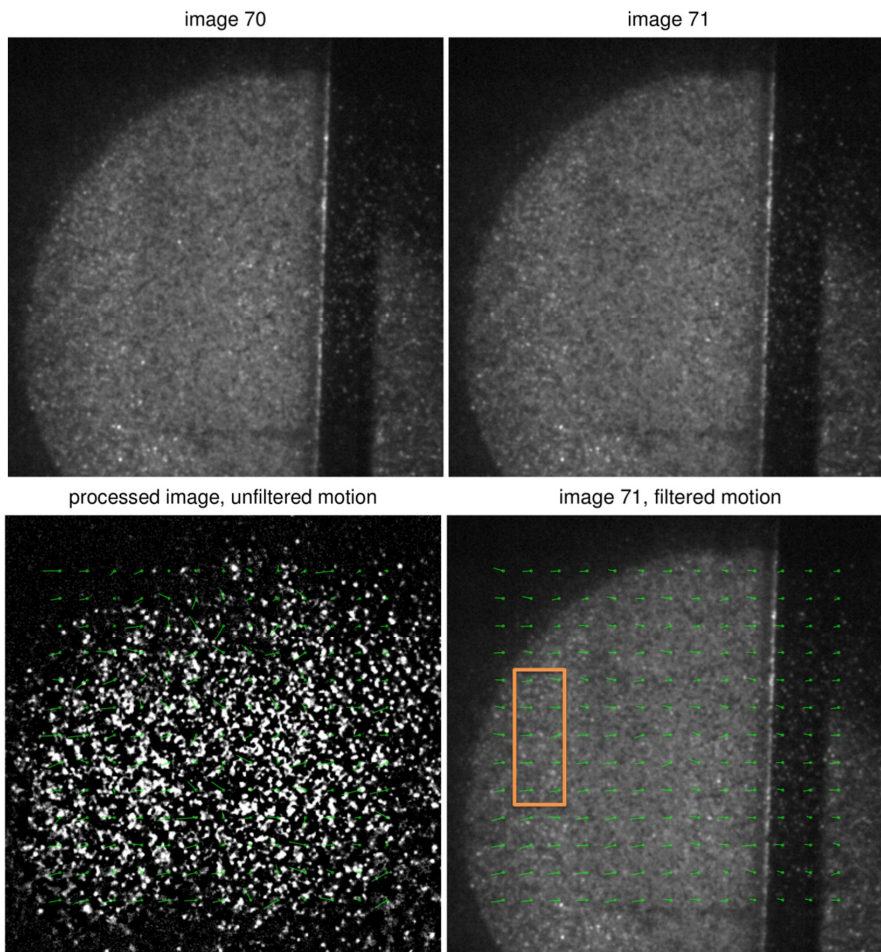


Figure 29. An example of two consecutive frames from the video (top row) analyzed with optical flow and Kalman filtering (bottom row). The green arrows are the estimated motion vectors for the local sub-windows. The orange square marks the spot where the declared / stated particle velocities were measured.

4. Review of publications

This section concentrates on summarizing the four research papers that constitutes the second part of this thesis. Table 4 presents how the different publications are related to each research problem.

Table 4. The research problems, and their relation to the research papers.

Research paper	Research problem
Publication 1	The possibility of the scanning amplitudes adjustment to adjust the clad beads dimensions. The scanned beam's effect on the melt pool behavior and how the melt pool's behavior changes together with the scanning amplitude
Publication 2	The effect of the scanned beam's dwell times on the stability of the process and how power modulation affect to it. Also the effect of the scanned beam's power modulations on the clad bead's geometry
Publication 3	Laser cladding with scanning optics: Effect of scanning frequency and laser beam power density on cladding process
Publication 4	Powder cloud behavior under the high power scanned laser beam; the effect of the powder feeding angle and feeding gas flow on the process stability, and how vaporization in the powder cloud can be detected

Altogether these four publications form overall view of matters that affect the qualitative results and process stability of laser cladding process when scanner optics is used. Results of these publications can be used when laser cladding is done with scanning optics and instability during the process is to be voided. Furthermore, these results can be also used if there is observed instability in the process, in order to identify and solve the problem. The first publication mainly deals with laser cladding using scanning optics at a general level and the following three publications treat more specific matters related to this subject.

4.1 Publication 1

Laser cladding using scanning optics

The first publication concentrated on explaining how scanning optics can generally be used in laser cladding, how the clad bead width can be adjusted by amplitude adjustment, and how this effects on the clad bead's geometry. Also matters of the defects in the clad beads, and the effect of the scanned beam on the melt pool's behavior are treated in this publication.

One of the most important matters that was reported in the first publication was the matter of the dual characteristics of the energy input and the effect of it on the melt pool behavior. Laser energy is introduced into the process via a relatively small laser spot which moves rapidly back and forth, distributing the energy to a relatively large area. This energy input mechanism was noticed to cause some unique behavior in the melt pool. The moving laser spot was noticed to cause dynamic movement in the melt pool. The basic case with this movement in the melt pool was that small spot caused a small amount of material to vaporize and form a “dent” in the melt pool. When this “dent” moved along with the laser beam it caused movement in the melt pool. If the melt pool size was large the laser beam formed a small dent in the melt pool, which movement caused the melt pool to wave. On the other hand, if the melt pool was small and narrow the melt pool was more likely to swing from side to side.

Scanning amplitudes adjustments effect to the width of the clad bead was also studied and it was determined that clad beads width can be adjusted by adjusting scanning amplitude. The scanning amplitude defines not only the clad bead’s width but also the overall geometry of the clad bead. With wider scanning amplitude the clad bead is naturally wide and low, in some cases almost rectangular. Respectively, with a narrow scanning amplitude clad bead form can be almost parabola-shaped. However, the clad bead’s shape was naturally also dependent on the cladding speed, but the scanning amplitude determined the basic shape of the clad bead. Three of these clad bead basic shapes were found in this study. This means that when cladding with scanning optics there are more factors that determine the clad bead’s shape than in laser cladding with static optics.

There were some additional factors found that affected the clad bead’s dilution in this type of cladding process. At low cladding speed the melt pool grows larger and pushes forward to cladding direction, which in turn covers the laser beam area of interaction. In this way, the laser beam does not interact directly with the substrate material. On the other hand, when the cladding speed is higher the melt pool size reduces and draws back against the cladding direction. Therefore, when the melt pool does not cover the whole laser beam material interaction area, the laser can interact directly with the substrate material. Hence, when this high intensity laser spot can react directly with the substrate material the substrate melting increases significantly and thus dilution increases. This is the way how at low cladding speeds the melt pool can, in one sense, act as a “protective shield” for the substrate material against the high intensity laser beam.

The last thing observed was formation of defects on the clad bead. With certain parameter combinations the couple different types of defect were discovered, such as lack of fusion or undercuts. When the cladding speeds were low and the scanning amplitude was wide the melt pool grew too large causing overflow of the molten material to the sides of the melt pool (outside of laser beam material interaction area). When this occurs, there is not enough energy in the molten material to melt the substrate surface to create a fusion bond between the clad layer and substrate. This mechanism can create lack of fusion at the clad bead’s border

regions. Undercuts, on the other hand, were noticed as forming at higher cladding speeds. Then scanned laser beams formed small “dent” forces molten material away from the melt pool’s border region (border area is area where melt pool ends and solid material begins). Due to a faster cladding speed, the molten metal does not have enough time to fill out this small dent completely before the molten metal solidifies and undercut forms.

4.2 Publication 2

Laser cladding with scanning optics: The effect of power adjustment

The second publication concentrated on the importance and usage of the power adjustment of the scanner in laser cladding. Power adjustment in scanner based laser cladding has two functions. Firstly, it can be used to stabilize the cladding process. The oscillating scanners unadjusted heat input pattern is the so called viper teeth pattern, where the energy input is higher at the far ends of the scanning amplitude. This is caused by change in the direction of movement of scanning mirror, when the mirror velocity is decelerated, stopped and accelerated at end of scanning amplitude. This creates a situation of excessive energy input at scanning amplitudes far ends which in turn can cause instability (vaporization) at the melt pool edge areas. The laser beam was actually noticed to momentarily form a small keyhole at edge regions of the scanning amplitudes where laser beams direction of movement changes. As this keyhole formed vapor flow rise from it. This vapor formation disturbs the cladding process and increases the dilution at this edge region. Using power adjustment to decrease the laser power at the scanning amplitudes edge regions this excessive heat input can be avoided and the process stabilized.

Secondly, the scanner’s power adjustment can be used to increase the flexibility of the cladding process. It was shown that power adjustment can be used to affect the clad bead’s cross-section geometry. As the energy input is adjusted across the scan line, there are different amounts of energy to melt the additive material across the melt pool. So, through this mechanism the cross section geometry of the clad bead can be adjusted. Using this mechanism e.g. the side-angle of the clad bead can be adjusted or simple shapes can be built, as was shown in this publication.

4.3 Publication 3

Laser cladding with scanning optics: Effect of scanning frequency and laser beam power density on cladding process

Third publication concentrated on two matters that affect the stability of the melt pool: scanning frequency and intensity of the laser spot. With both of these matters excessive vaporization inside the melt pool was found when certain parameters were used. When

vaporization occurred in the melt pool a small shallow keyhole was found where the vapor flow rise. This vapor flow was noticed to be harmful to the quality of the clad bead. Vapor flow rising from the keyhole prevented the additive powder material from reaching the melt pool, which in turn directly affected the dilution as an increasing factor. As the additive material cannot reach the melt pool properly the laser beam is melting the substrate material and dilution increases. Also the small keyhole digs in to the substrate material further increasing the dilution.

Scanning frequency directly affects the interaction time of laser beam at a specific point. So it also determines how long the laser provides energy to the specific point, thus the scanning frequency determines the local energy input. It was noticed that using low, below 40 Hz, scanning frequency, a significant amount of vaporization occurred inside the melt pool, forming a keyhole. This keyhole then moved with the scanned beam from side to side. Furthermore, this keyhole was able to reach quite deep into the substrate material. When this phenomenon occurred the dilution rate increased significantly and the process started to resemble more laser alloying than laser cladding. When the scanning frequency was 40 Hz or more vaporization stopped completely and the process became stable. As the scanning frequency increases, it equalizes the heat input inside the laser beam material interaction area. Thus, when the local spikes in specific energy input decreases there is less possibility of vaporization. It was determined that when specific local energy input was higher than 2.42 J/mm^2 chance for material vaporization increased.

As the laser spots intensity determines how large “packages” energy is imported to this process, it affects highly to process stability. If the intensity is too high, vaporization can occur even though laser is scanned at high frequency (100 Hz as in this case). The high peak intensity of laser spot caused a small keyhole to form, which effectly ruins the clad quality (high dilution). When the focal point distance from process was increased (defocusing) and thus spot peak intensity was decreased, vaporization stopped and process became stable and dilution decreased. It was determined that peak intensity of 191 kW/cm^2 is low enough to ensure stable cladding process, at scanning frequency of 100 Hz. In turn peak intensities higher than this causes unstable cladding process.

4.4 Publication 4

Laser cladding using scanning optics – Effect of the powder feeding angle and gas flow on process stability

Forth publication concentrated on powder cloud behavior under the scanned laser beam and how the powder feeding angle and gas flow influence on the behavior of the powder cloud. When certain parameter combinations were used, the powder material was noticed to vaporize in the air when it encountered the laser beam. When this vaporization occurred, it created a sort of plume on top of the melt pool, which in turn started to emit light in the wavelength

range of visible light. The intensity of light emitted by the powder cloud was noticed to have direct correlation to the vaporization / plume size. As the measured emitted intensity increased, the vaporization increased correspondingly; if there was no vaporization in the powder cloud region, the measured emission was very low.

The powder cloud's stability was noticed to be dependent on three things, the powder feeding angle, the powder feeding gas flow rate, and the scanning amplitude. The powder cloud behavior was more stable at higher gas flow rate and scanning frequency and with powder feeding angles of 40 ° and 60 ° degrees. In turn 70 ° and 50 ° degree feeding angles caused significant instability to the powder cloud. The effect of the scanning frequency to stability is the same as in the melt pool case. The high frequency equalizes the local heat input and thus a more stable process is achieved. The effect of the gas flow came from its effect on the formed vapor. If vapor plume formed it was noticed to increase laser energy absorption in to the powder cloud. Thus the vapor acts as a self-reinforcing factor in the powder cloud's instability. When the gas flow rate was higher it blew the formed vapor away and through this mechanism stabilized the powder cloud.

The powder cloud's stability had a significant effect on the quality of the clad bead. When vaporization occurred in the powder cloud it significantly affects the powder material's access to the melt pool. Discharging vapor pushed the powder stream aside from its original flight track and thus the powder particles did not reach the melt pool. This was noticed when the clad beads deposited cross-section areas were compared. When even a slight amount of vaporization was noticed, the deposited cross-section area was decreased and correspondingly the dilution rates increased. This is because the energy of the laser beam is then diverted to melting the substrate material instead of the additive powder material.

5. Conclusions and recommendations

This thesis focused on how scanning optics can be used in laser cladding and what kind of advantages and disadvantages this type of optics brings to the process. This led in two main research directions: firstly how scanning optics can be used to modify the shape and geometry of the clad bead. For this matter the effect of the laser beam scanning amplitude and the scanner's power adjustment on the geometry of the clad bead were studied. Second studied matter was the effect of different parameters on process stability and dilution. From the process stability and dilution point of view of following matters were studied: the power adjustment, the scanning frequency, laser beams intensity, the power feeding angle, and the effect of the powder feeding gas flow. This work aimed to identify, how different process parameters affect the process and its outcome.

The following conclusions were obtained from this study:

1. Scanning optics enables a higher flexibility in the cladding process. When the scanner enables numerical control of both the scanning amplitude and scanned beams laser power, the geometry of clad bead can be numerically adjusted more freely. The clad bead's width follows well the width of the scanning amplitude, and, in turn, the clad bead's geometry follows the power adjustment in a reasonable manner. This enables more versatile usage of laser cladding, because numerical control permits tailoring the clad bead geometry. For example, by using the numerical adjustment of the scanning amplitude and the scanned beam's power control it is possible to decrease the overlapping ratio by modifying the clad bead's geometry. This can be done by creating clad bead with wide and flat middle section and edges with suitable side angle so that it is possible to decrease the overall overlapping ratio.
2. Power adjustment has an important part in stabilizing the melt pool behavior. As the oscillating mirror experiences dwell time at mirror's movement turning point it also causes excessive energy input at the borders of the scanned area. This energy input can be high enough to enable formation of small keyhole. It is really important that energy input is compensated with the power adjustment across the clad layer. Decreasing the laser power at the edge regions prevents keyhole formation at the melt pool edge areas, and thus the cladding process can be stabilized. When the oscillating scanner is in use the power control is not only used for adjusting the clad bead's geometry but is an important factor in making the process stable.
3. The importance of parameter selection increases when the laser cladding is done using scanner optics. This is due to the dual characteristics of the heat input in the cladding process. Even though the scanned laser beam imports energy to a large area and on average the intensity is relatively low but locally laser beam still has a high intensity. The local intensity peak sets limits to the scanning frequency and the

laser beam's spot size or intensity. High scanning frequencies evens out the unevenness of the energy input caused by this local high intensity. As it was determined that scanning frequency of 40 Hz was high enough to produce an even heat input so that melt pools behavior was stable. Then specific local energy input was at most 2.46 J/mm^2 . Respectfully, it was determined that too high an intensity can cause keyhole formation in the melt pool, even though high scanning frequency is used. It was determined that 191 kW/cm^2 peak intensity of laser beam is low enough to produce a stable process where no keyhole formation in the melt pool is seen (when power control is used). Because of these issues, it is important to use high enough scanning frequencies with an appropriate spot size to ensure that the cladding process remains stable.

4. Powder cloud is also prone to excessive vaporization under the scanned laser beam. A steep powder feeding angle, low feeding gas flow, and low scanning frequency can cause powder material vaporization in a powder cloud. However, with correct parameter selection this instability can be completely avoided and the process remains stable. Vapor formation can be observed by the light emitted by the vapor in the visible wavelength range. This occurs when the vapor absorbs energy from the laser, is overheated and emits some of it away as a visible light. By measuring the intensity of the powder cloud's emitted light in a wavelength range of 450 to 650 nm, the powder cloud's stability can be monitored. Stable behavior of the powder cloud can be ensured with correct parameter selection and monitoring the powder cloud emissions in the aforementioned wavelength range.
5. Cladding process stability has a significant effect on dilution of the clad bead. All instability in the cladding process increases the dilution. Stability affects the dilution in two ways: firstly, if a small keyhole is able to form in the melt pool, the laser beam is able to penetrate in to the substrate material. This naturally increases the melting of the substrate material and thus the dilution. Secondly, another mechanism increasing the dilution is the vapor formation, which causes a disturbance in the additive material feeding. When the laser beam vaporizes material, the vapor forms a flow which pushes the additive powder material past the melt pool. As the powder material cannot reach the melt pool the energy of laser beam is used to melting the substrate material and the dilution increases. This is why it is important to make a careful parameter selection and use process monitoring to ensure the stability of the cladding process, and thus a good quality clad
6. Melt pool behavior has a significant effect on dilution. Since the scanned beam has a relatively high local intensity, it is preferable that the laser beam has minimal direct contact with the substrate material. As it was noticed, when the laser beam has direct contact with the substrate material dilution levels increase. This matter suggests that using lower cladding speeds is to be recommended when cladding is

done using scanning optics. This is because at lower cladding speeds melt pool covers better the laser beam material interaction area and laser has less direct contact with the substrate material. Hence, the effect of cladding speed on the melt pool behavior must be taken into account when laser cladding is done using scanning optics with dynamic powder feeding.

7. Even though keyhole formation is undesirable in the laser cladding process, because it increases dilution, this phenomenon could be utilized in laser alloying. In laser alloying, deep penetration to the substrate material, wide treatment zone and homogenous mixing of alloying elements could be exploited. However, this matter would need further research.

References

- [1] D. Gross. 2013. Obama's speech highlights rise of 3-D printing, article [referenced 3.7.2013][available : <http://edition.cnn.com/2013/02/13/tech/innovation/obama-3d-printing>] CNN.
- [2] J. Archambeault and L. Dubourg. Scientific and technological landscape of laser cladding: a bibliometric analysis of patents and publications. Proceedings of the laser materials processing conference ICALEO, Oct. 31- Nov. 3, 2005, Hyatt Regency Miami, Miami, FL USA, pp.570-579
- [3] E. Toyserkani, A. Khajepour & S. Corbin. 2004. Laser Cladding. CRC Press. 280 p.
- [4] US 3952180 A . 1976. Cladding. Avco Everett Research Laboratory, Inc., Daniel S. Gnanamuthu. US 05/529,379, Filled Dec 4, 1974, Published Apr. 20, 1976.
- [5] V.M. Weerasinghe & W.M. Steen. Laser cladding with pneumatic powder delivery. Applied Laser Tooling, Martinus Nijhoff Publishers, Dordrecht 1987, pp. 183-211.
- [6] A. W. Hammeke. Laser spray nozzle and method. US Patent, No. 4724299, Apr 15, 1988
- [7] G. Hass. Filmed surfaces for reflecting Optics. Journal of the optical society of America, 1955, vol. 45, no. 11, pp. 945-952.
- [8] Optics.org.2012. IPG set to ship 100 kW laser. 1 November 2012. Article. [referenced 23.10.2013] [available : <http://optics.org/news/3/10/44>] Optics.org
- [9] Belmont, A. & Castagna, M.: Wear-resistance coatings by laser processing. Thin solid films, 1979, Vol. 64, Iss. 2, pp. 249-256.
- [10] Bruck, G. J.: High-Power Laser Beam Cladding. Journal of Metals, 1987, Vol. 39, Iss. 2, pp. 10-13
- [11] Arlt, A. G. 2009 User's Manual ILV DC-Scanner. ILV, Schwalbach. 16 p.
- [12] F. Klocke, C. Brecher, D. Heinen, C.-J. Rosen, and T. Breitbach, Flexible scanner-based laser surface treatment, Proceedings of the Laser Assisted Net shape Engineering 6 (LANE 2010) Conference, Physics Procedia, Vol. 5, Part A, 2010, pp. 467–475
- [13] F. Klocke, C. Brecher, M. Wegener, D. Heinen, B. Fischera & D. Do-Khac. Scanner-based Laser Cladding. Proceedings of the Laser Assisted Net shape Engineering 7 (LANE 2012), Physics Procedia, Vol. 39, 2012, pp 346–353.
- [14] J. Pekkarinen, V. Kujanpää and A. Salminen. Laser cladding with scanning optics: Effect of power adjustment. Journal of Laser Applications, 2012, Vol. 24, No. 3, 7 pp.

- [15] I.J. Pekkarinen, V. Kujanpää and A. Salminen. Laser cladding using scanning optics. *Journal of Laser Applications*, 2012, Vol. 24, No. 5, 9pp.
- [16] G. A. Turichin, E. V. Zemlyakov, E. Yu. Pozdeeva, J. Tuominen, and P. Vuoristo. Technological possibilities of laser cladding with the help of powerful fiber lasers, *Metal Science and Heat Treatment*, 2012, Vol. 54, no. 3-4, pp. 139-144.
- [17] J. Tuominen, J. Näkki, H. Pajukoski, T. Peltola, P. Vuoristo, M. Kuznetsov, and G. Turichin, Laser cladding with 15 kW fiber laser, *Proceedings of the 13th NOLAMP Conference in Trondheim, 27–29 June 2011 (Norwegian University of Science and Technology, Trondheim)*, p. 12.
- [18] R. A. Hella. *Material Processing With High Power Lasers*. *Optical Engineering*, 1978, Vol. 17 Iss. 3 pp. 198-201
- [19] D. S. Gnanamuthu. Laser Surface Treatment. *Optical Engineering*, 1980, Vol. 19, Iss. 5 pp. 783-792.
- [20] J. C. Ion. 2005. *Laser Processing of Engineering Materials: Principles, procedure and industrial applications*. Oxford, Elsevier Butterworth-Heinemann. 556pp.
- [21] E.M. Birger , G.V. Moskvitin , A.N. Polyakov & V.E. Arkhipov. Industrial laser cladding: current state and future. *Welding International*, 2009, Vol. 25, No. 3, pp. 234-243
- [22] USRE29815 E. Cladding. Avco Everett Research Laboratory, Inc. Daniel S. Gnanamuthu. US 05/806,924, Filled Jun. 15. 1977, Published Oct. 24.1978.
- [23] Laser cladding services. [image gallery] [retrieved 18.11.2013] From: <http://www.lasercladding.com/Gallery/>
- [24] Fraunhofer ILT. System Engineering for Powder-Based Laser Cladding. [Fraunhofer ILT www-page] [retrieved 18.11.2013] From: http://www.ilt.fraunhofer.de/en/publication-and-press/brochures/brochure_System_Engineering_for_Powder-Based_Laser_Cladding.html
- [25] Di N. Longfield, S. Lester, J. Griffiths, J. Cocker, C. Staudenmaier and G. Broadhead. 2013. Modifiche sulle superfici con l'impiego del laser cladding. *Applicazioni Laser*. [Web article] [retrieved 18.11.2013] From: <http://www.publitedonline.it/applicazioni-laser/contenuti/trattamenti/item/792-modifiche-sulle-superfici-con-l%E2%80%99impiego-del-laser-cladding>
- [26] Fraunhofer ILT. Powder Nozzle Technology - COAX 11 - Wide beam nozzle. [Fraunhofer ILT www-page] [retrieved 18.11.2013] From: http://www.ccl-laser.fraunhofer.org/en/products/coax_11.html
- [27] M.U. Islam, L. Xue, and G. McGregor, "Process for manufacturing or repairing turbine engine or compressor components," U.S. Patent Number 6269540, August 7 2001.

- [28] P.F. Jeantette, D.M Keicher, J.A. Romero, and L.P Schanwald, "Mutiple and system for producing complex-shape objects," U.S. Patent Number 6046426, April 2000.
- [29] I. Smurov. Laser cladding and laser assisted direct manufacturing. *Surface & Coatings Technology*, 2008, Vol. 202, Iss. 18, pp. 4496–4502
- [30] J. Tuominen, P. Hayhurst, V. Eronen, P. Vuoristo T. Mantyla. Comparison of multifeed and off-axis high-power diode laser (HPDL) cladding. *Proceedings of igh-Power Diode Laser Technology and Applications*, San Jose, CA, January 25, 2003.
- [31] E. M. R. Silva, W. A. Monteiro, W. Rossi & M. S. F. Lima. Absorption of Nd:YAG laser beam by metallic alloys. *Journal of materils science letters*, 2000, Vol 19, pp. 2095-2097
- [32] L. C. Nistor, S. V. Nistor, V. Teodorescu, Eva Cojocar, and 1. N. MihAilescu. Calorimetric absorption coefficient measurements using pulsed CO2 lasers. *Applied optics*, 1979. Vol. 18, No. 20, pp.3517-3521.
- [33] D. Bergström. The Absorption of Laser Light by Rough Metal Surfaces. Luleå, Luleå University of Technology Department of Applied Physics and Mechanical Engineering Division of Manufacturing Systems Engineering 2008:08. Doctoral thesis. 226 pp.
- [34] Y. Akiyama, H. Takada, M. Sasaki, H. Yuasa and N. Nishida. Efficient 10 kW diode-pumped Nd:YAG rod laser. *First International Symposium on High-Power Laser Macroprocessing*, 2003, *Proceedings of SPIE* Vol. 4831, pp. 96-100.
- [35] G. Treusch and T. Koening. 2008. HIGH-POWER DIODE LASERS: High-power diode lasers boost power-beaming competition. *Laser Focus World Magazine* [www- journal] [retrieved 27.7.2010] From: <http://www.optoiq.com/index/photronics-technologies-applications/lfw-display/lfw-article-display/322032/articles/laser-focus-world/volume-44/issue-3/features/high-power-diode-lasers-high-power-diode-lasers-boost-power-beaming-competition.html>
- [36] L. Quintino, A. Costa, R. Miranda, D. Yapp, V. Kumar, C.J. Kong. Welding with high power fiber lasers – A preliminary study. *Materials and Design*, 2007, iss 28, pp. 1231–1237
- [37] Laserline. 2013. Technical data LDF. [Technical data sheet] [retrieved 30.10.2013] From: <http://www.laserline.de/technical-data-ldf.html>
- [38] Laserline. 2013. Technical data LDM. [Technical data sheet] [retrieved 30.10.2013] From: <http://www.laserline.de/technical-data-ldm.html>
- [39] Trumpf lasers. 2013. TruDisc lasers Technical Data. [Technical data sheet] [retrieved 30.10.2013] From: <http://www.trumpf-laser.com/en/products/solid-state-lasers/disk-lasers/trudisk.html>

- [40] J. Hecht. 2012. FIBER LASERS: Fiber lasers: The state of the art. [article] Laser Focus World. [retrieved 30.10.2013] From: <http://www.laserfocusworld.com/articles/print/volume-48/issue-04/features/the-state-of-the-art.html>
- [41] IPG Photonics. 2013. Industrial fiber lasers for materials processing. [brochure] [retrieved 30.10.2013] From: http://www.ipgphotonics.com/Collateral/Documents/English-US/HP_Brochure.pdf
- [42] E. Stiles. 2010 Fiber Lasers: The Flexible Tool for High Power Laser Welding. [presentation] New Welding Technologies Conference, June 15-16, 2010, Fort Lauderdale, FL [retrieved 30.10.2013] From: <http://www.aws.org/conferences/newweldingtech/stiles.pdf>
- [43] S. Santhanakrishnan, F. Kong and R. Kovacevic. An experimentally based thermo-kinetic hardening model for high power direct diode laser cladding. Journal of Materials Processing Technology, 2011, Vol. 211, Iss. 7, pp. 1247-1259.
- [44] K. Parker. Advanced 8kW Direct Diode Laser Optimized for Large Area / High Deposition Rate Processing. [presentation] Laser Additive Manufacturing Workshop, February 29 - March 1, 2012, Houston, TX, [retrieved 1.1.2013] From: <http://d12d0wzn4zozj6.cloudfront.net/pdf/LAM2012%20Presentation%2021.pdf>
- [45] F. Brückner, D. Lepski and E. Beyer. Modeling the Influence of Process Parameters and Additional Heat Sources on Residual Stresses in Laser Cladding. Journal of Thermal Spray Technology, 2007, Vol. 16, Iss. 3, pp. 355-373.
- [46] US 4195913 A. 1980. Optical integration with screw supports. Spawr Optical Research, Inc., D. D. Dourte, R. L. Pierce and W. J. Spawr. US 05/849,932, Filled Nov. 9. 1977, Published Apr. 1. 1980.
- [47] Kugler GmbH. Integrator mirror. [Kugler GmbH web-page] [retrieved 18.11.2013] From: <http://www.kugler-precision.com/index.php?Integrator-mirror>
- [48] M. Blomqvist, S. Campbell, J. Latokartano and J. Tuominen. Multi-kW Laser Cladding using Cylindrical Collimators and Square-formed Fibers. SPIE Photonics West 2012 Event News and Photos, 21-26 January 2012, Moscone Center, San Francisco, CA, USA, [retrieved 18.11.2013] From: <http://www.optoskand.se/assets/Uploads/PDF/Artiklar/20120131-PW-Artikel-2012-Non-symmetric-collimator.pdf>
- [49] E.W. Reutzel. Laser Cladding and Laser Additive Manufacturing: Recent Developments. [presentation slides] Laserpinnoitustekniikan päivä Kokkolassa, Feb. 10. 2011, Kokkola, Finland
- [50] J. Tuominen. 2009. Engineering coatings by Laser Cladding – The Study of Wear and Corrosion Properties. Tampere, Tampere University of Technology, Doctoral thesis, Publication 845, Tampere University of Technology. 223 pp.

- [51] U. de Oliveira, V. Ocelík, J.Th.M De Hosson, Analysis of coaxial laser cladding process conditions. *Surface and Coating Technology*, 2005 Vol. 197, Iss. 2-3, pp. 127-136
- [52] K. Partes, T. Seefeld, G. Sepold and F. Vollertsen. Increased Efficiency in Laser Cladding by Optimization of Beam Intensity and Travel Speed, *Proceedings of Workshop on Laser Applications in Europe, Conference Volume 6157, Dresden, Germany, Nov. 23, 2005*, 11pp.
- [53] A. J. Pinkerton and L. Li. Modelling the geometry of a moving laser melt pool and deposition track via energy and mass balances. *Journal of Physics D: Applied Physics*, 2004, Vol. 37, No. 14, pp.1885-1895
- [54] A. F. H. Kaplan and G. Grobth. Process Analysis of Laser Beam Cladding. *Journal of Manufacturing Science and Engineering*, 2001, Vol. 123, Iss. 4, pp. 609-614
- [55] J. M. Pelletier, M. C. Sahour, M. Pilloz & A. B. Vannes. Influence of processing conditions on geometrical features of laser claddings obtained by powder injection. *Journal of material science*, 1993, iss. 28, pp. 5184-5188.
- [56] A. F. A. Hoadley and M. Rappaz. A thermal model of laser cladding by powder injection. *Metallurgical Transactions B*, 1992, Vol. 23, Iss. 5, pp. 631-642
- [57] M. Qian L. C. Lim, Z. D. Chen & W. L. Chen. Parametric Studies of Laser Cladding Processes. *Journal of Materials Processing Technology*, 1997, iss. 63 pp. 590-593
- [58] M. Picasso, C.F. Marsden, J.-D. Wangnière, A. Frenk & M. Rappaz. A Simple but Realistic Model for Laser Cladding. *Metallurgical and materials transactions B*, 1994, Vol. 25B, pp.281-291
- [59] L. Han, K. M. Phatak & F. W. Liou Modeling of laser cladding with powder injection. *Metallurgical and Materials Transactions B*, 2004. Vol. 35, Iss. 6, pp. 1139-1150
- [60] E. Toyserkani, A. Khajepour & S. Corbin. Tree-dimensional finite element modeling of laser cladding by powder injection: Effect of powder feedrate and traveling speed on the process. *Journal of laser applications*, 2003, vol. 15, no.3, pp. 153-160
- [61] M. Schneider.1998. LASER CLADDING WITH POWDER effect of some machining parameters on clad properties. Doctoral thesis, Thesis University of Twente, Enschede, Netherlands. 177p.
- [62] O. O. D. Neto & R. M. S. Vilar. Interaction between the laser beam and the powder jet in blown powder laser alloying and cladding. *Proceedings of the laser materials processing conference ICALEO'98, Part 2* , November 16-19, 1998, Sheraton World Resort Hotel, Orlando, FL. pp. 180-189.

- [63] Y-L. Huang, G-Y. Liang, J-Y. Su & J-G. Li. Interaction between laser beam and powder stream in the process of laser cladding with powder feeding. *Modelling and Simulation in Materials Science and Engineering*, 2005, vol. 13 no. 1, pp. 47-56.
- [64] C-Y. Liy & J. Lin. Thermal processes of a powder particle in coaxial laser cladding. *Optics & Laser Technology*, 2003, vol. 35, iss.2, pp. 81-86.
- [65] J. Lin. Temperature analysis of powder streams in coaxial laser cladding. *Optics & Laser Technology*. 1999, vol. 31, iss. 8, pp. 565-570
- [66] Y. Fu, A. Loredó, B. Martín & A.B Vannes. A theoretical model for laser and powder particles interaction during laser cladding. *Journal of materials processing technology*, 2002, vol. 128, iss. 1-3, pp. 106-112
- [67] W.-B. Li, H. Engström, J. Powell, Z. Tan & C. Magnusson. Redistribution of the beam power in laser cladding by powder injection. *Lasers in Engineering*, 1996, vol. 5, no. 3, pp. 175-183.
- [68] J. Lin. Laser attenuation of the focused powder streams in coaxial laser cladding. *Journal of Laser Applications*, 2000, vol. 12, Iss. 1, 28 p.
- [69] J. Lin. A Simple model of powder catchment in coaxial laser cladding. *Optics & Laser Technology*, 1999, Vol. 31, Iss. 3, pp. 233-238
- [70] C.F. Marsden, A. Frenk & J.-D. Wagnière. Power absorption during the laser cladding process. *European Conference on Laser Treatment of Materials (ECLAT'92)* (B.L.Mordike, ed.), D.G.M. Informationsgesellschaft, Adenauerallee 21 Oberursel, Germany, 1992, pp. 365-380.
- [71] M. Picasso, C.F. Marsden, J.-D. Wagnière, A. Frenk & M. Rappaz. A simple but realistic model for laser cladding. *Metallurgical and materials transactions B*, 1994, vol. 25B no. 2, pp. 281-291.
- [72] O.O. Diniz Neto & R. Vilar. Physical-computational model to describe the interaction between a laser beam and a powder jet in laser surface processing. *Journal of Laser Applications*, 2002, vol. 14, no. 1, pp.46-51
- [73] W.-B. Li, H. Engstrom, J. Powell, Z. Tan & C. Magnusson. Modeling of the laser cladding process - Pre-heating of the blown powder material. *Lasers in Engineering*, 1995, vol. 4 pp.329-341.
- [74] L. Sexton, S. Lavin, G. Byrne and A. Kennedy. Laser cladding of aerospace materials. *Journal of Materials Processing Technology*, 2002, Vol. 122, Iss. 1 pp. 63-68
- [75] J. M. Yellup.] Laser cladding using the powder blowing technique. *Surface and Coatings Technology*, 1995, Vol. 71, Iss. 2, pp. 121-128

- [76] J. Mazumder, A. Schifferer and J. Choi. Direct materials deposition: designed macro and microstructure. *Material Research Innovations*, 1999, Vol. 3, Iss. 3, pp. 118-131
- [77] M. R. Boddu, R. G. Landers and F. W. Liou. Control of Laser Cladding for Rapid Prototyping--a Review. *Proceedings of 12th Solid freeform fabrication symposium*, The University of Texas at Austin, Austin, Texas, 2001, pp. 460-467
- [78] E. Capello, D. Colombo and B. Previtali. Repairing of sintered tools using laser cladding by wire. *Journal of Materials Processing Technology*, 2005, Vol. 164-165, pp.990-1000
- [79] G. K. Lewis and E. Schlienger. Practical considerations and capabilities for laser assisted direct metal deposition. *Materials & Design*, 2000, Vol. 21, Iss. 4, pp. 417-423
- [80] A. Fathi, E. Toyserkani, A. Khajepour and M. Durali. Prediction of melt pool depth and dilution in laser powder deposition. *Journal of Physics D: Applied Physics*, 2006, Vol 39, No 12, pp.2613-2623
- [81] D.F. de Lange, J.T. Hofman and J. Meijer. Influence of intensity distribution on the melt pool and clad shape for laser cladding. *Proceedings of the Third International WLT-Conference on Lasers in Manufacturing LIM 2005 ; Munich, Germany, June 13th - 16th, 2005*. 5 pp.
- [82] J-D. Kim and Y Peng. Melt pool shape and dilution of laser cladding with wire feeding, *Journal of Materials Processing Technology*, 2000, Vol. 104, Iss. 3, pp. 284-293
- [83] Y. Huang. Characterization of dilution action in laser-induction hybrid cladding. *Optics & Laser Technology*, 2011 Vol. 43, Iss. 5 pp. 965-973
- [84] G. Zhao, C. Cho and J-D. Kim. Application of 3-D finite element method using Lagrangian formulation to dilution control in laser cladding process. *International Journal of Mechanical Sciences*, 2003 Vol. 45 Iss. 5, pp. 777-796
- [85] F. Vollertsen, K. Partes, G. Habedank and T. Seefeld. Deep penetration dispersing of aluminum with TiB₂ using a single mode fiber laser. *Production Engineering*, 2008, Vol. 2 Iss. 1, pp.27-32.
- [86] K. Zhang, W. Liu and X. Shang. Research on the processing experiments of laser metal deposition shaping. *Optics & Laser Technology*, 2007, Vol. 39, Iss.3, pp.549-557
- [87] Y. Huang & S. Yuan. Modeling the geometric formation and powder deposition mass in laser induction hybrid cladding. *Journal of Mechanical Science and Technology*, 2012, Vol. 26, Iss. 8, pp. 2347-2351
- [88] D. M. Goodarzi. 2012. Analysis the influence of process variables in laser cladding of the stainless steel 316L on the structural steel S355. Lappeenranta, Lappeenranta University of Technology. Master's Thesis. 147 pp.

- [89] J. Tuominen. Katsaus laserpinnoituksen kehityssuuntiin Suomessa (Innovations& Network–tutkimusohjelma/Trilaser-projekti) “Recent laser cladding developments in Finland (Innovations& Network–programme/Trilaser-project)”. [presentation slides] Presentation in Laserpinnoitustekniikan päivä, 10 February 2011, Kokkola, Finland
- [90] A. G. Arlt. Laser Welding: Line Scanners for Beam Shaping and Guiding. [presentation slides] Presentation in Joining in Car Body Engineering conference, 17 – 19 April 2012, Bad Nauheim, Germany.
- [91] De Castro, E. & Morandi, C. (1987) Registration of Translated and Rotated Images Using Finite Fourier Transforms, IEEE Transactions on pattern analysis and machine intelligence
- [92] Simon, D. (2006) Optimal State Estimation. John Wiley & Sons

PART II: THE PUBLICATIONS

PUBLICATION 1

Pekkarinen, I. J., Kujanpää, V. and Salminen, A. (2012)

LASER CLADDING USING SCANNING OPTICS

This paper has been published in the
Journal of Laser Applications, **24**,

Printed with permission

Laser cladding using scanning optics

I. J. Pekkarinen, V. Kujanpää, and A. Salminen

Laboratory of Laser Processing, Department of Mechanical Engineering, Lappeenranta University of Technology, Tuotantokatu 2, 53850 Lappeenranta, Finland

(Received 10 February 2012; accepted for publication 25 July 2012; published 16 August 2012)

Laser cladding using scanning optics is a relatively little studied matter. Scanning optics makes the adjustment of laser beam interaction zone numerically possible and it is, therefore, a more flexible optical tool than the conventional static optics. A series of cladding test were conducted using a 5 kW fiber laser and an oscillating linear scanner with dynamic powder feeding to determine the process characteristics and their possibilities and limitations. This study was carried out using 316L powder as an additive material and S355 mild steel plate as a substrate material. It was noticed that by using scanning optics, it is possible to vary the width and thickness of clad beads on a large scale. With scanning optics, it is possible to affect clad bead geometry so that only a 20% overlapping ratio is used. However, certain cladding parameter combinations expose the clad bead to cladding defects. Also, a fast moving scanned laser beam causes a wave formation to the melt pool which further causes stirring in the melt pool. Another studied matter was the effect of the cladding speed to dilution in laser cladding with scanning optics. The dilution was increased with increase in the cladding speed. However, the increase of the dilution was dependent on the scanning amplitude. © 2012 Laser Institute of America.

Key words: laser cladding, scanning optics, oscillating scanner

I. INTRODUCTION

Laser cladding is a process where coating material is melted on the surface of substrate material with laser beam. This is typically done for improving surface properties or repairing worn surfaces. There are a few variations of the basic principle of laser cladding process. The coating material can be preplaced prior to laser melting or additive material can be dynamically fed into the process during it. Cladding process with high brightness laser beam requires spreading of the laser beam using some optical solution. This can be done simply by just using defocusing or using specialized integrating optics. Another mean is using dynamic beam forming which typically refers to beam modifications with scanner optics. The earliest studies using scanning optics in laser cladding were reported in the late 1970s by Belmont and Castagna.¹ In late 1980s, Bruck² used scanning optics in his studies. Both of these studies were performed using preplaced powder. Even though laser cladding with scanning optics has been known more than 30 years, the subject is still relatively little studied. However, in recent years, the development in both laser and scanner technology has increased interest toward use of scanning optics in laser cladding. Cladding with scanning optics has been studied in recent years at least by Klocke *et al.*³ and Palmer.⁴ The difference from the previous studies was that in these studies, the additive material was fed directly to the process. In Klocke *et al.* study, the additive material was wire³ and in Palmer's study powder.⁴ In these studies, scanning optics was mainly used as an optical tool for expanding the laser beam interaction area. The study by Vollertsen *et al.*⁵ on alloying is one of the few where the effect of scanned beam on process dynamics

is studied in laser surface modification. There is quite little information available on changes of the cladding process when adopting scanning optics into use. Due to this, there is need of better understanding of the limits and opportunities of this type of cladding process.

The principle of the laser cladding process with dynamic powder feeding is relatively simple. Additive material is injected into the interaction zone of the laser beam, where the laser beam melts as much as possible the additive material and as little as possible the substrate material. When the laser beam moves forward, the melt left behind the interaction zone of the laser beam solidifies, forming a clad bead.⁶⁻⁸

For the laser cladding process, the power intensity (W/cm^2) of the laser beam plays a more important role than laser power. In laser cladding, the intensity of the laser beam has to be within certain limits in order for the process to work properly. With too low an intensity, the laser beam does not melt material sufficiently to form a dense clad bead.^{2,8,9} With too high an intensity, the laser beam melts too much substrate material, increasing the dilution, or it can even start to vaporize material when the process may become unstable.^{2,9,10} The task of the optics in laser cladding is to distribute the energy of the laser beam to the desired area by keeping the beam intensity appropriate for the process.¹¹

A linear scanner, a so-called 1D scanner, has the ability to move the beam in one direction. Linear scanner can be used in the same manner as a line integrating mirror for widening the interaction area of the laser beam. The scanner makes a small laser spot which is moved back and forth on top of the work piece, thus creating a wide area of influence for laser beam. Inside of this area influenced by the laser

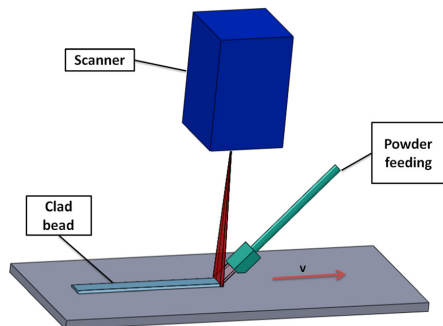


FIG. 1. Principle of cladding with scanning optics. The scanner spreads the laser beam to the desired width and the additive powder is fed to the melt pool generated by the laser.

beam, Fig. 2, the energy distribution is constantly changing since laser can only bring energy to one point at a time.^{9,11}

Laser cladding with scanning optics is otherwise mainly similar to laser cladding with static optics. The scanning amplitude along with the spot size gives the interaction area of the laser beam. Inside this area, the laser beam melts material, creating a melt pool, and in this melt pool, the additive material is injected (Fig. 1). Figure 2 presents the terminology and parameters of scanner based laser claddings. The difference from cladding with static optics is that the interaction area of the laser beam can be adjusted numerically by adjusting the scanning amplitude.

A. Overlapping

Overlapping is an important factor when large areas need to be coated. When laser cladding is used to cover large surfaces, clad beads need to be overlap with each other to get a uniform clad layer. The shape of the clad bead has a remarkable influence on the overall efficiency of the process. Traditionally, in order to get a flat surface, the clad layers must overlap with each other by 60%–70%.¹³ This means that on an average 2/3 of a new clad bead goes on top of an old one and only 1/3 of the width of a new clad increases the overall width of the clad layer. The need for such a large overlapping comes from the cross-sectional profile of the “normal” clad bead. Commonly, the clad bead is a convex shaped due to static beam forming via the use of de-focus, and because of this shape, the clad beads need to overlap so much with each other in order to create a flat clad layer.^{12–14}

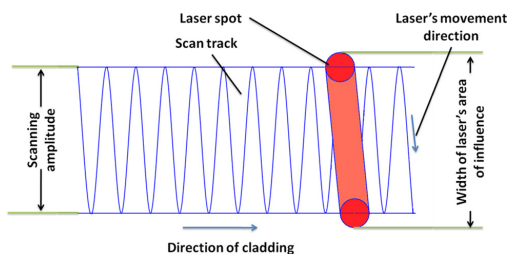


FIG. 2. Terminology and parameters in laser cladding with scanning optics.

The quality of the overall clad layer is highly dependent on the geometry of a single clad bead. In order to produce a defect free clad layer consisting of several layers beside each other, the side angle of the clad bead should be more than 120°. If the side angle is significantly smaller than 120°, the chance for trapping impurities or forming joint defects or pores between clad beads is increased.^{2,6}

B. Dilution

It is important that a certain amount of substrate material is melted during the cladding process. This enables the metallurgical bond between the clad bead and substrate material. However, the melting of the substrate material dilutes the composition of the additive material.^{8,9,12,15} Dilution is highly dependent on the cladding process parameters, laser power, additive feed rate, and cladding speed.^{2,16–18} The effect of laser power on dilution can be understood through specific energy input.

$$\text{Specific energy input [J/mm}^2\text{]} = \frac{\text{laser power [W]}}{\text{beam width [mm]} \times \text{cladding speed [mm/s]}}$$

Specific energy input determines how much material laser can melt per square millimeter. If the additive material is not able to absorb most of this energy, the excessive energy is used to melting the substrate material and dilution increases.^{2,19}

In dilution point of view, the task of additive feeding in the cladding process is to ensure that there is enough additive material for a certain laser power to absorb most of the laser energy and to prevent the excessive melting of substrate material. If powder feeding rate is insufficient in contrast to other cladding parameters, the substrate material melts excessively.^{16,17} A study by Pelletier *et al.*¹⁶ showed that an increase in the powder feeding rate decreases dilution when other cladding parameters remain constant. This is due to two factors: first, there is more material for the laser to melt when the feed rate is higher. Second, increasing the feed rate turns the powder cloud, created by powder feeding, more opaque. This how less laser light get's directly contact with the substrate material.^{2,16,20}

The influence of the cladding speed on dilution is twofolded. On one hand, an increase in the cladding speed decreases the specific energy input. In consequence, there is less energy to melt material and therefore, an increase in cladding speed can decrease the dilution. This was concluded in a study conducted by Zhao *et al.*¹⁹ On the other hand, in this case, the power feeding rate must be high enough to ensure sufficient powder feeding also at high cladding speeds. Studies by Qian *et al.*¹⁷ and Fathi *et al.*²¹ concluded the opposite observation compared to Zhao *et al.*¹⁹ The two former studies argued that the dilution increases when the cladding speed increases. An increase in dilution with an increase in cladding speed is connected to the powder feeding and growth of the melt pool. An increase in dilution is a result of less powder volume fed per unit length when the cladding speed is increased.¹⁷ Low cladding speeds enable

the melt pool to grow sufficiently for the melt pool to work as a protective shield against the laser light. An increasing cladding speed decreases the melt pool size and the laser light can interact better with the substrate material.²¹

C. Motivation of this work

Laser cladding with scanning optics has some unique characteristics that make the end result and the process different from traditional laser cladding. This study attempts to clarify the possibilities and special features of this type of cladding process. The study can be divided into three sections. First, this study focuses on explaining how the scanning optics can be used to create different types of clad bead geometries and how the geometry of the clad bead is dependent on cladding and scanning parameters. Second, this study aims to explain how the use of scanning optics in laser cladding changes the process dynamics and behavior of the melt pool. The third focus area is defects in clad bead and dilution and the mechanisms behind them.

II. EXPERIMENTAL PROCEDURE

The experimental setup can be divided into four branches: laser equipment, powder delivery, scanner, and process imaging. The laser equipment consists of IPG 5 kW multimode fiber laser, beam parameter product of 4.6 mm mrad. The working fiber diameter used was 150 μm. The focal length of the collimation lens was 150 mm and the focal length of the focusing lens was 500 mm. The focusing optics used was a Precitec YW50 welding head. The position of the focal point was placed 60 mm above the top surface of the substrate. The laser beam diameter on work piece with this setup was 2.43 mm, average intensity being 369 W/mm², and local peak intensity inside laser spot being 1920 W/mm² on top of work piece. These values were measured using Primes FocusMonitor. The substrate material was 6 mm thick S355 structural steel of company Rautaruukki. The laser beam was moved by a numerically controlled X-Y portal robot. The cladding speed (speed in direction of cladding) was varied from 1.67 to 8.3 mm/s.

Powder feeding was off-axis using pneumatic powder delivery, where powder is injected straight into the melt pool. The powder feeding machine was a Plasma-Technik Twin-System 10-C powder feeder and with argon as the carrying gas. Three different size powder feeding nozzle were designed and used such that the width of the powder feeding matched with the scanning width. The powder feeding angle was 40° and the additive powder mass flow rate was kept constant in all tests at a level of 0.5 g/s. The additive powder was AISI 316L stainless steel with a particle size between 53 and 150 μm.

Scanning optics was used to distribute the laser beam to the desired area. Scanner is located between the collimator and focusing lens. An ILV DC linear scanner was used in this study. The scanner includes features for laser power adjustment. This scanner works in oscillating principle so that the scanning mirror oscillates from side to side in the desired frequency. When forward movement of process is taken into account, scanned beam forms one sort of sinusoidal wave on

top of work piece. This enables adjusting the laser power in 32 points along the scan track. Figure 3(a) presents how these 32 adjustment points are located in the sinusoidal wave. In this study, the power was adjusted such that a cross-section diagram of the laser power distribution is formed as presented in Fig. 3(b). The laser power was set so that 100% in the power adjustment diagram means 5 kW. The power was adjusted in order to avoid energy build-up in the turning points of scanning at the edge of clad layer by the dwell time at the end of each scan. Due to the power adjustment, the average laser power input is 74% of the maximum laser power or 3.7 kW in this test series when the maximum laser power was 5 kW. Three different scanning amplitudes were tested in order to see how the shape of the clad bead changes according to the scanning amplitude. The tested amplitudes were 3.1, 9.6, and 17.5 mm. In all tests, the scanning frequency was 100 Hz.

The analysis of the melt pool behavior was based on video imaging of the process. It was carried out using a CCD video camera with Cavilux laser illumination by the company Cavitar Oy. Laser illumination combined with optical filtering enables a clear video image from the melt pool regardless of the bright illumination of the process. The

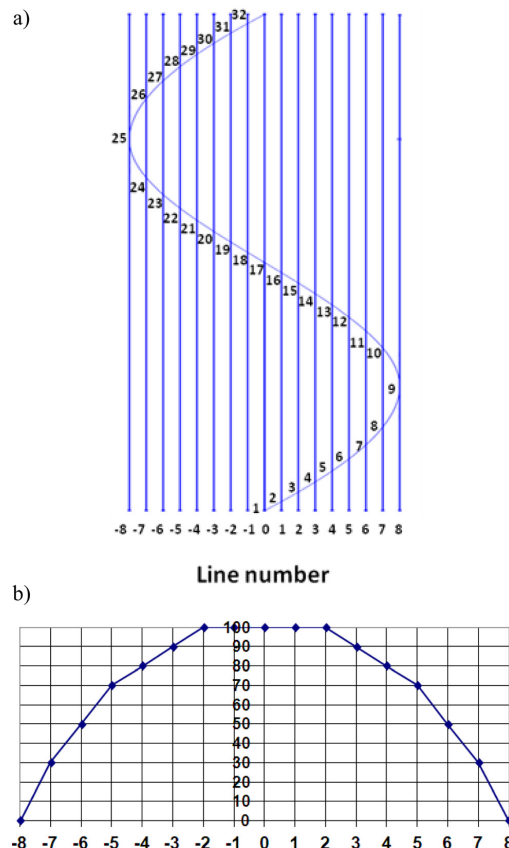


FIG. 3. Power adjustment points placed in a sinusoidal wave (a) and the power adjustment diagram created by 32 adjustment points (b).

frame speed of the video image was 20–25 fps. The other analyzing method was metallographic cross-section images from the clad bead. From these images, it was possible to measure the thickness of the clad bead, the width and the angle between the substrate material surface (clad bead side angle) and the clad bead wall tangent, and to calculate the geometrical dilution degree of the clad bead. The thickness of the clad bead was measured in the middle of clad bead. These measurements were performed with a program of Carl Zeiss AxioVision.

III. RESULTS AND DISCUSSION

A. Shape of clad bead

The most considerable advantage of scanning optics is the possibility to adjust the interaction area of the laser beam numerically by adjusting the scanning amplitude. Numerical control gives more freedom to adjust the interaction area of the laser beam compared to the static optics. This how it is possible to clad a large range of different width clad beads using the same optical setup.

Three different basic geometries were found for a clad bead, shown in Fig. 4. These geometries are highly dependent on the scanning amplitude and the cladding speed. It was also noticed that it is important to match the width of the powder feed to the interaction area of the laser beam in order for the process to work properly. Too wide a powder feed results in powder loss and the clad bead is not build up properly. Correspondingly, too narrow powder feed increases the possibility to undercut formation.

Using wide scanning amplitude, 17.5 mm, and low cladding speed, 1.67 mm/s, the clad bead obtains a rectangular shape [Fig. 4(a)]. With these parameters, the width of the clad bead was 19 mm and the thickness was 1 mm. By increasing the cladding speed to 3.33 mm/s and by reducing the scanning amplitude to 9.6 mm, the thickness of the clad bead grows to 1.3 mm and the width decreases to 13 mm. Simultaneously, the form of the clad bead changes from rectangular to convex at the edges, but the middle section of clad bead remains flat [Fig. 4(b)]. By decreasing the scanning amplitude further to 3.1 mm, the walls of the clad bead turn to a relatively vertical position but the top section of the clad bead curves to a convex shape [Fig. 4(c)]. The dimensions of the clad bead were then 2.8 mm thickness and 5.3 mm width.

The scanning amplitude determines the width and basic geometry of the clad bead, and the cladding speed determines the height and bead side angle of the clad bead. Figure 5 presents the height and the bead side angle of the clad bead according to cladding speed. It is common knowledge that the thickness of the clad bead is highly dependent on the cladding speed. The increase of the cladding speed decreases the

height of the clad bead and at the same time the clad bead side angle is increased. These two factors are connected to each other: when the clad bead thickness decreases, the clad bead side angle does not increase as steeply as with a thicker clad bead height. The clad bead width can vary significantly when using a scanner in laser cladding. This is one of the main difference from cladding using static optics compared with cladding with scanning optics. Scanning amplitude also effects on how much the shape of the clad bead is altered when the cladding speed changes. Scanning amplitude affects how drastically the side angle of the clad bead is increased when the cladding speed is increased, as can be seen in Fig. 5. Scanning amplitude of 3.1 mm enables the clad bead to grow noticeably thicker; hence the same amount of additive material is added to a narrower surface area. Therefore, the clad bead holds its shape better and clad beads side angle does not grow as swiftly as with longer scanning amplitudes, 9.6 mm or 17.5 mm.

The basic geometry of the clad bead changes visibly with the change of the scanning amplitude and the change of cladding speed. For short scanning amplitude, 3.1 mm, the clad bead height decreases quite linearly and the clad bead holds its overall shape fairly well when cladding speed is increased. The main difference between the speeds of 3.3 mm/s and 5.0 or 8.3 mm/s is that the vertical part of the clad bead does not form and only the convex top part remains. Correspondingly, by using long scanning amplitude, 17.5 mm, the cladding speed increases from 1.67 mm/s to 3.3 or 5.0 mm/s makes the clad bead height decreases rapidly. This makes the clad bead relatively shallow, in which case the clad bead geometry turns from rectangular to a shallow convex shape. By using a medium scanning amplitude length, 9.6 mm, the clad bead holds the shape presented in Fig. 4(b). Only the height is decreased and the clad bead side angle is changed when the cladding speed is increased from 3.3 mm/s. However, if the cladding speed is decreased from 3.3 to 1.7 mm/s, the clad bead obtains a geometry which is completely different. Then, the clad bead crows to a convex, almost semicircular shape. This is due to the fact that the melt pool has grown large enough that the surface tension of the molten material can pull it to this shape.

When laser cladding is carried out by using scanning optics, the clad bead geometry is dependent on more factors than laser cladding carried out by static optics. The clad bead geometry is mainly dependent on powder feeding, cladding speed, laser power, and spot size when cladding is performed using static optics. On the other hand, when using scanning optics, many new variables affect how the clad bead geometry forms, as previously was shown. It must be considered that the clad bead geometry changes along with the scanning amplitude when cladding parameters are chosen.

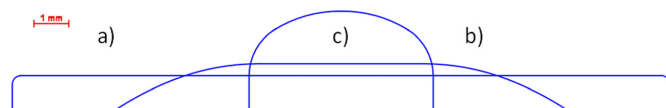


FIG. 4. The dependence of the geometry of a clad bead cross-section on scanning amplitude. (a) $A = 17.5$ mm and $v = 1.67$ mm/s; (b) $A = 9.6$ mm and $v = 3.33$ mm/s; and (c) $A = 3.1$ mm and $v = 3.33$ mm/s.

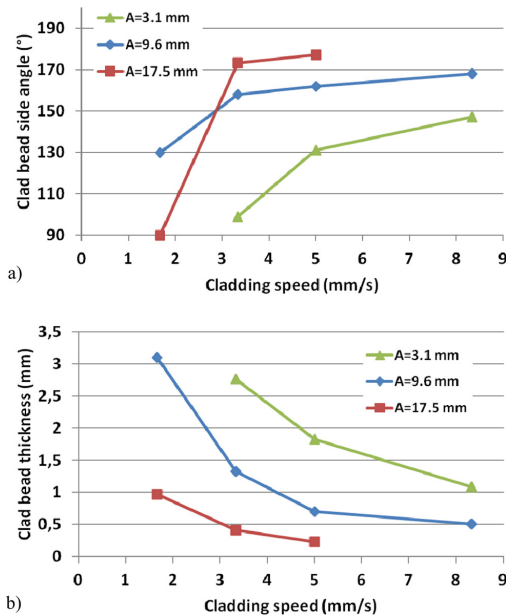


FIG. 5. Dependence of (a) the clad bead side angle and (b) the clad bead thickness on the cladding speed.

B. Overlapping

Scanning optics can be used to increase the overall efficiency of cladding process. An increase in cladding efficiency can be achieved by eliminating the need for a high overlapping ratio. This can be done by designing the clad bead to include a flat middle part, which constructs a new clad layer, and edge areas that have the desired bead side angles for defect free overlapping. Then, overlapping is only required between the edge areas of the clad bead. These types of clad beads can be created using scanning optics, as previously shown in Fig. 3(b).

With scanning amplitude of 9.6 mm, it was possible to create a clad bead that has a flat middle section and a bead side angle of more than 120°, which is desirable. The tests showed that for these types of clad beads, the overlapping ratio of 20% was enough to produce a flat and uniform clad layer. Between the clad beads, there were minimum gaps or discontinuity points. An increase of the overlapping ratio from 20% to 30% creates a large number of intersection points between the first and the second clad bead. Then, the edge of the second clad bead rises on the top of the flat middle section of the first clad beads. A decrease in the overlapping ratio to 10% creates a dent between the clad beads because the second clad bead is too far away from the first one.

C. Behavior of the melt pool

The main difference between cladding with scanning optics and with static optics can be found in the energy distribution of the laser interaction area on top of the work piece. Static optics distributes the laser’s energy in such a way

that the laser energy distribution stays constant across the laser interaction area. With static optics, the laser interaction area can be called the laser spot. However, with scanning optics, the concepts of laser spot and laser interaction area must be separated.

With scanning optics, a relatively small laser spot moves rapidly back and forth, creating a larger interaction area between the laser beam and material. This fundamental difference appears when the power densities of a laser spot in these two types of optical systems are compared. A large spot of static optics has a relatively small power density, while a laser spot of scanning optics has a relatively high local power density. However, in static optics, the spot stays still while the laser spot of scanned optics moves rapidly back and forth, spreading out the energy of the laser beam in a large area. Within this area, the average power density is again relatively small, comparable to that one off static optics. Nevertheless, this rapidly moving small spot, the power density of which is high, creates some unique features to the cladding process.

The moving laser spot of scanned optics creates horizontal waves in the melt pool. The small, rapidly moving laser spot vaporizes small quantities of metal, creating a “dent” in the melt pool [Fig. 6(a)], and the movement of the dent creates waviness. Figure 6(a) is one frame from the video that was recorded in the melt pool of the cladding process. The dent is formed in the melt pool when small amount of vaporized material erupts, creating a force directed to the melt pool [Fig. 6(b)]. At the same time, it must be noticed that even though laser is directed at one small area at a time, the laser beam moves fast enough to keep the melt pool in melted state for width of the scanning amplitude in most cases. This represents well the two-folded nature of the laser

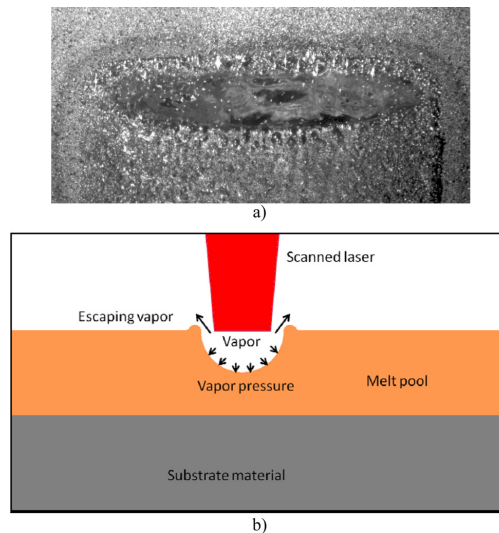


FIG. 6. (a) Melt pool behavior under the scanned beam. $f=100$ Hz, $A=17.47$ mm, $P_{max}=5$ kW, $v=1.67$ mm/s, used power adjustment diagram, see Fig. 3(a). (b) Free body diagram of how escaping vapors create a dent in the melt pool.

interaction zone created by scanning optics: on one hand, the spot intensity is high enough to create a dent in the melt pool, but on the other hand, the spot moves fast enough to distribute the laser energy evenly so that the melt pool stays molten along the full scanning amplitude.

The cladding speed and scanning amplitude have a significant effect on how the melt waves during the process. In the scanning system used, the traveling speed of the scanning beam spot across the melt pool is dependent on the scanning amplitude. Naturally when scanning frequency is constant, also the time that laser spot travels length of the amplitude is constant. In such cases, the amplitude determines the traveling speed of the laser beam across the melt pool. An increase in the scanning amplitude increases the number and size of waves. Correspondingly, with a short scanning amplitude, the melt pool rather swings from side to side or pulse instead of waving. This is a result of melt pool becoming narrower. When laser beam is directed in either aside of melt pool, force of escaping vapor pushes molten material to the other side of melt pool. Respectively, when laser is directed to the middle of melt pool, vapor pressure pushes molten material away from the middle of melt pool. This mechanism makes melt pool motion looking like swinging or pulsing when scanning amplitude is short, e.g., 3.1 mm. In Fig. 10, it can be seen that the melt pool is quite smooth with a short scanning amplitude, but the melt pool surface is rippled with a wide scanning amplitude.

Since the cladding speed affects the melt pool size, it also affects the melt pool behavior. When cladding speeds are low, the laser beam crates a larger wave which moves back and forth along with the scanned laser beam. This is because there is a larger amount of molten material in which this wave can form. When the cladding speed increases, the melt pool grows shallower and an equivalent larger wave cannot form. Consequently, the melt pool surface rather ripples than waves.

The cladding speed also affects the way the melt pool stays molten during scanning cycle. With long scanning amplitude and a high cladding speed, the melt pool can start to solidify partially. With scanning amplitude of 17.5 mm and a cladding speed of 5 mm/s was used, partial solidification during cladding was observed. In this case, the specific energy input of the scanned beam is not high enough to keep the melt pool completely molten state while new additive material is injected into it. This type of partial solidification was not discovered in any other combination of cladding parameters in this study. The scanned beam is able to keep the melt pool open if the cladding speed is adapted to the scanning amplitude.

The back-and-forth movement of the laser beam causes a stirring motion in the melt pool which can mix the melted substrate material with the melted additive material and, therefore, dilute the clad material. Preliminary tests have shown that with certain scanning parameter combinations, the melt pool is strongly mixed, creating metallurgically a relatively homogenous structure. Even in a micro image (Fig. 7), two types of solidification structures can be seen, primary ferritic (F-A solidification) on the right and primary austenitic (A-F solidification) on the left, which is supposed

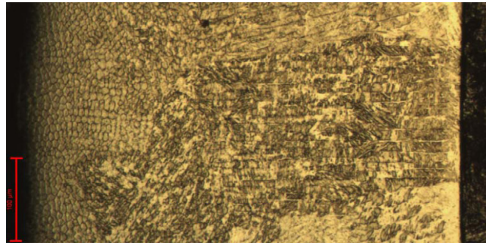


FIG. 7. Clad bead microstructure. A clad with 17.5 mm scanning amplitude and 33 mm/s cladding speed, geometrical dilution 34%.

to indicate the uneven mixing of alloying elements, especially of chromium and nickel. This is because the solidification mode is dependent on two issues: the solidification rate and the composition of steel, the Cr/Ni equivalent ratio. The solidification rate can be considered relatively even through the entire clad bead. Therefore, in this case, the difference in the solidification mode is mainly dependent on the Cr/Ni equivalent ratio. However, an energy-dispersive x-ray spectroscopy (EDS) analysis showed that the alloying elements were divided relatively evenly. Nevertheless, this matter needs further study to determine the dependence of mixing on the parameters.

D. Defects in clad bead

Certain cladding-scanning parameter combinations are likely to produce defects on a clad bead, such as a lack of fusion between the clad bead and substrate material and undercuts on the edges of clad beads. With long scanning amplitude and a slow cladding speed, the melt pool tends to grow slightly wider than the width of the laser interaction zone. This is due to the growth of the melt pool, which causes the molten metal to push to the surrounding area. Because this melted metal does not have enough energy to melt the substrate material below it and it is out of the interaction zone of the laser beam, a lack of fusion may form between the edge of the clad bead and substrate. In this study, lack-of-fusion defects were found in one sample. In that case, the clad was done using a cladding speed of 1.67 mm/s and scanning amplitude of 17.5 mm [Fig. 8(a)]. A lack of fusion can be seen on both sides of the clad bead.

An undercut is formed more typically when the cladding speed is high and when the forces caused by the vaporizing material push the melted material away, creating a small dent in the melt pool at the turning point of scanning. The mechanism is shown in Fig. 6(b). Due to a faster cladding speed, the molten metal does not have enough time to fill out this small dent completely before the molten metal solidifies. At a lower cladding speed, this does not seem to be a problem because the molten metal has more time to fill up the dent and the volume of molten material is high enough to fill it up. Additionally, when the melt pool grows larger, it shields the substrate material against the laser beam. If these types of dents are formed, they form in the added layer and do not dig into the substrate material or dilute the composition of the

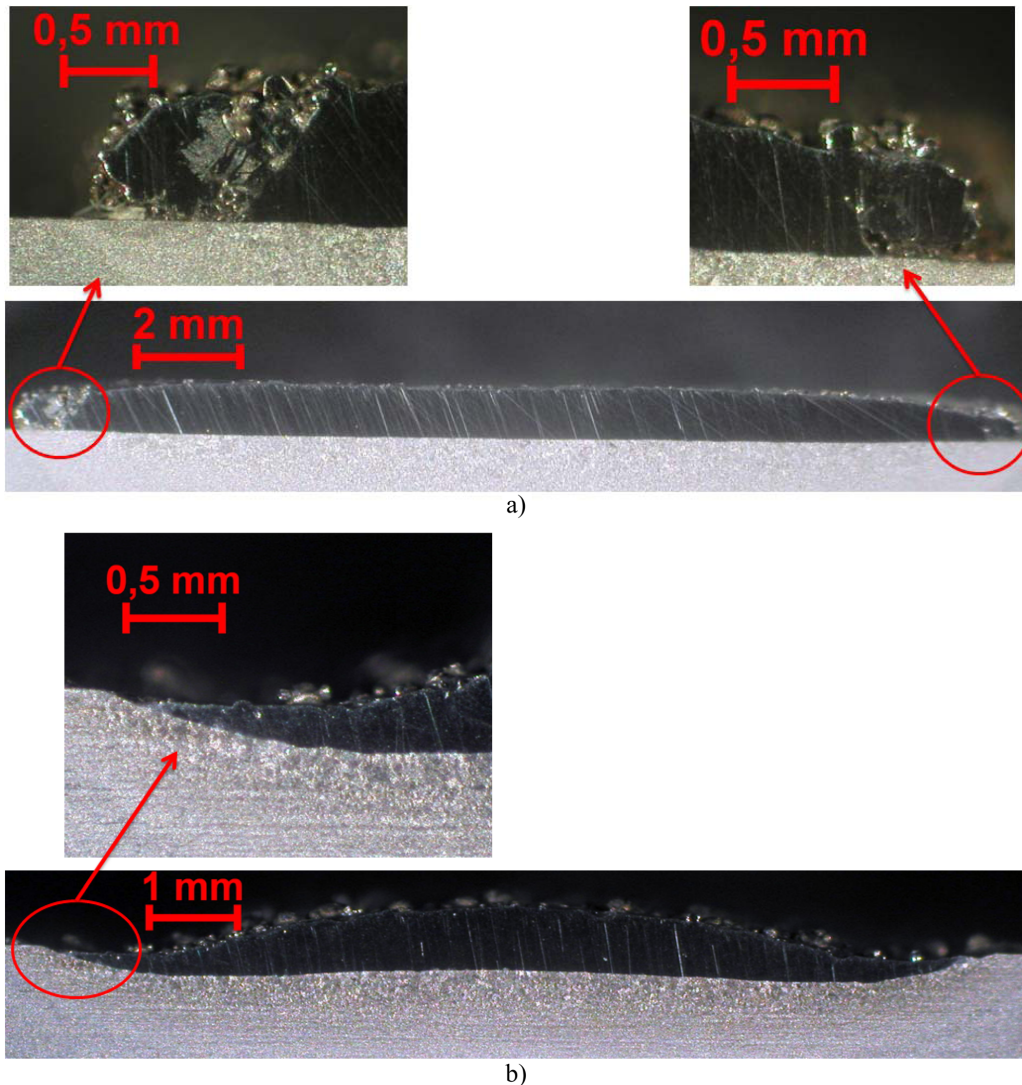


FIG. 8. Defects formed in clad beads: (a) lack of fusion and (b) undercut.

clad. Undercuts were found in the clad surface with scanning amplitude of 9.6 mm at a cladding speed of 8.33 mm/s [Fig. 8(b)]. Undercuts can be seen in Fig. 8(b) on the left side of the clad bead.

E. Dilution

The degree of dilution with an increase in cladding speed depends on the scanning amplitude (Fig. 9). At short scanning amplitudes, the dilution is increased more slowly than at long scanning amplitudes. This is a result of two factors: the cover effect of powder feeding and the thickness of the melt pool. With short cladding amplitude, the powder feeding width is also narrower when the powder cloud is

more opaque. The opacity growth is caused by the fact that same amount powder goes through narrower nozzle. In such cases, the powder cloud can work better as a protective shield for the substrate material against the laser light and protect the substrate material from excessive melting. These results are aligned with the results of Pelletier *et al.*¹⁶ and Huang *et al.*²⁰ studies on how powder stream density effects on laser power attenuation in powder stream. They concluded that denser powder stream absorbs more laser light.

Melt pools thickness effect on dilution shows well when short and long scanning amplitudes melt pool behavior are compared. With short scanning amplitude, the formed melt pool is narrower but thicker. A thick melt pool on top of the substrate is pushed forward, creating a cover for the substrate

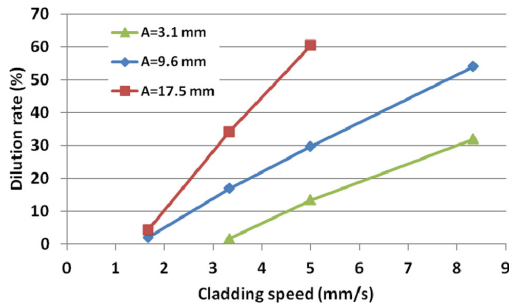
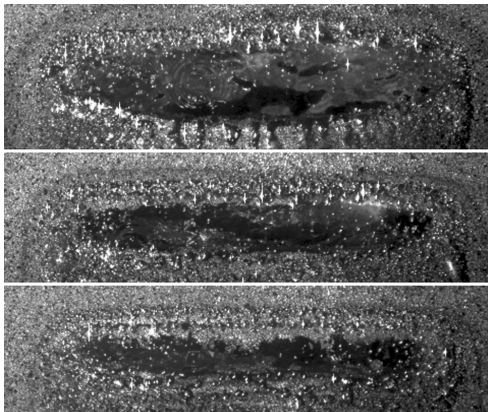
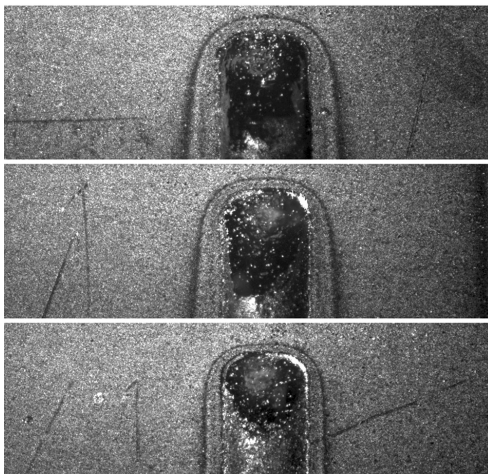


FIG. 9. Dependence of dilution of clad bead on cladding speed with different scanning amplitudes.



(a)



(b)

FIG. 10. Change in the melt pool geometry with cladding speed and scanning amplitude. (a) Amplitude 17.5 mm and cladding speeds from top to bottom 1.67, 3.33, and 5 mm/s. (b) Amplitude 3.1 mm and cladding speeds from top to bottom 3.33, 5, and 8.33 mm/s.

material. With short scanning amplitude, the cover effect is reduced since the cladding speed is increased, but the melt pool is still pushed forward to cover the substrate material against the laser light. Figure 10 shows how the melt pool is pulled back when the cladding speed is increased. By comparing Figs. 10(a) and 10(b), it can be seen that when the scanning amplitude is longer, the melt pool is narrower and the laser light hits the substrate material directly, but when the scanning amplitude is shorter, the laser only hits the melt pool. The laser beam in these pictures is pale white.

With long scanning amplitude, the melt pool is shallow. Therefore, an increase in the cladding speed affects the dilution more than with short scanning amplitude. Increase of cladding speed with long scanning amplitude, the substrate material under the front end of the melt pool is revealed. In consequence, the front end of the laser beam spot interacts directly with the substrate material. Meanwhile, the melt pool interacts with the back end of the laser spot. The front end of the laser spot directly melts the substrate material, and this can increase the dilution dramatically. These results are in line with Qian *et al.*¹⁷ and Fathi *et al.*²¹ observation of dilutions increase with increase of cladding speed.

As mentioned above, the thickness of the clad bead is rapidly decreased and the dilution is increased when the cladding speed is increased. Therefore, it can be argued that at high cladding speeds with long scanning amplitudes, the process starts to resemble more laser alloying than laser cladding. However, it must be remembered that in this study, the powder feeding rate was kept constant. By increasing the powder feeding rate, the thickness of the clad bead could be increased and at the same time excessive dilution could be prevented.

IV. CONCLUSIONS

Using scanning optics in laser cladding creates some advantages compared to laser cladding with static optics. Scanning optics creates flexibility to adjust the shape and size of a clad bead by adjusting the cladding speed and scanning amplitude numerically. Consequently, it is possible to manufacture the geometry of the clad bead according to the need and not only to what is possible. Laser cladding flexibility enables making such a clad bead that the overlapping ratio can be reduced. Therefore, it is possible to increase the overall efficiency of laser cladding when large surfaces are clad and high laser power is available.

A laser beam moving rapidly back and forth creates a unique characteristic for the melt pool behavior. As shown in this paper, the laser beam can create pressure on the melt pool and the rapid back-and-forth movement of the laser beam can create waves in the melt pool. This stirs the melt pool and creates a relatively metallurgically homogenous clad bead even if the dilution is high.

In certain cases, either the movement of the melt pool or the growth of the melt pool may create defects in the clad bead: undercuts or a lack of fusion. Undercuts can form when the cladding speed is high and the melted metal is not able to fill up the dent created by the laser beam in the scanning's turning area (melt pool's border region). Respectively, a lack

of fusion may occur when the melt pool becomes wider than laser beams area of influence. This is most likely happen when cladding speed is low and melt pool is thereby large.

The dilution of the clad bead is highly dependent on the cladding speed and the scanning amplitude. The dilution decreases along with the decrease of the cladding speed because the melt pool becomes large enough to act as a protective shield for the substrate material against laser light. An increase in cladding speed reveals the substrate material under the melt pool, and the front end of the laser beam spot has direct contact with the substrate material. This mechanism increases the dilution. It is also concluded that dilution increase with cladding speed is highly dependent on scanning amplitude. Short scanning amplitude creates more easily higher clad beads and the melt pool is pushed further forward. Consequently, the melt pool better shields the substrate material from the effect of the laser beam.

ACKNOWLEDGMENTS

The authors wish to express their gratitude to the Regional Council of Päijät-Häme and the European Regional Development Fund for funding the research.

¹A. Belmont and M. Castagna, "Wear-resistance coatings by laser processing," *Thin Solid Films* **64**(2), 249–256 (1979).

²G. J. Bruck, "High-power laser beam cladding," *J. Met.* **39**, 10–13 (1987).

³F. Klocke, C. Brecher, D. Heinen, C.-J. Rosen, and T. Breitbach, "Flexible scanner-based laser surface treatment," in Proceedings of the LANE 2010 Conference [Phys. Procedia **5**(Part 1), 467–475 (2010)].

⁴T. A. Palmer, "Implementation of laser cladding for Virginia class submarine main propulsion shaft repair," in *CTMA 2010 Symposium, MCB Quantico, VA*, 22–24, March 2010.

⁵F. Vollertsen, K. Partes, G. Habedank, and T. Seefeld, "Deep penetration dispersing of aluminium with TiB₂ using a single mode fiber laser," *Prod. Eng.* **2**(1), 27–32 (2008).

⁶V. M. Weerasinghe and W. M. Steen, *Laser Cladding with Pneumatic Powder Delivery*, Applied Laser Tooling (Martinus Nijhoff Publishers, Dordrecht, 1987), pp. 183–211.

⁷R. Vilar, "Laser cladding," *J. Laser Appl.* **11**(2), 64–79 (1999).

⁸E. Toyserkani, A. Khajepour, and S. Corbin, *Laser Cladding* (CRC Press, Boca Raton, FL, 2004), 280 p.

⁹J. C. Ion, *Laser Processing of Engineering Materials: Principles, Procedure and Industrial Applications* (Elsevier Butterworth-Heinemann, Oxford, 2005), 556 p.

¹⁰A. F. A. Hoadley and M. Rappaz, "A thermal model of laser cladding by powder injection," *Metall. Trans. B* **23**, 631–642 (1992).

¹¹Laser Institute of America, *LIA Handbook of Laser Material Processing*, edited by J. F. Ready (Magnolia Publishing, Inc. Orlando, FL, 2001), 715 p.

¹²W. M. Steen, *Laser Material Processing* (Springer, London, 2003), 408 p.

¹³Y. Li and J. Ma, "Study on overlapping in the laser cladding process," *Surf. Coat. Technol.* **90**, 1–5 (1997).

¹⁴J. Liu, "Formation of cross-sectional profile of a clad bead cross-sectional profile," *Opt. Laser Technol.* **39**, 1532–1536 (2007).

¹⁵W. M. Steen and K. G. Watkins, "Coating by laser surface treatment," *J. Phys.* **III 3**, 581–590 (1993).

¹⁶J. M. Pelletier, M. C. Sahour, M. Pilloz, and A. B. Vannes, "Influence of processing conditions on geometrical features of laser claddings obtained by powder injection," *J. Mater. Sci.* **28**, 5184–5188 (1993).

¹⁷M. Qian, L. C. Lim, Z. D. Chen, and W. L. Chen, "Parametric studies of laser cladding processes," *J. Mater. Process. Technol.* **63**, 590–593 (1997).

¹⁸L. Han, F. W. Liou, and K. M. Phatak, "Modeling of laser cladding with powder injection," *Metall. Mater. Trans. B* **35**, 1139–1150 (2004).

¹⁹G. Zhao, C. Cho, and J.-D. Kim, "Application of 3-D finite element method using Lagrangian formulation to dilution control in laser cladding process," *Int. J. Mech. Sci.* **45**, 777–796 (2003).

²⁰Y.-L. Huang, G. Y. Liang, J. Y. Su, and J. G. Li, "Interaction between laser beam and powder stream in the process of laser cladding with powder feeding," *Modell. Simul. Mater. Sci. Eng.* **13**, 47–56 (2005).

²¹A. Fathi, E. Toyserkani, A. Khajepour, and M. Durali, "Prediction of melt pool depth and dilution in laser powder deposition," *J. Phys. D: Appl. Phys.* **39**, 2613–2623 (2006).

PUBLICATION 2

Pekkarinen, J., Kujanpää, V. and Salminen, A. (2012)

LASER CLADDING WITH SCANNING OPTICS: EFFECT OF POWER ADJUSTMENT

This paper has been published in the
Journal of Laser Applications, **24**

Printed with permission

Laser cladding with scanning optics: Effect of power adjustment

Joonas Pekkarinen, Veli Kujanpää, and Antti Salminen

Laboratory of Laser Processing, Department of Mechanical Engineering, Lappeenranta University of Technology, Tuuantokatu 2, 53850 Lappeenranta, Finland

(Received 21 October 2011; accepted for publication 10 April 2012; published 1 May 2012)

Laser cladding with fiber laser using scanning optics is a relatively new way of laser cladding. Modern oscillating scanners enable laser power adjustment according to scanning direction. This is a versatile tool for making process more stable as well as modifying the shape of clad bead. Laser cladding was made using 5 kW IPG fiber laser with ILV-oscillating scanner, using 316L powder as clad material and S355 mild steel plate as substrate material. These tests showed that power adjustment is necessary for cladding process stability when sinusoidal scanning is used. Power adjustment can be used also for adjusting the geometry of clad bead and for constructing simple geometries. The oscillating scanner enables flexibility for controlling the geometry of clad bead and process stability compared to the conventional laser cladding with static optics. © 2012 Laser Institute of America.

Key words: laser cladding, scanning optics, oscillating scanner, power adjustment

I. INTRODUCTION

Laser cladding with pneumatic powder delivery has been studied during almost a quarter of century, first study made by Weerasinghe and Steen¹ and the first tests with cladding using scanning optics were done even earlier in late 1970s by Belmont and Castagna with preplaced powder.² Even though both cladding with pneumatic powered delivery and cladding using scanning optics are relatively old techniques, their combination is relatively unstudied. There have been made some studies in late 1980s in Lappeenranta University of Technology concerning laser cladding using scanning optics with dynamic powder feeding, for example, by Kauppila.³ However, in recent years, interest toward using scanning optics in laser cladding has been growing, and there have been some studies concerning this matter.⁴⁻⁶ In these studies, scanning optics has been used mainly as an optical tool to spread out the energy of laser beam and not focusing on how scanning optics changes the process or what kind of opportunities it creates.

Laser cladding using scanning optics is a very similar process to traditional laser cladding using static optics. Difference between these two cladding methods can be found in guiding of laser light. Static optics scatter laser light to the desired pattern where a melt pool is formed. Clad material is fed to this melt pool, when laser beam is moved forward; clad bead is formed from molten material, when it is solidified.⁷⁻⁹ The process using scanning optics works same way in principle. The difference is that laser light is guided using scanner instead of the static optics. Scanning optic adds flexibility to cladding process compared to using static optics.⁴ Flexibility of cladding process is based on possibility to adjust numerically the dimensions of laser interaction area, scanning amplitude. Scanning amplitude of laser beam on the top of work piece is mainly dependent on scanning mirrors tilting angle. When this angle can be adjusted numerically, it means also that laser interaction area can be

adjusted numerically.^{4,10,11} Figure 1 shows the principle of cladding with scanning optics.

Some scanners include the feature of power adjustment, which means that laser power can be adjusted according to the target location of laser beam or, in other words, according to tilting angle of scanning mirror.¹² This kind of feature increases process flexibility even more when numerically can be adjusted how much laser power is input in certain part of melt pool. This study concerns on this matter.

Laser cladding quality is typically graded by dilution ratio, such that the lower the dilution is, the better is the quality.¹³⁻¹⁵ Laser cladding dilution ratio is highly dependent on the specific energy input of laser cladding process which is in turn dependent on three basic cladding parameters: laser power, cladding speed, and the dimensions of the interaction zone of laser beam (the laser spot diameter/size; Fig. 2).¹⁶ Specific energy input determines how much material laser light can melt on square millimeter, and this affects directly to dilution ratio.¹⁶⁻¹⁸ Dilution ratio increases in most cases along with the increase of specific energy input.^{16,19-22} Both an increase of laser power and a decrease of laser beam spot size increase specific energy, thus increasing the dilution ratio.^{16,21,22} The influence of cladding speed on the dilution ratio is two-folded. A decrease of cladding speed increases the specific energy input and, thus, dilution ratio.^{21,22} On the other hand, a decrease in cladding speed increases the melt pool size. When melt pool grows larger, it creates thicker and better shield for substrate material against laser light. Then laser cannot get touch with substrate material as well, and this decreases dilution.^{19,20} Because the specific energy input takes into account more factors than linear energy input or power density, it is a good measure to interpret the laser energy input of laser cladding (Fig. 2).

This study concentrates on the suitability of the power control feature of linear scanner for laser cladding. Scanning optics create some unique challenges and possibilities in

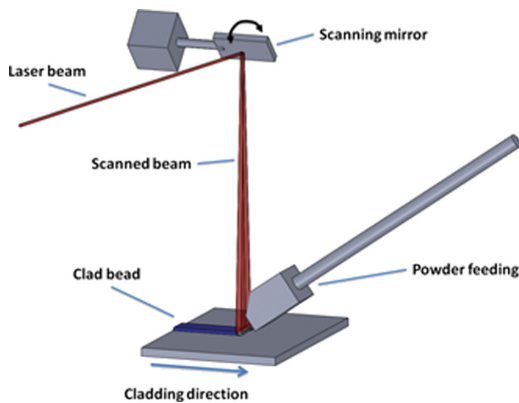


FIG. 1. Principle of cladding using scanned beam.

comparison to laser cladding with static optics. Dwell time of oscillating mirror at far ends of scanning range can create problems if the increase of specific energy input caused by dwell time is not corrected with power adjustment. The first part of this study deals with this matter. The second part of this study concerns how the power control feature of scanner can be used to influence the geometry of clad bead.

II. EXPERIMENTAL PROCEDURE

The experimental setup of this study can be divided in four branches: laser equipment, powder delivery, scanner, and process imagine. Laser equipment consists of IPG 5 kW multimode fiber laser and beam parameter product of 4.6 mm mrad, with 150 μm thick optical fiber and 150 mm focal length collimator. Used focusing optics were Precitec YW50 welding head with 500 mm focal length focusing lens. Focal point position located 60 mm on the top of substrates top surface. Substrate material was 6 mm thick S355 low alloyed steel, produced by company Rautaruukki Oy. The process head and cladding process movement were carried out with numerically controlled X-Y workstation.

Powder injection was carried out off-axially using pneumatic powder delivery, which injected the powder straight to melt pool. Used powder feeding machine was Plasma-Technik Twin-System 10-C powder feeder with argon as a

carrying gas. Two different sizes of powder feeding nozzle were used such that powder feeding width was matched with the scanning width. Powder feeding angle was 40°, powder mass flow rate was 0.5 g/s, and powder flow leaving from the nozzle was evenly distributed. Clad powder was AISI 316L stainless steel with particle size in a range of 53–150 μm .

Scanning optics were used to distribute laser beam to the desired area. ILV DC linear scanner was used in this study. This scanner works in oscillating principle so that one scanning mirror oscillates from side to side in a wanted frequency in a sine scan wave form. Scanner includes a powder adjustment feature. This enables to adjust laser power level in 32 points along one sine wave. This power adjustment feature was used to vary the energy distribution pattern of laser beam. Altogether, six different kinds of power adjustment profiles (PAPs) were tested in this study, presented later in this paper. Scanning amplitude was 9.6 mm, and laser spot size was 2.43 mm. It means that the width of laser beam interaction zone is 12.03 mm.

Analysis of melt pool behavior is based on video imaging from the process. Video recording was carried out using CCD video camera with Cavitar Cavilux active laser illumination technology. Laser illumination enables clear video image from the melt pool regardless of bright light generated by the process. Video image picture rate was 20–25 fps. The other analyzing methods were cross-section images from the clad beads. These samples were cut off from the middle of the clad bead. From these images, it was able to measure the height, width, and side bead angle of clad bead and to calculate the geometrical dilution ratio of clad bead. These measurements were done using Carl Zeiss AxioVision program.

III. RESULTS AND DISCUSSION

A. Power adjustment

As previously mentioned, the feature of laser power control is build inside the ILV scanner. Laser power can be adjusted in the range of 0%–100 % in 32 different points along the scanned sinusoidal wave. In Fig. 3, it can be seen how the power adjustment points are placed along the sine wave. These 32 power control points form 17 lines, and trough these lines, it can be drawn the PAP (Fig. 8). Power adjustment profiles represent how laser power is distributed in respect of laser spot position in the scan line.

Laser power adjustment according to the scanning direction is a beneficial tool in laser cladding because then the energy distribution of laser beam can be adjusted numerically. This creates two advantages. First, oscillating scanners typically work at some sort of sinusoidal waveform which causes higher fraction of laser energy to be introduced to the border areas of scan width than in the middle regions (Fig. 4).⁷ The laser power adjustment can be used to even the irregular laser energy distribution. This is how the maximum power of laser can be utilized at least in some part of the scanning track, and laser power levels are not needed to set up according to what kind of power levels the melt pool can endure at scanning border areas. Second, laser power adjustment enables the shape of the cross-section of the heat input

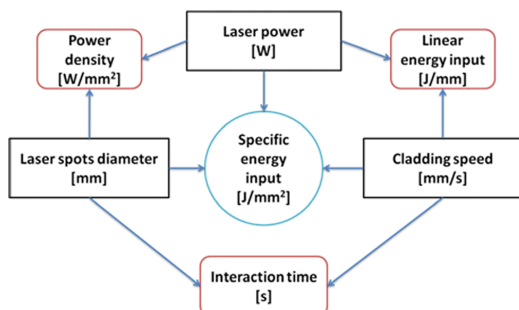


FIG. 2. The interdependency of parameters to laser energy input.



FIG. 3. The places of adjustment points of scanner power along the sinusoidal wave.

numerically to be adjusted. This enables the shape of clad bead to be adjusted to a certain degree through the power control, which will be discussed later in this paper.

The accumulation of the laser beam energy to the border areas of the scan lines is due to the dwell time of scanning mirror movement. The reason for this dwell time comes from Newton’s laws of motion. In order to change the moving direction of the scanning mirror at end of scan, it has to undergo deceleration and acceleration which leads to the dwell time and a sinusoidal waveform. In order to eliminate the dwell time completely, the deceleration and the acceleration should be indefinite. Therefore, since the acceleration in a real life cannot be indefinite, all the oscillating scanners suffer from the dwell time at the end of each scan, at least in some extent.⁷

The local energy beam input of laser beam is a sum of laser power and the duration of laser beam in each location. The local energy input can be adjusted either by adjusting laser beam—material interaction time, process speed, or laser power. The local energy input can be kept even by the scan track (Fig. 5), regardless of sinusoidal waveform by lowering locally the laser power at the edge areas of scanning.

The investigation for the effect of dwell time on cladding process was done by using two different settings of power adjustment. The first test series was done by using power adjustment, presented in Fig. 8(b), and in the second test series, laser power was kept constant through the whole scanning track.

It was noticed that in laser cladding, the dwell time of scanner causes the specific energy input to be increased at the end of each scan if the energy input is not leveled using the power adjustment. The increase in local energy input in the edge areas of scanning can make the process unstable and cause excessive melting of substrate material.

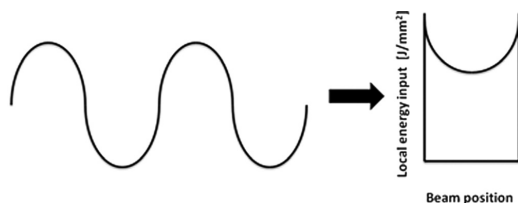


FIG. 4. Principle of local energy input accumulation on the scanning’s border area in sine scan wave form (Ref. 7).

When the power adjustment of Fig. 8(b) was used, cladding process was stable and the substrate material melted relatively evenly underneath the clad bead [Figs. 7(a)–7(c)]. However, when power adjustment is turned off and the power level is kept constant through the scanning track, the process becomes unstable [Figs. 7(d)–7(f)]. In this case, the local energy input increases near the turning point of scan and the material starts to vaporize at these areas. Then a shallow key-hole can be formed, as can be seen in Figs. 7(e) and 7(f) at left side of melt pool. Vaporization of material in border areas of melt pool was noticed in all clad processes which were done without using the power adjustment. The formation of key-hole creates an eruption of vaporized metal which disturbs the powder feeding. Erupting of the vapors prevents powder entering to the process at the border areas of scanning.

There is a significant difference in the amount of melted substrate (Fig. 6) between the cases, when power adjustment is used and when it is not in use. When power adjustment is not used, the substrate near the edges of clad bead is excessively melted [Figs. 7(d)–7(f)], compared to the case where laser power is adjusted [Figs. 7(a)–7(c)]. The excessive melting in the border areas originates from the increase of local energy input when power adjustment is not used. When power adjustment is used, the average power input is 26.4% less than in the case of no power adjustment. Difference in dilution ratio between these two test series were on the average 24% (Fig. 6), which is relatively close to the difference in average laser power input.

Vaporization in the border area of the melt pool additionally enhances the melting of the substrate in two ways. First, powder stream is not able to be accessed to the process, as mentioned previously, and when there is no additive material to melt lasers, energy goes to melting substrate material. Second, vaporizing of the material pushes the molten metal

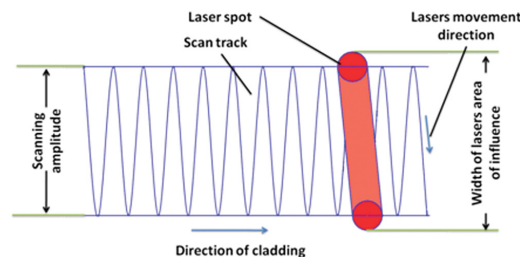


FIG. 5. Terminology and parameters in laser cladding with scanning optics.

outward from the melt pool. Due to the vaporization, a small keyhole is formed and laser light is able to import energy closer or even directly to substrate material. These two mechanisms increase the melting of substrate material and the dilution ratio. Lowering the laser power in areas where laser passes longer time prevents in the questioned vaporization and excessive melting.

From Fig. 6, it can be seen that dilution rate is highly dependent on cladding speed regardless whether the power adjustment is used or not. As the cladding speed increases, the melt pool grows thinner and so the melt pool does not create sufficient cover to substrate material, and hereby, laser energy is able to melt the substrate material better. This is how dilution rate can increase with the cladding speed even though the specific energy input decreases along with the increase of cladding speed. Similar results were also concluded by Qian *et al.*¹⁹ and Fathi *et al.*²⁰ However, it must be remembered that in this study, the powder feeding was kept at a constant level all the times. Increasing the powder feeding rate so that more of the laser power would go to melting, the additive powder instead of substrate material dilution rates could be smaller in higher cladding speeds.

Both the dilution ratio and the process stability are dependent on the specific energy input. An increase in specific energy input increases the dilution ratio and can make the process unstable. According to the previous result, it can be concluded that when the specific energy input of laser cladding using scanning optics is calculated, more factors must be considered than just the laser power, the cladding speed and the interaction area between laser beam and base material. Also the power adjustment diagram and dwell time of the scanner must be considered. Both of these factors affect the input of the laser energy. The dwell time defines how long the laser energy is interacting with a certain area, and the power adjustment defines how much of laser beam energy is brought to this area. Increase in the specific energy input does not only cause the increase of dilution, but it also makes the process unstable by material vaporization.

In all cases, the overall surface roughness of the clad bead was relatively rough independently of the use of power adjustment. The rough surface is caused by the powder particles attaching to the solidified clad bead surface. This is the result of some particles going through laser beam without

hitting melt pool but going over it and hitting to warm but already solidified clad bead. Then these particles can attach to clad beads surface and lower the clad beads surface quality.

B. Geometry shaping of clad bead

The feature of power adjustment of the scanner can be used also in a more versatile way than just by making cladding process stable. The power adjustment can be also used to give a shape for the geometry of the clad bead. By using the laser power adjustment, many types of power adjustment profiles can be created. Laser beam can only construct the clad bead when the energy intensity of the laser beam is high enough to melt both the clad material and the surface of substrate.^{13,17} When these two concepts are combined, we get a

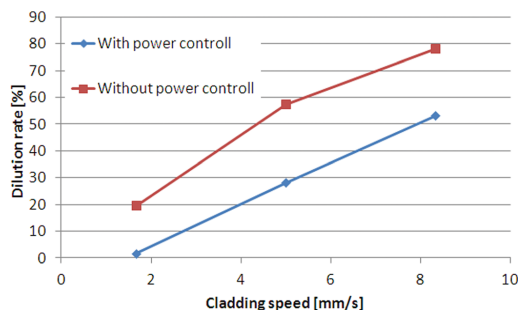


FIG. 6. The dilution ratios according to the speed when power control of the scanner is used and when it is turned off.

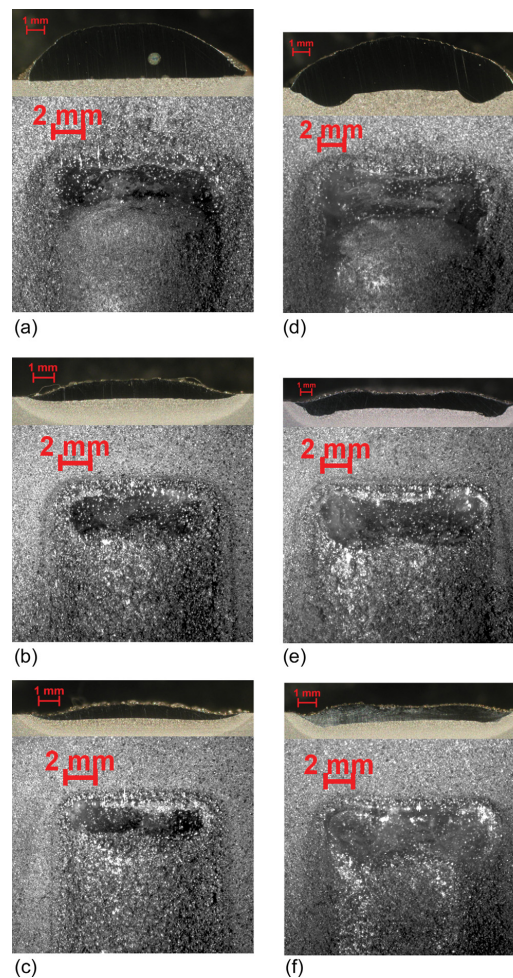


FIG. 7. Clad bead cross-sections and melt pools behavior figures. (a)–(c) When power adjustment is used; (d)–(f) when power control is turned off. (a) and (d) Cladding speed 1.67 mm/s; (b) and (e) cladding speed 5 mm/s; and (c) and (f) cladding speed 8.33 mm/s.

mechanism, which can be used to modify clad beads shapes geometry.

In this study, six different types of power adjustment profiles were used (Fig. 8). This test series showed that the geometry of clad bead can be shaped using the power control feature of the scanner. This test series was divided into two main branches: how the basic shape of clad bead can be modified [Figs. 8(a)–8(c)] and which types of more detailed geometries can be constructed using the power control [Figs. 8(d)–8(f)].

Two features in the basic geometry of clad bead can be adjusted by using power control: side angle of the clad bead (Fig. 9) and the shape of the middle section of the clad bead. When the power adjustment profile has a flat middle section (T-shape PAP), then also the geometry of clad bead gains flat section in the middle [Fig. 8(a)]. Changing the power adjustment profile so that it resembles parabola, D-shape PAP, the flat middle section of clad bead is narrowed [Fig. 8(b)], and when the power control resembles triangle, V-shape PAP, the clad bead becomes a round shape [Fig. 8(c)].

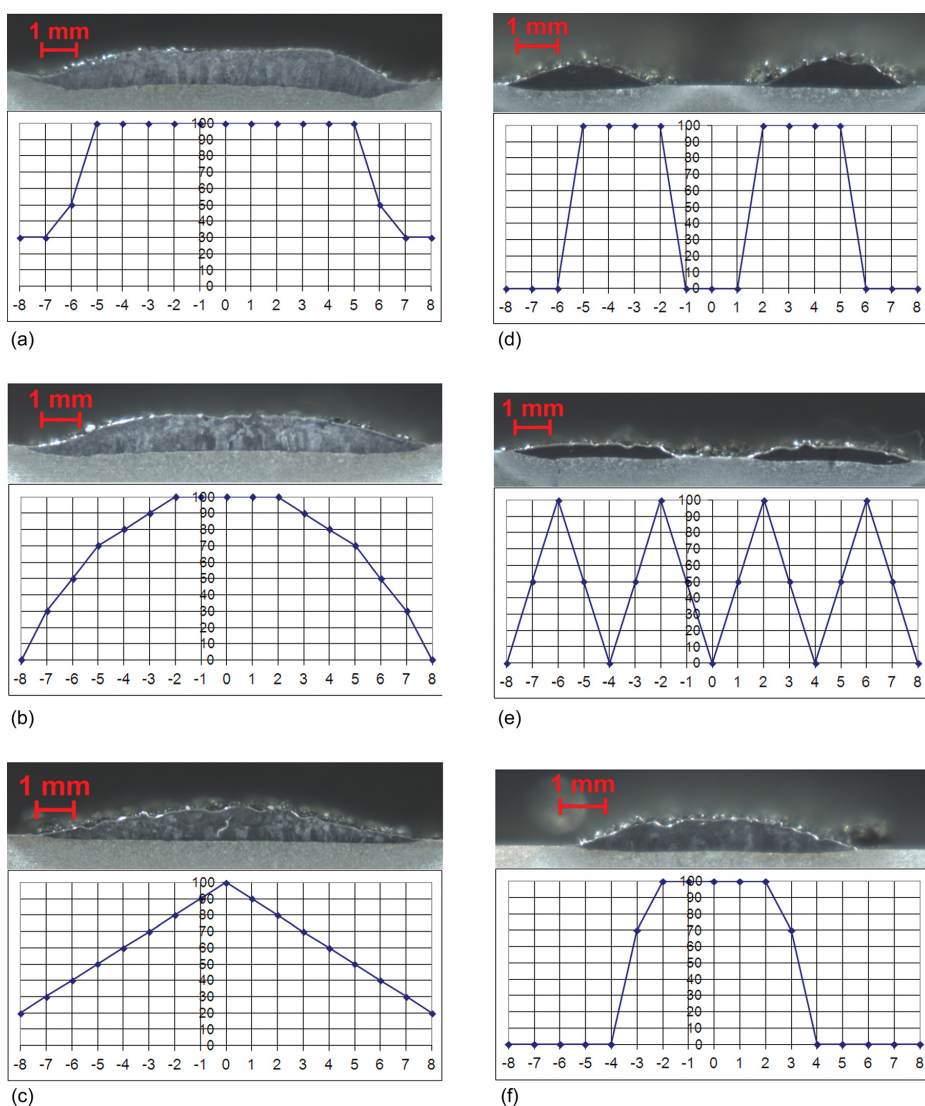


FIG. 8. Geometries of clad bead according to the power control diagrams. Cladding speed $v = 5$ mm/s and average laser power input: (a) T-shape PAP $P_{avg} = 4.16$ kW, (b) D-shape PAP $P_{avg} = 3.68$ kW, (c) V-shape PAP $P_{avg} = 3.10$ kW, (d) B-shape PAP $P_{avg} = 2.58$ kW, (e) WW-shape PAP $P_{avg} = 2.07$ kW, and (f) U-shape PAP $P_{avg} = 2.58$ kW.

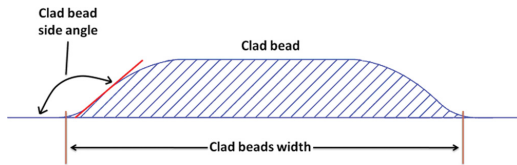


FIG. 9. Side angle of clad bead.

When clad beads flat middle section width increases, then side angle of the clad bead decreases. This is due to the increase of flat section width. Then the clad bead has a shorter way to settle to the level of substrate, and the angle is decreased. The side angle of clad bead is 157° , 164° , and 169° in Figs. 8(a), 8(b), and 8(c) cases, respectively.

The shape of power adjustment profile has also an effect to the dilution ratio. The dilution ratio was the highest with a T-shape PAP, 42.8%, and the lowest in a V-shape was 21.3%. The bead clad using a D-shape power control diagram gained to the dilution ratio of 29.7%. A decrease in the dilution ratio from case (a)–(c) in Fig. 8 is a result of a decrease in a specific energy input of the same order. This result indicates that at least in the power adjustment diagram cases T and D, the laser power levels has been little too high for this type of power control diagrams. There was too much “excessive laser energy” to melt the substrate material, and thereby increase the dilution ratio. In these parameter combinations, the optimal laser power would be 1–2 kW smaller, but this case need further study.

Power adjustment can be also used for creating simple geometries as Figs. 8(d)–8(f) demonstrate. In Fig. 8(d), it is demonstrated a case where laser cladding was used to construct a canal using a B-shape PAP. In this case, laser was “turned off” in the middle of the scan amplitude such that no cladding was occurred in the middle of the track. This way, it is possible to create two narrow clad beads during one cladding run and to construct a canal shape. When power spikes were increased from two to four, a WW-shape PAP was resulting [Fig. 8(e)]. Then, it can be noticed same type of two clad beads to be formed next to each other. This shows that there is a limit for how little features can be made using this cladding technique. Four power spikes created four small melt pools, and two of those melt pools in each side of center line got touched with each other and were combined forming one clad bead in each side of center line.

When narrow clad beads need to be constructed, scanning optics can be used in two ways, adjusting amplitude narrower or adjusting power diagram to U-shape like in Fig. 8(f). An adjusting power diagram has one advantage against to adjusting the cladding amplitude. Laser beam works as one type of pulsed mode because laser is on only when laser is directed in middle of scan line and it is cut off at the edges of a scan. This is how the power control of scanner can be used as a numerical control of heat input of laser cladding process. Using a U-shape power control diagram, the melt pool stayed in melted state at all times throughout the process at scanning frequency of 100 Hz.

IV. SUMMARY OF ADVANTAGES AND DISADVANTAGES

Main advantage of using numerically adjusted scanning optics in laser cladding is scanners created flexibility to process control. Using the power control options of the scanner, the laser energy input can be adjusted versatile as in this paper has been demonstrated. This way, the clad bead geometry can be adjusted relatively easily. Also when the scanning optics makes it possible to control the heat a sensitive material or object, it can be clad more easily.

The main disadvantages of using the scanner optics in laser cladding come from the amount of parameters, and the fact that it is not possible to utilized all potential laser power to cladding purposes. Because scanner optics enables significantly more adjustability in laser cladding compared to laser cladding using static optics, it also means that there is more parameters to be determined. If these scanning parameters are not determined correctly, the process can become more unstable. Also, when the power control option of scanner is used to stabilize the cladding process, some of the potential laser energy is not used. This is because laser power needs to be decreased at the edge areas of scan; consequently, all of the lasers power reserve cannot be utilized to cladding.

V. CONCLUSIONS

When laser cladding is done by using an oscillating scanner, it is important to use a power control to even the specific energy input in the turning points of a scan line. Typically, the increase of specific heat input in the turning points of scan line is caused by the dwell time of the movement at these areas. If this increase in the specific heat input caused by the dwell time is not compensated, the process is changed to be unstable. In this case, laser beam starts to evaporate material in the turning points of scan line, and melting of the substrate materials will be increased which in turn increases the dilution ratio.

Power adjusting makes it possible to effect on the geometry of clad bead. This is how it is possible to create simple geometries using laser cladding with scanning optics. Power adjustment enables the creation of clad bead that has a flat middle section and the adjustment of a clad bead side angle. Laser power adjustment enables the creation of canals with one clad pass. Also one type of pulsing is possible to carry out by using power adjustment when a narrow clad bead is made.

This study shows that the power control feature of scanner is a beneficial and important tool for laser cladding done with scanning optics. However, a further study is needed to find out the full potential and the limits of this technology.

ACKNOWLEDGMENTS

The authors wish to express their gratitude to Päijät-Hämeen Liitto (The regional council of Päijät-Häme) and the European Regional Development Fund for funding the research carried out.

¹V. M. Weerasinghe and W. M. Steen, “Laser cladding with pneumatic powder delivery,” in *Applied Laser Tooling* (Martinus Nijhoff Publishers, Dordrecht, 1987), pp. 183–211.

- ²A. Belmont and M. Castagna, "Wear-resistance coatings by laser processing," *Thin Solid Films* **64**(2), 249–256 (1979).
- ³J. Kauppila, "Laser cladding with dynamic powder feeding," Master's thesis, Lappeenranta University of Technology, Lappeenranta, 1988.
- ⁴F. Klocke, C. Brecher, D. Heinen, C.-J. Rosen, and T. Breitbach, "Flexible scanner-based laser surface treatment," in *Proceedings of the LANE 2010 Conference* [Phys. Procedia **1**, 467–475 (2010)].
- ⁵T. A. Palmer, "Implementation of laser cladding for Virginia class submarine main propulsion shaft repair," in Proceedings of the CTMA 2010 Symposium, MCB Quantico, VA, 22–24 March 2010.
- ⁶J. Tuominen, J. Näkki, H. Pajukoski, T. Peltola, P. Vuoristo, M. Kuznetsov, and G. Turichin, "Laser cladding with 15 kW fiber laser," in *Proceedings of the 13th NOLAMP Conference in Trondheim*, 27–29 June 2011 (Norwegian University of Science and Technology, Trondheim), p. 12.
- ⁷*LIA Handbook of Laser Material Processing*, edited by J. F. Ready (Laser Institute of America, Oxford, FL; Magnolia Publishing, Inc., Orlando, FL, 2001), p. 715.
- ⁸J. C. Ion, *Laser Processing of Engineering Materials: Principles, Procedure and Industrial Applications* (Elsevier, Oxford, FL, 2005), p. 556.
- ⁹E. Toyserkani, A. Khajepour, and S. Corbin, *Laser Cladding* (CRC Press, Boca Raton, FL, 2004), p. 280.
- ¹⁰K. Kim, K. Yoon, J. Suh, and J. Lee, "Laser scanner stage on-the-fly method for ultra fast and wide area fabrication," in *Proceedings of the Sixth International WLT Conference on Lasers in Manufacturing, Munich, Germany*, 23–26 May 2011 [Phys. Procedia **12**(2), 455–461 xx].
- ¹¹J. F. Ready, *Industrial Applications of Lasers* (Academic Press, London, 1997), p. 597.
- ¹²A. G. Arlt, *User's Manual: ILV DC-Scanner* (ILV GmbH, Schwalbach, 2009), p. 29.
- ¹³W. M. Steen and K. G. Watkins, "Coating by laser surface treatment," *J. Phys.* **IV** **3**(C9), 581–590 (1993).
- ¹⁴W. M. Steen, *Laser Material Processing* (Springer, London, 2003), p. 408.
- ¹⁵J. T. Hofman, D. F. de Lange, B. Pathiraj, and J. Meijer, "FEM modeling and experimental verification for dilution control in laser cladding," *J. Mater. Process. Technol.* **211**, 187–196 (2011).
- ¹⁶G. J. Bruck, "High-power laser beam cladding," *J. Metals* **39**(2), 10–13 (1987).
- ¹⁷A. F. A. Hoadley and M. Rappaz, "A thermal model of laser cladding by powder injection," *Metall. Trans. B* **23**, 631–642 (1992).
- ¹⁸J. M. Pelletier, M. C. Sahour, M. Pilloz, and A. B. Vannes, "Influence of processing conditions on geometrical features of laser claddings obtained by powder injection," *J. Mater. Sci.* **28**, 5184–5188 (1993).
- ¹⁹M. Qian, L. C. Lim, Z. D. Chen, and W. L. Chen, "Parametric studies of laser cladding processes," *J. Mater. Process. Technol.* **63**(1–3), 590–593 (1997).
- ²⁰A. Fathi, E. Toyserkani, A. Khajepour, and M. Durali, "Prediction of melt pool depth and dilution in laser powder deposition," *J. Phys. D: Appl. Phys.* **39**, 2613–2623 (2006).
- ²¹G. Zhao, C. Cho, and J.-D. Kim, "Application of 3-D finite element method using Lagrangian formulation to dilution control in laser cladding process," *Int. J. Mech. Sci.* **45**, 777–796 (2003).
- ²²J. M. Yellup, "Laser cladding using the powder blowing technique," *Surf. Coat. Technol.* **71**(2), 121–128 (1995).

PUBLICATION 3

Pekkarinen, J., Salminen, A. and Kujanpää V. (2014)

LASER CLADDING WITH SCANNING OPTICS: EFFECT OF SCANNING
FREQUENCY AND LASER BEAM POWER DENSITY ON CLADDING PROCESS

This paper has been published in the
Journal of Laser Applications, **26**

Printed with permission

Laser cladding with scanning optics: Effect of scanning frequency and laser beam power density on cladding process

Joonas Pekkarinen^{a)} and Antti Salminen

Laboratory of Laser Materials Processing, Lappeenranta University of Technology, Tuotantokatu 2, 53851 Lappeenranta, Finland

Veli Kujanpää

VTT Technical Research Centre of Finland, Tuotantokatu 2, 53851 Lappeenranta, Finland

(Received 8 March 2013; accepted for publication 7 March 2014; published 7 April 2014)

Scanning optics is an effective way to manipulate a laser beam for laser cladding. The numerical adjustment of the scanner gives a great deal of flexibility to the cladding process. However, the effect of the scanned beam on the cladding process itself has not been studied very thoroughly so far. This study concentrates on explaining how the scanning frequency and power density of the laser beam affect the stability of the cladding process. The results showed that both of these factors significantly influence the process stability and the outcome of the cladding process. If the local specific energy input was over 2.46 J/mm^2 , the process was noticed to be unstable. This limit was crossed when scanning frequency was under 40 Hz. Power density's limit value for stable process was found to be 191 kW/cm^2 and higher power densities than this was found to produce unstable process. If the cladding process was found to be unstable, dilution increased significantly and process started to resemble more laser alloying. © 2014 Laser Institute of America.

[<http://dx.doi.org/10.2351/1.4868895>]

Key words: fiber laser, scanner, scanning frequency, cladding, focal position, power density, melt pool behavior, process stability

I. INTRODUCTION

Laser cladding using scanning optics is a technique with a relatively long history; the first reference to this process is from late 1970s by Belmont and Castagna.¹ The optical setup of Belmont and Castagna¹ for laser cladding experiments included 2D scanner, and thus, they proved that scanner optics can be used in laser cladding. In 1980s, at least two laser cladding studies have been done where scanning optics have been used. Bruck² showed in his study that over 2 in. wide clad bead can be cladded using scanning optics with a high power CO₂ laser. Kauppila³ in turn defined that widening laser beam material interaction area (LMIA) (Fig. 1) by increasing scanning amplitude decreases slightly the dilution. It is also known that the process has been used since the late 1980s for air carried catapult rail cladding with a CO₂ laser of power up to 20 kW. However, scanner technology has improved significantly from those days. Nowadays, scanners are computer guided which enables a better process control and even a modification of the geometry of clad bead through the power control of the scanner.^{4,5}

The interest toward using scanning optics in laser cladding and other surface modification processes has risen in recent years. Klocke *et al.*⁶ show in their study that scanner optics can be used to increase the flexibility of laser cladding process. In terms of laser cladding, flexibility mainly means numerical adjustment of the size of laser beam material

interaction zone (Fig. 1) and modification of energy input. The numerical adjustment of scanning amplitude enables the width adjustment of the laser beam material interaction zone,⁴⁻⁶ and energy input modification can be achieved by using the power adjustment feature of the scanner.⁴ Power adjustment in turn enables laser power adjustment across the clad bead when cross-section shape of the clad bead can be modified.^{4,7} Palmer⁸ and Tuominen *et al.*⁷ both have shown in their independent studies that scanner optics with high power fiber laser enables laser cladding of wide clad beads and thus increase the productivity of the laser cladding process. Palmer⁸ showed that using powder material wide clad beads can be cladded with low dilution. This was confirmed in Tuominen *et al.*⁷ study, and they added that also wire material can be used as an additive material but then dilution

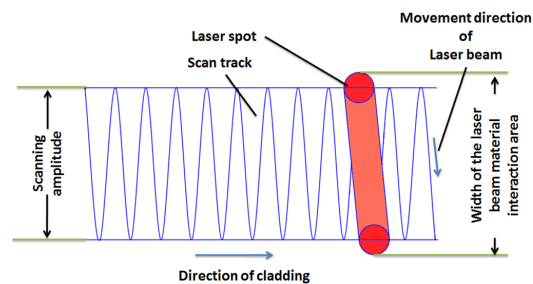


FIG. 1. Relation of scanning amplitude to width of the LMIA.

^{a)}Author to whom correspondence should be addressed; electronic mail: Joonas.pekkarinen@lut.fi; Telephone: +358 40 482 3840.

control is more difficult. Vollertsen *et al.*⁹ in turn showed that scanning optics can be used also in deep penetration surface alloying. However, even though this technique has been known for over 30 yr for laser cladding, there have been only a few studies^{4,5,9,10} about how the scanned beam changes the process dynamics and the effect of scanning parameters on the overall quality of the clad bead. Major part of these studies has been done in Lappeenranta University of Technology by Pekkarinen *et al.*^{4,5,10} These studies have shown that scanner's oscillating mirror dwell time can cause vaporization at the edge areas of LMA (Fig. 1). This phenomena decrease clad bead quality and also changes the clad bead geometry.

The basic idea of laser cladding using scanning optics is the same as laser cladding with static optics. Laser beam melts the substrate material as little as possible and at the same time as much as possible additive material; this way low dilutions can be achieved. When the laser beam moves forward, the melted material left behind the laser beam interaction zone solidifies, creating a clad bead.¹⁰⁻¹³ The main difference between laser cladding with scanning optics and that with static optics is the way how the laser beam is controlled and spread to the desired interaction area. With a scanner, the laser beam is controlled using one or more moving mirrors and dynamic computer control. This way the effective area of the laser beam is not tied to fixed focusing properties, as with, e.g., integrating mirrors or lenses, but it can be adjusted numerically by modifying the scanning amplitude and frequency.^{4,5,10} Figure 1 shows the effect of the scanning amplitude on the area of influence.

The impact of the energy input on cladding process stability and the quality of the clad bead is substantial.^{2,4,5,10-17} The energy input of the laser beam to a specific point can be defined by two factors: laser power and the interaction time of the laser beam with the specific point.^{2,17} Laser cladding using a scanned laser beam has one special feature compared to laser cladding using static optics: The width of the scanning amplitude of the laser beam forms an overall interaction area of the laser beam where the average energy input is relatively low. However, the laser energy is transmitted through a small, rapidly moving laser spot with a high power density, and therefore, locally the energy input can be relatively high.^{4,5,9,10,18,19} Dilution—the melted substrate material volume compared to the overall clad bead volume—typically increases with the increase of energy input if powder feeding is not used to compensate the increased energy input.^{15-17,20-30}

Laser power determines ultimately how much energy is imported to the cladding process.^{2,13} However, the power does not solely determine the phenomena that take place when the laser beam interacts with the material; the laser beam spot size also has effects on this. The power and the spot size together determine the power density which in turn defines how the material acts when the laser encounters it: whether it warms up, melts, or vaporizes.^{12,13,20} For laser cladding purposes, the power density should be high enough to melt the material but low enough not to vaporize it.

The laser beam material interaction time in turn defines how long the laser beam imports energy to the specific point and thus defines how high the energy input is at each

location. The interaction time between beam and material is understandably defined by the traveling speed and diameter of the laser beam (spot size).¹¹⁻¹³ The interaction time defines the time during which the laser beam delivers energy to a certain point (thermal impact time). Therefore, it also determines together with laser power how much material temperature can raise during this interaction and thus how the material acts at this point.^{12,13,31} By combining the laser power, the traveling speed, and spot size of the laser beam, the specific energy input of the process can be defined as follows:²

$$\begin{aligned} \text{Specific energy input} & \left(\frac{\text{J}}{\text{mm}^2} \right) \\ & = \frac{\text{Laser power (W)}}{\text{Beam width (mm)} \times \text{Cladding speed} \left(\frac{\text{mm}}{\text{s}} \right)}. \end{aligned} \quad (1)$$

It must be remembered that the energy input of laser cladding with scanning optics has a dual character. The overall specific energy input can be relatively low when it is calculated as an average from the entire interaction area formed by the scanned beam. On the other hand, one should also consider that inside this interaction area there is a small, fast moving laser spot which possess high power density. Because of this cladding process, energy inputs limit value may be exceeded locally and laser can start to vaporize the material.⁴ In order to get a well-functioning cladding process, this matter must be recognized.

This study focuses on clarifying how the scanning frequency and the laser beams power density influence to the cladding process stability and what is the process mechanism behind unstable cladding process. Also this study aims to clarify threshold value for scanning frequency and focal point position of process change from unstable to stable.

II. EXPERIMENTAL PROCEDURE

The laser equipment in the study consists of an IPG 5 kW fiber laser with a 150 μm fiber diameter and a 150 mm focal length collimator. The focusing optics used was the Precitec YW50 welding head with a focusing lens of a focal length of 500 mm. The focal point position was +60 mm over the top of the work piece surface in frequency tests, and scanning amplitude used in all of these tests was 9.7 mm, resulting in the interaction zone of 12.3 mm in width. In the power density effect tests, focal point positions of 0, +20, +40, +60, and +80 mm were applied. Scanning amplitude in these tests was 8.7 mm and the corresponding interaction zone width was 9.2, 9.6, 10.4, 11.2, and 12.1 mm at 0, +20, +40, +60, and +80 mm focal position level, respectively. The difference in the width of laser interaction zone in different focal positions comes from growth of spot diameter along with the increase of focal position. The used substrate material was S355 low alloyed steel plate. Plates dimensions were 6 \times 50 \times 150 mm. The substrate was at room temperature before cladding, and the substrate temperature rise was

not controlled during cladding. Changes in the substrate temperature during the process were not taken into account. Cladding length for a single clad test was 120 mm, and for this cladding length, cladding parameters stayed constant, excluding scanners power adjustment (Fig. 2). Two cladding speeds were used in scanning frequency tests, 3.33 and 5.00 mm/s. During the power density tests, cladding speed of 5.00 mm/s was used.

The ILV DC linear scanner was used in this study. In the scanner, one scanning mirror oscillates from side to side at the desired frequency in sine scan wave form. The scanner includes a power adjustment feature. This enables adjusting the laser power at 32 points along one sine wave. The power was adjusted such that the laser energy decreased when the scanner directed the laser beam at the scanning turning area at the both ends of the amplitude. Figure 2 presents the power adjustment profile used in this study. The laser power at 100% was set to 5 kW. The laser power was adjusted in this way such that the dwell time of the scanning mirrors does not cause unnecessary vaporization and disturbance to the cladding process. The importance of power adjustment for process stability is discussed in previous study of authors.⁷ The average laser power experienced by the work piece was 3.7 kW.

Powder feeding was implemented by using an off-axial powder feeding with argon as a carrying gas. Powder was fed in 40° angle (angle between powder stream and work piece surface) in mass feed rate of 0.5 g/s. Powder feeding nozzle formed laminar powder stream where powder was distributed uniformly through the powder stream. Powder stream leaving from the feeding nozzle was aligned straight to the melt pool and laser beam's area of influence (Fig. 1) so that the formed powder stream covered the whole melt pool. The used powder feeding machine was the Plasma-Technik Twin-System 10-C powder feeder with argon as the carrying gas. The cladding powder was AISI 316L stainless steel with a particle size in a range of 53–150 μm .

The power density distribution of the laser spot and spot size in different focal positions was analyzed using the Primes FocusMonitor. The analysis of the melt pool behavior is based on video imaging of the process using a CCD video camera with Cavitax Cavilux active laser illumination technology and dichroic window filtering. The system provides a clear video image from the melt pool regardless of the bright

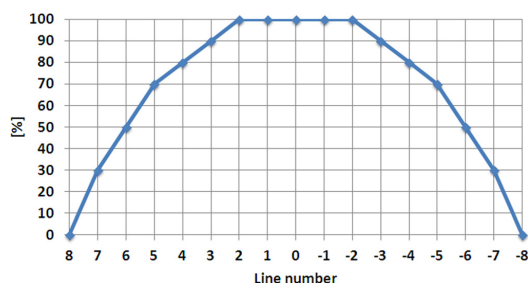


FIG. 2. Presentation of laser power in different locations of scan track with used power adjustment.

light generated by the process. The video imaging rate was 20–25 fps. The other analyzing method was metallographic cross-section images of the clad beads. These samples were cut off from the middle of the clad bead. From these images, it was possible to measure the clad bead cross-section area and to calculate the geometrical dilution of the clad bead.

III. RESULTS AND DISCUSSION

A. Laser cladding process stability

In both of the studied matters (scanning frequency and focal position), excessive vaporization was noticed when certain parameter ranges, i.e., a low scanning frequency or high power density were used. In these cases, the laser was even able to vaporize the material in that extend that a small keyhole, moving rapidly with the scanned beam, was able to be formed in the melt pool. This caused an excessive vapor eruption from the keyhole, preventing the powder from reaching the melt pool properly [Fig. 3(a)]. The erupting vapor flow from the keyhole creates a type of local moving barrier for powder flow which either takes powder with it or forced powder flow to go around it. This mechanism was first noticed during the experiments and confirmed by the video image from the melt pool, example presented in Fig. 3(b), and by comparing clad beads added to the cross-sectional area of stable and unstable processes (Fig. 8).

Overall, vaporization is a highly undesirable phenomenon in laser cladding because it prevents additive powder from reaching the melt pool properly. This directly affects the dilution, which will be shown later. When vapor eruption occurs, the vapor either blocks the additive powder for entering the process or vapor flow takes with it some or most of additive powder. Figure 3(b) shows video frames from the unstable process. In this figure, erupting vapor can be seen in the left side of the melt pool as a light grey cloud flowing backward (opposite of the cladding direction). At this time because additive material is not able to enter the process properly, the laser beam no longer melts the additive material, but it melts the substrate material, which causes increase of dilution (see Figs. 5 and 8). When this vapor formation occurs, the process does not work as a proper cladding process, but it starts to resemble more like laser alloying due high dilution and deep penetration of melt pool to the substrate material (Figs. 5 and 6). Similar results for the prevention of powder entering the melt pool in the case of vaporization are reported by the authors in an earlier study.⁴ This is the way how vaporization sets its own limits for an applicable scanning frequency and focal point position.

B. Effect of scanning frequency

The scanning frequency has a significant impact on the process stability. The laser beam needs to be scanned with a high enough frequency so that the local specific energy input does not grow excessively high. If the local specific energy input becomes too high (Table I), the material starts to vaporize [vapor can be seen in Fig. 4(a)], disturbing the cladding process as presented above. This was noticed in experiments on the effect of the scanning frequency on the

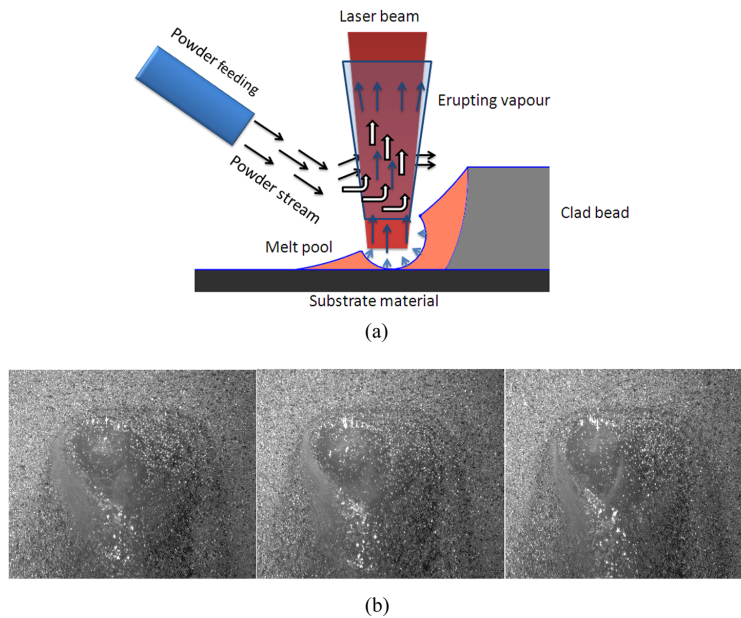


FIG. 3. The mechanism how erupting vapor prevents additive powder from entering the process. Black and black/white arrows represent powder particle movement. Green arrows represent vapor movement from the keyhole. Figure series (b) is from unstable process, where erupting vapor can be seen as a light grey cloud, $v = 3.33$ mm/s and $f = 5$ Hz (enhanced online) [URL: <http://dx.doi.org/10.2351/1.4868895.1>].

cladding process stability [Fig. 5(b)]. When the scanning frequency was set to 5 or 10 Hz, a tiny keyhole formed in the melt pool which caused instability to the process. In laser cladding, the keyhole formation is highly undesirable phenomenon because it increases dilution [Fig. 5(a)]. The increase in dilution is due to two factors. First, the laser beam is able to dig a melt pool into the substrate material due to the keyhole. Second, as previously mentioned, the vapor erupting from the keyhole prevents the additive powder from entering the cladding process properly.

In order to determine the threshold value for local specific energy input, the local velocity of the scanned beam needs to be calculated. The scanned beam works at sine wave mode. Therefore the local velocity can be calculated by using the formula of harmonic oscillations

$$v_{sb} = 2\pi\dot{y}f \cos 2\pi ft, \quad (2)$$

where v_{sb} is the velocity of scanned beam at a specific point, \dot{y} is the peak amplitude of scan (half of scanning amplitude, Fig. 2), f is the scanning frequency, t is time where scanned beams velocity is calculated. From this, we can solve the velocity of scanned beam in every power adjustment point using formula

$$v_{sb} = 2\pi\dot{y}f \cos 2\pi f \frac{n}{mf}, \quad (3)$$

where n marks the adjustment point number and m is the total number of power adjustment points. Local specific energy input can be calculated by using formula (1)

TABLE I. Local specific energy inputs in power adjustment lines.

		Frequency (Hz)								
		5	10	20	40	80	100	150		
Line number	0	12.82	6.41	3.20	1.60	0.80	0.64	0.43	100	Power adjustment (%)
	±1	13.07	6.53	3.27	1.63	0.82	0.65	0.44	100	
	±2	13.87	6.94	3.47	1.73	0.87	0.69	0.46	100	
	±3	13.87	6.94	3.47	1.73	0.87	0.69	0.46	90	
	±4	14.51	7.25	3.63	1.81	0.91	0.73	0.48	80	
	±5	16.15	8.08	4.04	2.02	1.01	0.81	0.54	70	
	±6	16.75	8.38	4.19	2.09	1.05	0.84	0.56	50	
	±7	19.71	9.86	4.93	2.46	1.23	0.99	0.66	30	
	±8	0.00	0.00	0.00	0.00	0.00	0.00	0.00	0	
Local specific energy input (J/mm ²)										

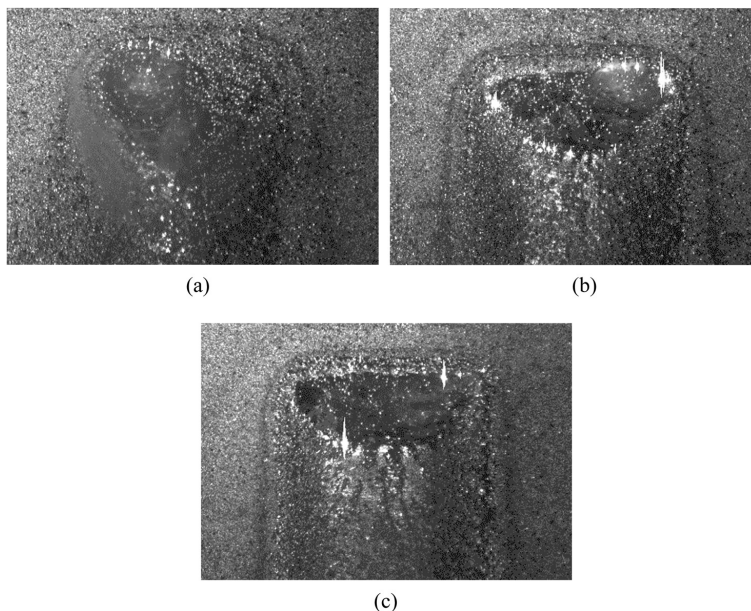


FIG. 4. Melt pool at different frequencies (a) 5 Hz, (b) 40 Hz, (c) 150 Hz. Vapor formation can be seen in (a); light gray cloud in left side of melt pool. Cladding speed of these tests is 3.33 mm/s.

$$Q_{sl} = \frac{a_p \times P}{D_f \times (2\pi y f \cos 2\pi \frac{y}{m})}, \tag{4}$$

where Q_{sl} is the local specific energy input, a_p is power adjustment factor, P is laser power, and D_f is the spot diameter. Using this formula, the local specific energy input in every adjustment point can be calculated. In Table I, the used local specific energy input is presented by every power adjustment lines (Fig. 2) presented earlier.

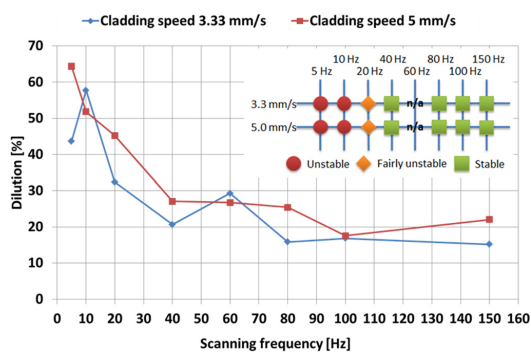


FIG. 5. Effect of scanning frequency on dilution and stability. Average laser power is 3.7 kW, focal point diameter is 2.4 mm and amplitude is 9.7 mm, and maximum power density is 191 kW/cm² (Table III). Specific energy input with cladding speed of 3.33 mm/s was 94.4 J/mm² and with cladding speed of 5 mm/s was 62.7 J/mm². Unstable marks that a small keyhole is able to be formed and it causes a heavy vapor formation. Fairly unstable marks that a small keyhole forms and a small amount of continuous vapor formation is detected. Stable marks that there is no keyhole formation.

From Fig. 5 and Table I, it can be concluded that if the local specific energy input is at most 2.46 J/mm², the cladding process remains stable. This limit value from that process is stable at scanning frequency of 40 Hz and above it (Fig. 5), and 2.46 J/mm² is the maximum local specific energy input at 40 Hz. Higher local specific energy input causes vaporization in the melt pool. Even though the energy input is relatively low, it must be remembered that this energy amount is delivered to this point in short time (Table II). Therefore, when heat has no time to conduct away, it starts to vaporize the material in order to consume this excessive energy.

When low scanning frequencies (5 or 10 Hz) were used, the process resembles more laser alloying than laser cladding due to high dilution [Fig. 5(a)] and the penetration depth of the laser into the substrate material (Fig. 6). These cross-section images show quite explicitly how deep melt the laser

TABLE II. Scanned beam interaction within a specific point.

		Frequency (Hz)						
		5	10	20	40	80	100	150
Line number	0	16.80	8.40	4.20	2.10	1.05	0.84	0.56
	1	17.14	8.56	4.28	2.14	1.07	0.86	0.57
	2	18.18	9.09	4.55	2.27	1.14	0.91	0.61
	3	20.21	10.10	5.05	2.53	1.26	1.01	0.67
	4	23.77	11.88	5.94	2.97	1.49	1.19	0.79
	5	30.24	15.12	7.56	3.78	1.89	1.51	1.01
	6	43.90	21.96	10.98	5.49	2.74	2.20	1.46
	7	86.11	43.06	21.53	10.77	5.38	4.31	2.87
	8	—	—	—	—	—	—	—
		Laser beams interaction time with specific point (ms)						

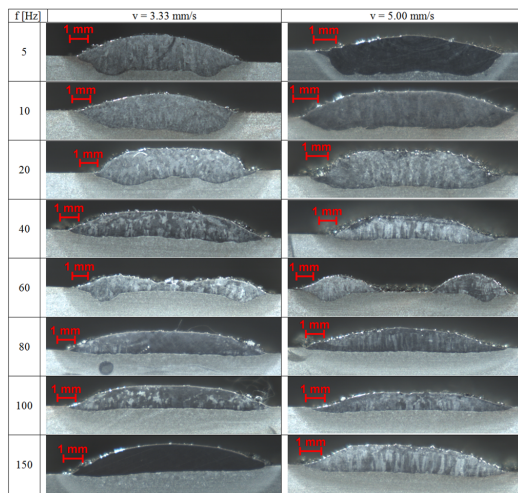


FIG. 6. Cross-section of clad bead in different tested frequencies and cladding speeds. Specific energy input with cladding speed of 3.33 mm/s was 94.4 J/mm² and with cladding speed of 5 mm/s it was 62.7 J/mm².

beam is able to form into the substrate material when the scanning frequency is low. When scanning frequency is increased, substrate melting decreases significantly (Fig. 6).

When the scanning frequency reaches 20 Hz and local specific energy input is in a range of 3.2–4.93 J/mm², the melt pool behavior started to stabilize. Even though the keyhole formation is significantly diminished, it does not completely disappear. This is shown as an elevated dilution [Figs. 5(a) and 6]. A 20 Hz scanning frequency is still too low to distribute the laser energy evenly since the local specific energy input may increase so high that the material can start to vaporize occasionally, at least with the power density of 191 kW/cm² (Table III). If a lower power density would be in use, laser cladding process could be stable with a 20 Hz scanning frequency, but this matter needs further research.

At a scanning frequency of 40 Hz or higher, the melt pool behavior is calm and stable, and no keyhole formation is detected with the used power density. At the scanning frequency of 40 Hz, laser beam moves fast enough to distribute the laser energy evenly to lasers interaction zone so that the material does not start to vaporize during the cladding process [Figs. 4(b), 5(b), and 6]. Thus, maximum local specific energy input that is low enough to ensure stable cladding process is 2.46 J/mm².

The absence of keyhole significantly affects the dilution, as shown in Figs. 5(a) and 5(b). When keyhole is not formed, the dilution decreases significantly. Figure 5(a) shows that 40 Hz is one type of saturation point for speed of dilution

TABLE III. Spot size and peak power density in different focal positions.

Focal position (mm)	0	+20	+40	+60	+80
Beam size on work piece(mm)	0.54	0.89	1.73	2.56	3.44
Peak power density (kW/cm ²)	2836	1424	413	191	102
Average power density (kW/cm ²)	982.3	303.0	79.51	35.36	20.61

change. From this point on, dilution changes moderately along with the increase of the scanning frequency, except in the case of 60 Hz. Experiments performed with 60 Hz can be disregarded because the scanner does not work properly when this frequency–amplitude combination was applied, and these results are not discussed further in this article. Figure 6 shows that when cladding is done using 60 Hz scanning frequency, the clad bead is deformed compared to the others.

When an even higher scanning amplitude was used (80, 100, or 150 Hz), the dilution stabilized and slightly decreased compared to the frequency values of 40 Hz. This can be considered to be a result of more even energy distribution. When the laser beam scans faster, heat has less time to build up locally and to conduct to the substrate material and thus to vaporize or melt it [Fig. 4(c)].

The effect of the scanning frequency on the cladding process is significant because it determines maximum allowed local specific energy input. When the scanning frequency is low, the local specific energy input can be so high that the laser beam starts to vaporize the material. When this is compared to the higher scanning frequencies, the dual characteristics of the heat input of the scanner based laser cladding can be understood. Even though the overall heat input is the same in the scanning frequency of 5 and 150 Hz, there is locally a significant difference in the energy input.

C. Effect of laser beam power density

The focal point position in relation to the surface of the work piece, i.e., laser beams power density, has a significant effect on the stability of the cladding process. Even though the laser beam moves rapidly back and forth, spreading the laser energy in a fairly wide area, it must be pointed out that the laser energy is introduced through a small spot which has relatively high power density. Therefore, if the laser spot on top of the work piece is too small, the local energy density can be then correspondingly too high so that the laser beam starts to vaporize the material. These types of results were seen in a video from the cladding process. When the focal point position (distance between the focal point and surface of the work piece) is close to substrates surface, the laser power density is relatively high due to the small laser beam spot size (Table III and Fig. 7). This high power density can cause vaporization during the cladding process, which disturbs the cladding process, as stated above. The laser beam spot size can be increased with an increase in the distance of the focal point from the work piece surface (Table III).

The focal point position determines spots peak power density (Table III) in or other words how “sharply” the laser energy is introduced into the process. At the same time, it also determines how stable the cladding process is (Fig. 8). The dilution of the clad bead decreases along with the increase of the focal position. When the laser spot peak power density was 191 kW/cm² or below it, the laser cladding process was stable and there were no signs of excessive vaporization in the melt pool. This indicates that 191 kW/cm² power density is not high enough to cause vaporization at 100 Hz scanning frequency. The dilution in

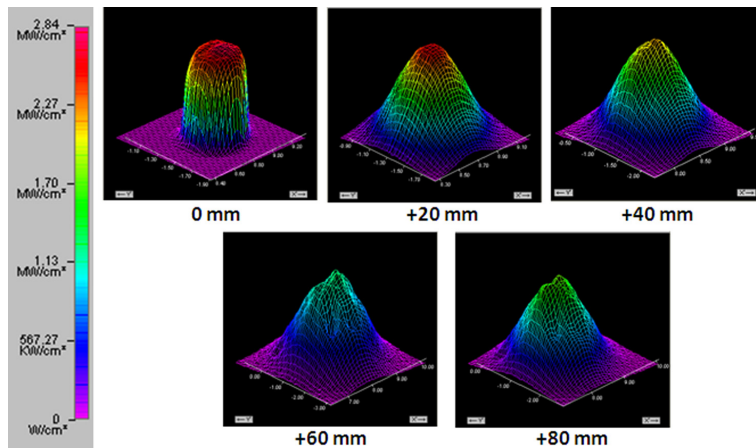


FIG. 7. Power distribution and peak power density of the laser beam on top of the work piece in different focal positions at 5 kW of laser power.

these cases was at a reasonable level compared to the dilution with clads that were made using focal positions closer to the work piece surface (0, +20 and +40 mm), when laser spot peak power density was significantly higher [Fig. 9(a)].

As the power density on the laser spot increased, excessive melting of the substrate was noticed (Figs. 8 and 9). This was caused by a small keyhole which developed in the melt pool penetrating to the substrate material but also by the erupting vapor from the keyhole, which was mentioned earlier to prevent additive materials from entering properly to the melt pool. This is how the experiments conducted using higher power density (i.e., shorter defocusing distance) results in higher dilution rates when process was unstable (Fig. 8). High dilution and deep melting of the substrate material using high peak power density (413–2836 kW/cm²) made the process resemble again more laser alloying than laser cladding [Figs. 9(a)–9(c)]. This in other hand indicates

that if the peak power density of laser spot is 413 kW/cm² or above at scanning frequency of 100 Hz, laser can vaporize the material and cause instability to the process.

The blocking of entrance of additive powders to the melt pool can be seen when the lines of melted substrate materials and clad beads in the overall cross-section area in Fig. 8 are compared. For example, when the peak power density of laser spot was 2836 kW/cm² (focal point on the top surface of the workpiece), the overall melted cross section area is approximately 5.2 mm² where 3.2 mm² is melted substrate material [Fig. 9(a)]. This is compared to a clad bead clad with the peak power density of 102 kW/cm² where the overall melted cross section area is approximately 7.4 mm² of which only 1.1 mm² is melted substrate material [Fig. 9(e)]. Considering that in both cases the powder feeding volume is the same (0.5 g/min), it is clear that in the case of higher power density used, the additive material has problems in

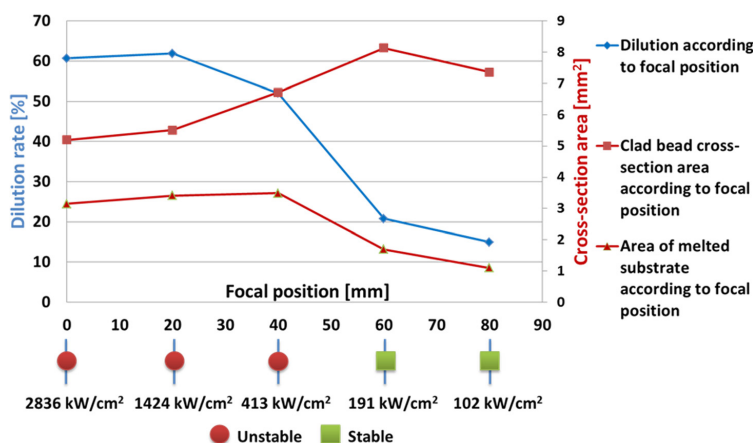


FIG. 8. Dilution and clad bead cross section areas according to focal position and stability according to peak power density (focal position). Scanning frequency is 100 Hz and cladding speed is 5.00 mm/s. Specific energy input is 62.7 J/mm². “Unstable” marks that a small keyhole is able to form. “Stable” marks that there is no keyhole formation.

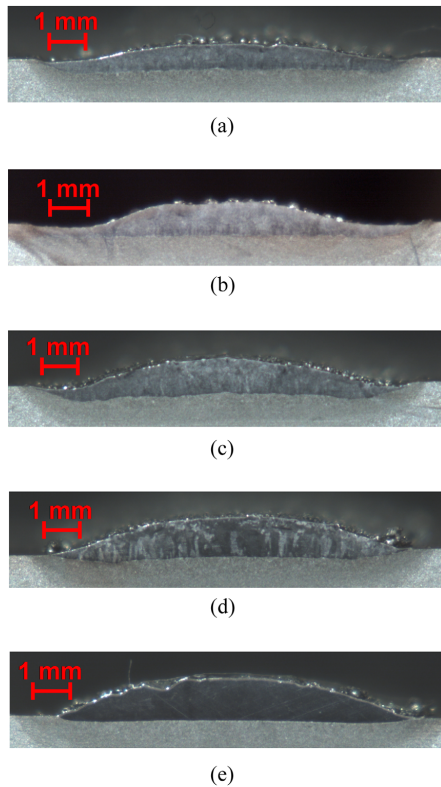


FIG. 9. Clad bead cross-sections clad with different peak power densities of (a) 2836 kW/cm², (b) 1424 kW/cm², (c) of 413 kW/cm², (d) 191 kW/cm², and (e) 102 kW/cm².

entering the melt pool. This is due to erupting vapor caused by gas flow (Fig. 3). So, when the additive material cannot properly enter melt pool, the overall cross-section area of the formed clad bead is decreased (Fig. 8).

As the scanning frequency determines the interaction time, i.e., how long time the laser beam gives energy to a certain point during the scan sweep, the power density determines on how large “packages” this energy is brought to the process. If the energy is attempted to be brought with excessively high power density, the laser beam starts to vaporize the material and the process does not work properly. However, when the laser beam power density on top of the work piece is low enough to melt material instead of vaporizing it, the process is smooth and works properly.

As laser spot power density can be decreased by increasing laser beams spot diameter or decreasing laser power, increasing spot diameter is preferable via, e.g., increasing the defocusing distance. If laser power is decreased, the productivity of the process is decreased alongside of it. When there is less energy to melt the material, the productivity of the process is decreased, as less additive material can be melted on top of substrate material. In productivity point of view, it is better to use higher laser power with a large spot

to decrease power density than decrease power density by decreasing the laser power.

IV. CONCLUSIONS

Both the scanning frequency and the laser beam power density are important factors when laser cladding is performed using the scanning optics. The scanning frequency should be high enough to avoid the excessive increase of the local specific energy input of the scanned beam. Excessive energy input can cause vaporization in the melt pool, which, respectively, increases the dilution. As presented above, a scanning frequency of 40 Hz was high enough to keep the cladding process stable. At this scanning frequency, the highest local specific energy input was 2.46 J/mm². This was a locally low enough energy input to ensure the stable cladding process. Higher scanning frequencies, 80 Hz and above it, decreased dilution slightly when the local specific energy input of the laser beam decreased due to a more rapidly moving scanned beam.

The effect of the laser spot power density on the stability of the cladding process is logical. If the power density is too high, the laser beam starts to vaporize the material creating a small keyhole. In these tests, it was concluded that 413 kW/cm² was too high a peak power density to stable process at 100 Hz scanning frequency. Decreasing laser spots peak power density keyhole formation, and thus, excessive vaporization was avoided. When the laser beam peak power density on top of the work piece was 191 kW/cm², the laser beam was not able to vaporize the material but is able to create a stable melt pool.

If the scanning frequency is low and the laser spot power density is high, the process becomes unstable, which is caused by keyhole formation which in turn leads to vapor eruption from the melt pool. This eruption of the vaporized material prevents additive powder from entering the cladding process properly. When a keyhole is formed, the process resembles more laser alloying than laser cladding.

ACKNOWLEDGMENTS

The authors wish to express their gratitude to the Finnish Metals and Engineering Competence Cluster (FIMECC)’s Innovation and Network program, Regional Council of Päijät-Häme, Tekes, and the European Regional Development Fund for funding the research.

¹A. Belmont and M. Castagna, “Wear-resistance coatings by laser processing,” *Thin Solid Films* **64**, 249–256 (1979).

²G. J. Bruck, “High-power laser beam cladding,” *JOM* **39**, 10–13 (1987).

³J. Kauppila, “Laser cladding with dynamic powder feeding,” Master’s thesis, Lappeenranta University of Technology, Lappeenranta, 1988.

⁴J. Pekkarinen, V. Kujanpää, and A. Salminen, “Laser cladding with scanning optics: Effect of power adjustment,” *J. Laser Appl.* **24**, 032003 (2012).

⁵I. J. Pekkarinen, V. Kujanpää, and A. Salminen, “Laser cladding using scanning optics,” *J. Laser Appl.* **24**, 052003 (2012).

⁶F. Klocke, C. Brecher, D. Heinen, C.-J. Rosen, and T. Breitbart, “Flexible scanner-based laser surface treatment,” *Phys. Procedia* **5**, 467–475 (2010).

⁷J. Tuominen, J. Näkki, H. Pajukoski, T. Peltola, P. Vuoristo, M. Kuznetsov, and G. Turichin, “Laser cladding with 15 kW fiber laser,” in *Proceedings of the 13th NOLAMP Conference, Trondheim, 27–29 June (2011)*, 12 p.

- ⁸T. A. Palmer, "Implementation of laser cladding for Virginia class submarine main propulsion shaft repair," in *CTMA 2010 Symposium*, MCB Quantico, VA, 22–24 March 2010, symposium presentation 24 March 2010.
- ⁹F. Vollertsen, K. Partes, G. Habedank, and T. Seefeld, "Deep penetration dispersing of aluminum with TiB₂ using a single mode fiber laser," *Prod. Eng.* **2**, 27–32 (2008).
- ¹⁰J. Pekkarinen and A. Salminen, "Laser Cladding with modern high power fiber laser—Dynamic beam modification characteristics to the cladding process," in *LAM 2012 Laser Additive Manufacturing Workshop, Sheraton North Houston Hotel, 29 February–1 March 2012*, workshop presentation 1 March.
- ¹¹E. Toyserkani, A. Khajepour, and S. Corbin, *Laser Cladding* (CRC Press, Boca Raton, FL, 2005), 280 p.
- ¹²J. C. Ion, *Laser Processing of Engineering Materials: Principles, Procedure and Industrial Applications* (Elsevier Butterworth-Heinemann, Oxford, 2005), 556 p.
- ¹³W. M. Steen and J. Mazumder, *Laser Material Processing*, 4th ed. (Springer, London, 2010), 408 p.
- ¹⁴V. M. Weerasinghe and W. M. Steen, "Laser cladding with pneumatic powder delivery," *Appl. Laser Technol.* 183–211 (1987).
- ¹⁵G. Zhao, C. Cho, and J.-D. Kim, "Application of 3-D finite element method using Lagrangian formulation to dilution control in laser cladding process," *Int. J. Mech. Sci.* **45**, 777–796 (2003).
- ¹⁶J.-D. Kim and Y. Peng, "Melt pool shape and dilution of laser cladding with wire feeding," *J. Mater. Process. Technol.* **104**, 284–293 (2000).
- ¹⁷J. M. Pelletier, M. C. Sahour, M. Pilloz, and A. B. Vannes, "Influence of processing conditions on geometrical features of laser claddings obtained by powder injection," *J. Mater. Sci.* **28**, 5184–5188 (1993).
- ¹⁸H. Zhou, "Temperature rise induced by a rotating or dithering laser beam," *Adv. Stud. Theor. Phys.* **5**, 443–468 (2011).
- ¹⁹J. E. Moody and R. H. Hendel, "Temperature profiles induced by a scanning cw laser beam," *J. Appl. Phys.* **53**, 4364–4371 (1982).
- ²⁰A. F. A. Hoadley and M. Rappaz, "A thermal model of laser cladding by powder injection," *Metall. Trans. B* **26B**, 631–642 (1992).
- ²¹M. Picasso, C. F. Marsden, J.-D. Wangnière, A. Frenk, and M. Rappaz, "A simple but realistic model for laser cladding," *Metall. Mater. Trans. B* **25**, 281–291 (1994).
- ²²L. Han, F. W. Liou, and K. M. Phatak, "Modeling of laser cladding with powder injection," *Metall. Mater. Trans. B* **35**, 1139–1150 (2004).
- ²³A. Fathi, E. Toyserkani, A. Khajepour, and M. Durali, "Prediction of melt pool depth and dilution in laser powder deposition," *J. Phys. D: Appl. Phys.* **39**, 2613–2623 (2006).
- ²⁴M. Schneider, "Laser cladding with powder effect of some machining parameters on clad properties," Doctoral thesis, University of Twente, Enschede, The Netherlands, 1998, 177 p.
- ²⁵O. O. D. Neto and R. M. S. Vilar, "Interaction between the laser beam and the powder jet in blown powder laser alloying and cladding," in *Proceedings of the Laser Materials Processing Conference ICALEO'98, Part 2, Sheraton World Resort Hotel, Orlando, FL, 16–19 November (1998)*, pp. 180–189.
- ²⁶C.-Y. Liy and J. Lin, "Thermal processes of a powder particle in coaxial laser cladding," *Opt. Laser Technol.* **35**, 81–86 (2003).
- ²⁷Y.-L. Huang, G.-Y. Liang, J.-Y. Su, and J.-G. Li, "Interaction between laser beam and powder stream in the process of laser cladding with powder feeding," *Modell. Simul. Mater. Sci. Eng.* **13**, 47–56 (2005).
- ²⁸Y. Fu, A. Loredò, B. Martin, and A. B. Vannes, "A theoretical model for laser and powder particles interaction during laser cladding," *J. Mater. Process. Technol.* **128**, 106–112 (2002).
- ²⁹J. Lin, "Temperature analysis of powder streams in coaxial laser cladding," *Opt. Laser Technol.* **31**, 565–570 (1999).
- ³⁰W.-B. Li, H. Engström, J. Powell, Z. Tan, and C. Magnusson, "Redistribution of the beam power in laser cladding by powder injection," *Lasers Eng.* **5**, 175–183 (1996).
- ³¹*Laser Processing of Materials: Fundamentals, Applications and Developments*, edited by P. Schaaf (Springer, London, 2010), 241 p.

PUBLICATION 4

Pekkarinen, J., Salminen, A., Kujanpää V., Ilonen, J., Lensu, L. and Kälviäinen, H.

LASER CLADDING USING SCANNING OPTICS – EFFECT OF THE POWER FEEDING
ANGLE AND GAS FLOW ON PROCESS STABILITY

This paper has been published in the
Proceedings of The International Congress on Applications of Lasers & Electro-Optics
(ICALEO), Oct. 6-10 2013, Miami, FL, USA. 10 pp.

Printed with permission

LASER CLADDING USING SCANNING OPTICS - EFFECT OF THE POWDER FEEDING ANGLE AND GAS FLOW ON PROCESS STABILITY

2001

Joonas Pekkarinen¹, Antti Salminen¹, Veli Kujanpää², Jarmo Ilonen³, Lasse Lensu³, Heikki Kälviäinen³

¹Laboratory of laser processing, Department of mechanical engineering, Lappeenranta University of Technology, Tuotantokatu 2 53850 Lappeenranta, Finland

²VTT Technical Research Centre of Finland, Tuotantokatu 2, 53851 Lappeenranta, Finland

³Lappeenranta University of Technology, Machine Vision and Pattern Recognition Laboratory (MVPR), Department of Mathematics and Physics, Skinnarilankatu 34, 53850, Lappeenranta, Finland

Abstract

Powder feeding is one of the single most important factors which defines the qualitative outcome of the cladding process. If the powder feeding or a powder cloud suffers from any form of interference, it will directly affect the quality of the clad bead. This study thus focuses on the effect of the powder feeding angle and the flow rate of the powder carrying gas on powder cloud behavior under the scanned laser beam during the laser cladding process. In this study, powder feeding angles from 40 to 70 degrees were tested with powder feeding gas flow rates of 3 and 6 l/min and with laser scanning frequencies ranging from 80 to 150 Hz. Additive material used was 316L, and the substrate material was low alloyed steel. Powder cloud behavior was simultaneously monitored in situ with a high-speed camera and spectrometer. The results showed that the stability of the powder cloud was highly dependent on the tested parameters. Also, a direct correlation between the vaporization of the powder cloud and the increase of dilution was noticed.

Introduction

Laser cladding has been in existence for several decades for coating and repair purposes [1-3], and has been proven with time to be a viable coating technique. When co-axial powder feeding was introduced for cladding purposes in the late 1980s [4], the laser cladding process became easier to control and enabled more freedom of movement. However, nowadays when lasers with even higher power have become more common, off-axial powder feeding is back in vogue. This is because higher laser power makes it possible to clad wider clad sections at a time using a wide spot, and this process would be difficult to complete with a coaxial nozzle structure. With an off-axial powder feeding system, the powder feeding angle is relatively easy to adjust. In doing so, the powder stream length of travel in relation to the laser beam can be adjusted, which in turn directly affects the degree of the power attenuation effect of the powder cloud (see

Figure 1) [5-8]. However, no reports exist on the behavior of the powder cloud under the effect of the scanned laser beam or on how this behaviour affects cladding process dynamics.

Laser cladding with a scanned beam has some peculiarities lacking from an ordinary laser cladding process performed with static optics. One important factor is the dual nature of energy input. This means that when a scanned laser beam is used in laser cladding (or in any other surface treatment process), energy is brought through a small, fast-moving laser spot of relatively high energy density. However, this small spot redirects energy to a larger area (the interaction area of the laser beam) of relatively low average energy density. This dual nature of the energy input sets limitations on process parameters such as scanning frequency and the spot size. Too low of a scanning frequency or too small of a laser spot size can cause vaporization of material, leading to an unstable cladding process and low clad quality [9,10]. The upside of laser cladding with scanning optics is that it enables the cladding of wide clad beads using high laser power [11,12] and the adjustment of the width of the clad beads using scanning amplitude adjustment[10]. These render the process more productive [11,12] and flexible [10,13].

The powder cloud causes an attenuation effect on the laser beam. Attenuation occurs when the powder cloud absorbs laser light [5-8], which causes powder particles temperature to increase [6,14]. Due to this temperature increase, powder particles can merely warm up, melt, or in the worst case scenario, even start to vaporize during the flight from the feeding nozzle into the melt pool [5,6,14,15]. The resulting vaporization is how powder particle temperature can affect process stability. The temperature rise of a powder particle depends highly on the powder feeding angle (the angle between the powder feeding direction vector and the substrate surface, Figure 1), powder particle speed and power density of the laser beam [5-7,14-19]. The effect of the powder feeding angle on

attenuation and powder particle heating originates from the flight pattern under the laser light. The feeding angle directly affects powder particle flight length under the laser light (see Figure 1) [5,6,14-16] and thus it determines the height of the powder cloud relation to the laser beam. With this height increase, the powder cloud absorbs more energy from the laser, and thus its attenuation effect increases [6,14].

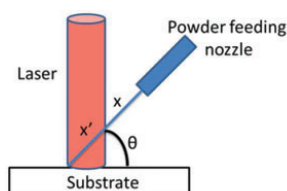


Figure 1. θ is the powder feeding angle, x is the maximum powder particles flight tracks from nozzle to spots back corner, and x' is the maximum travel length of the powder particle under the laser light.

As attenuation increases, the temperature of the powder particle / powder cloud also increases. The larger fraction of laser energy goes to the heating of powder material in the powder cloud, and less laser energy is thus directly involved with the melt pool or substrate material [14]. When the powder particle temperature increases to above the melting temperature point, the probability that the powder particle will adhere to the surface to form a clad bead increases. This is because the powder particle will stick to the surface only when either the particle surface or substrate surface or both are at the melted stage. The Solid-solid encounter leads to powder particles ricocheting away. [20]

If the energy intensity level of the laser beam is too high, it may result in vaporization in the powder cloud. In this case, the powder material temperature can rapidly increase to vaporization temperature. Other factors that can cause vapor formation are the same ones affecting the temperature rise in powder material; i.e., the particle speed and the particle radius [5,14,15]. Particle speed determines how long a powder particle is under the exposure of the laser beam, and thus it determines how much energy the particle will receive [14].

Dilution is highly dependent on powder feeding. Dilution is the result of the balance between the energy input and powder feeding; i.e., the energy-mass balance. If there is more energy than the melting of additive material volume requires, the energy will start to melt the substrate material and dilution will increase [21-25]. The significance of the powder cloud

concerning dilution can be viewed through the powder efficiency. Powder efficiency increases with an increase in the powder feeding angle [5]; thus, when a larger portion of additive powder is used for increasing the volume of the clad bead, less energy remains for the melting of substrate material, which is a matter of energy-mass balance, and dilution can decrease.

This study attempts to clarify how a powder cloud behaves when it is heated under a scanned laser beam during the cladding process. Also, it focuses on determining 1) threshold values for the powder feeding angle, scanning amplitude and powder feeding gas flow; 2) how these parameters change process dynamics; and 3) how much process stability affect to the dilution.

Experimental procedure

The laser equipment used for this study consisted of an IPG 5 kW multimode fiber laser with 150 μm fiber, beam parameter product of 4.6mm*mrad. The used optics was 150 mm focal length collimator and 500mm focal length focusing lenses. The focusing optics used were a Precitec YW50 welding head with an ILV DC linear scanner. With 60 mm defocusing the laser beam diameter on top of the workpiece was 2.43 mm, and local peak intensity being 1920 W/mm². These values were measured using a Primes FocusMonitor.

Process analyzing equipment consisted of a spectrometer and high-speed camera. The spectrometer used was an Ocean Optics HR200+, and it measured the light spectrum within the range of 192 to 652 nm. The spectrometer was used to analyze the light emitted by the powder clouds under the scanned laser beam. The spectrometer was aligned parallel to the substrate surface so that it measured only the radiance emitted from the powder clouds (see Figure 2). A high-speed camera was used with a Cavilux laser illumination system. The camera frame rate used was 2000fps and the wavelength of the laser illumination system was 808 nm. High-speed imaging was used to study the powder cloud movement during the process.

The laser beam was moved by a numerically controlled X-Y portal robot. The cladding speed used was 5 mm/s. The powder feeding rate was set at 0.57 g/s and two powder feeding gas flows were used, 3 l/min and 6 l/min. The gas flow rate was measured between the nozzle entry chamber and the powder feeding tube (Figure 6). Four powder feeding angles were used: 40°, 50°, 60° and 70°.

The laser was scanned using three different scanning frequencies of 80, 100 and 150 Hz and with a scanning amplitude (beam scanning width plus beam diameter)

of 12.1 mm. To ensure that the cladding process would not be affected by the dwell time of the scanning mirrors, the power adjustment option of the scanner was used. The power adjustment effect on the process stability is better explained in our previous study [9,10]. The principle behind power adjustment is that the laser beam power level is adjusted according to the pointing location of the scanning mirror. For this scanner type, there are 32 adjustment points in one scan wave, at each of which laser power can be adjusted. A cross-section image of the power adjustments can be drawn from these points, as can be seen in Figure 3. Figure 3 depicts the power adjustment figure used in our tests. With this kind of power adjustment, laser power is decreased while the scanning mirror is directing the laser beam in the edge areas of the amplitude. Laser power was set up in such a way that 100% equaled 4.1kW, and the measured average power with the power adjustment was 3.33 kW.



Figure 2. Experimental setup. 1. Precitec welding head. 2. High-speed camera. 3. Illumination system. 4. Spectrometer 5. Powder feeding nozzle.

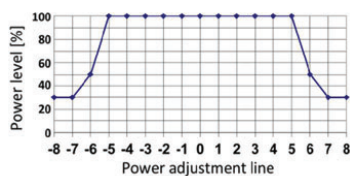


Figure 3. Cross-section image of power adjustments.

Powder particle velocities were estimated from the videos captured with a high-speed camera. The images in the sequences were 400x400 pixel grayscale frames with 256 intensity levels, and the movement of particles in the image sequences was estimated as follows. The background removal was performed by subtracting the previous frame from the current one

and by limiting the values in the resulting image from 0 to 10. The particles were brighter than the background, and thus both bright spots and dark "holes" in the image sequence were created after the background removal, facilitating following of the motion. The translational motion was determined by using a Fourier transform-based phase correlation optical flow algorithm [26], which is highly resistant to noise. The images were divided into 100x100 pixel subwindows and the windows were positioned at every 25th pixel, resulting in 13x13 motion vectors for each image. The motion was tracked separately in each subwindow after application of the Hann windowing function to avoid edge effects in the Fourier transform. The resulting motion vectors were not stable between the frames due to the noise in the original images and the difficulty of detecting even single particles reliably. Therefore, a Kalman filter [27] was used to smooth the noisy motion vectors between the different frames. Two consecutive frames from an analyzed video are shown in Figure 4.

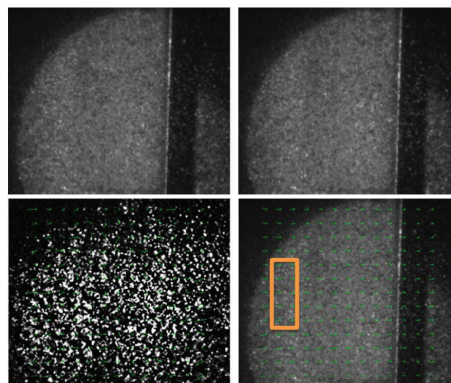


Figure 4. An example of two consecutive frames from video (top row) analyzed with optical flow and Kalman filtering (bottom row). The green arrows are estimated motion vectors for the local subwindows. The orange square marks the spot where announced particle velocities were measured.

Results

Powder velocity

Powder particle velocities were measured in order to define to what extent particle velocity can explain stability differences encountered in the cladding process. The measured particle velocities are shown in Figure 5. The growth of powder particle velocity as a function of an increase in feeding angle can be explained by gravity. As powder particles drain along

bottom plate at steeper angle they reach higher velocities (see Figure 5 and 6) Since the carrying gas has space to expand inside the nozzle, there is little difference in powder particle velocity between the 3 and 6 l/min carrying gas flow rates.

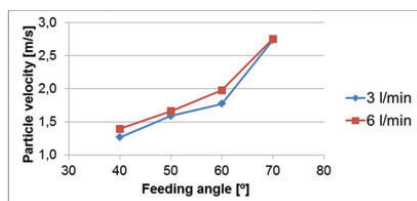


Figure 5. Powder particle average feeding velocity at different feeding angles and gas flows.

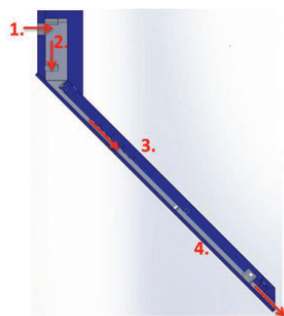


Figure 6. Cross-section of the powder feeding nozzle apparatus and powder route inside the nozzle (red arrows). 1. Connector to the powder feeding tube. 2. Powder entry chamber. 3. Nozzle frame. 4. Bottom plate.

Powder particle velocity directly affects the amount of time the particle is exposed to laser light, and the powder feeding angle determines how far the powder particle will travel while exposed to laser light. However, because powder velocity increases alongside the increase in feeding angle, the calculated time of the powder particle under the exposure of laser light stayed relatively constant throughout the test series. On average, a powder particle was under the laser light for 2.47 ms when the gas flow was 3 l/min, and for 2.34 ms when the gas flow was 6 l/min. The difference in time length for the powder particle under the laser light between the shortest time (2.24 ms at 40° and 6 l/min) and the longest time (2.60 ms at 60° and 3 l/min), was only 0.36 ms.

Powder cloud glow under the laser light

It was observed with the use of a spectrometer that the laser energy absorbed by the powder could make

the powder cloud glow. It was also observed that the intensity of the light emitted by the powder cloud was highly dependent on process stability.

The powder cloud was observed to emit light during the cladding process. The intensity of the light emitted was highly dependent on process stability and powder material vaporization. As observed from the video, when process stability was at its most unstable and a high amount of vapor formation was noticeable, powder cloud / plume emitted light intensities were at their highest. Because the highest measured intensities were at a wavelength range of 450 to 650 nm, which differs to lasers 1070 nm and illumination lasers 808 nm wavelength light, it can be deduced that powder cloud / plume absorbs energy from the laser beam and emits the energy as visible light.

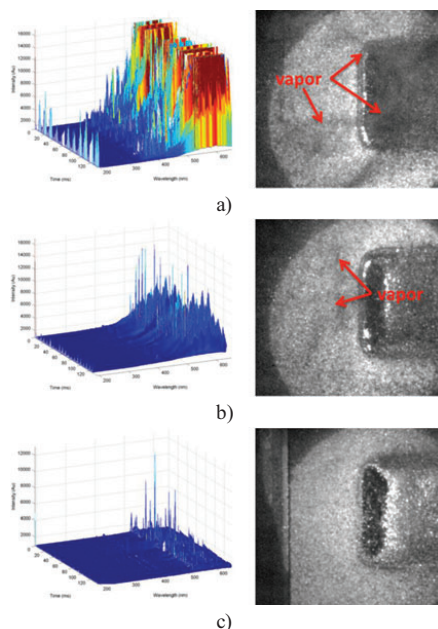


Figure 7. Plume illumination spectra and material vaporization during cladding. Vapor can be seen in 7a and 7b in the form of dark lines. 7a. Unstable process with continuous vapor formation. 7b. Discontinuous vapor formation. 7c. Stable process with no vapor formation noticed.

The intensity of light emitted by the powder cloud was noticed to be highly dependent on the level of vaporization inside the powder cloud. When powder vaporization occurred, the vapor began to absorb energy from the laser beam. This energy absorption

was noticeable with the spectrometer when the plume emitted energy within the range of the spectrometer (see Figure 7a). It should be emphasized that because of the upper limit of the measurement range, the spectrometer did not measure longer wavelengths, such as those of thermal emissions. In this case, increased intensity of light emissions in the powder cloud / plume meant that the cloud had absorbed more energy from the laser beam. When vaporization decreased, emitted light intensity also decreased. However, also noticed was another kind of vaporization inside the powder cloud; i.e., discontinuous vaporization. During discontinuous vaporization, the powder vaporized only at intervals. The discontinuous vaporization did not emit as high intensity of light as did continuous vaporization, as can be seen from Figure 7b.

When the process was stable with no vapor formation observed, the intensity of light emitted by the powder cloud was low, as shown in Figure 7c. In this case, the laser beam heated up the powder particles in the powder cloud such that they started to emit light. However, when the vapor plume — which patently increases absorption of the laser light by the plume and powder cloud — was not formed, the intensity of emitted light was significantly lower.

Powder behavior under the laser light

Powder material behavior in the powder cloud was noted to be highly dependent on three factors: the powder feeding angle, the carrying gas flow rate and the scanning frequency. Powder cloud behavior was noticed to change from stable to unstable, meaning there was a large amount of vaporization in the powder cloud, but depending on the above-mentioned parameters.

Powder cloud behavior became unstable when the powder material started to vaporize in a continuous fashion under the exposure of laser light before the powder reached the melt pool. In this case, the forming vapor expanded and formed a pressure wave which pushed the powder material away. In other cases, powder cloud behavior could seem relatively calm momentarily. In these cases, a small amount of continuous vapor formed and moved away from the powder cloud, in the opposite direction to the cladding direction. However, when either the vapor movement direction turned or the vapor remained stationary, powder cloud behavior became unstable when the powder started to vaporize at an accelerating rate. This caused almost exploding type of vaporization in the powder cloud (see Figure 8). Vapor moved away from the powder cloud mainly when higher gas flow rates (6 l/min) were in use.

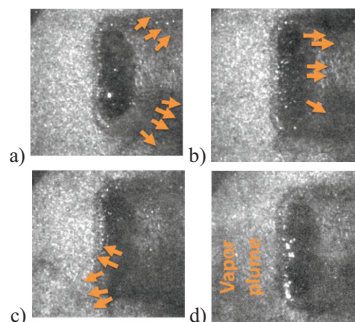


Figure 8. Vapor movement during an unstable process phase, from the test powder feeding angle of 70°, 80 Hz scanning frequency and 3 l/min gas flow. The arrows in the images mark the flow direction of the vapor plumes. 8a. When the vapor moves away from the powder cloud, the process is relatively stable. 8b. Vapor movement changes direction towards the powder cloud. 8c. Vaporization increases when an exploding type of vaporization commences. 8d. A large vapor plume forms.

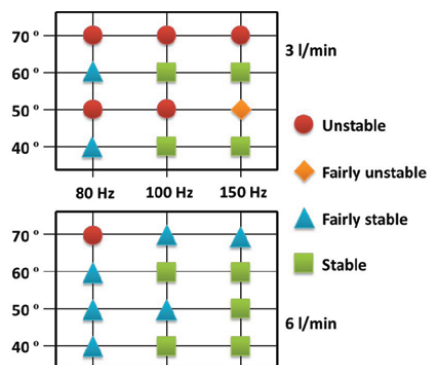


Figure 9. Powder cloud stability under the laser light with different scanning frequencies and powder feeding angles.

“Unstable” means that the powder material continuously and heavily vaporizes
“Fairly unstable” means that there is a small amount of continuous vaporization
“Fairly stable” means that there is occasional vapor formation in the powder cloud
“Stable” means that no vapor formation is found in the powder cloud

At 80 Hz scanning frequency with a low gas flow rate (3 l/min), vaporization was noticed in the powder cloud region with all tested powder feeding angles. With 70° and 50° powder feeding angles, vaporization

was severe. Respectively, with 60° and 40° powder feeding angles, a decrease in amount of vaporization was noticed, but the vaporization did not completely disappear. When the gas flow rate was increased to 6 l/min, overall vapor formation decreased, and the cladding process stabilized slightly, but the vapor formation did not completely disappear (see Figure 9). Only at a 70 degree feeding angle was significant instability noticed with 6 l/min gas flow. However, the process was more stable than it had been with a gas flow rate of 3 l/min. With 40°, 50° and 60° powder feeding angles, occasional vapor formation in the powder cloud was observed, and thus the process proved to be more stable with a gas flow rate of 6 l/min than with flow rate of 3 l/min (see Figure 9).

When the scanning frequency was increased, the behavior of the powder cloud under the laser light calmed down. With a 100 Hz scanning frequency, the process started to stabilize and there were fully stable process parameter combinations, as in Figure 9. With a 3 l/min powder feeding gas flow rate, there was fully unstable powder cloud behavior at 50° and 70° feeding angles. However, when the gas flow was increased, the process stabilized even further (see Figure 9). With a higher gas flow rate, vapor formation in the powder cloud decreased, stabilizing the process. Our best results from the standpoint of process stabilization were obtained using a scanning frequency of 150 Hz, with which powder cloud behavior was in most cases either stable or fairly stable (again, see Figure 9). Only at a 70° feeding angle with a low gas flow rate was powder cloud behavior found to be unstable.

Dilution

Large variation was noticed both in dilution levels and in the cross-section area of the added material between the different powder feeding angles (see Figures 10a and 10b and Figure 11). In terms of dilution, the 60° powder feeding angle yielded the best results. The lowest dilution levels were found throughout all scanning frequencies with the 60° powder feeding angle (Figure 10 a and b). When the powder feeding angle diverged from 60°, dilution levels increased. In some cases, this could be explained by the instability in the powder cloud (Figure 9); e.g., because of high dilution levels alongside a 70° powder feeding angle. Another noticeable difference is that with a higher carrying gas flow rate, dilution rates are also higher, as Figure 10 shows.

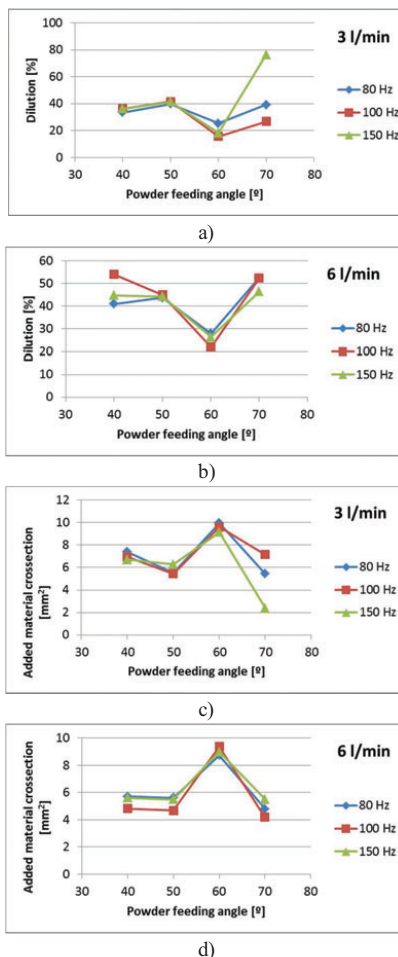


Figure 10. Powder feeding angle effect on dilution rates and clad bead added material cross-section expressed in area.

High dilution levels were linked to a low level of added surface volume, as can be seen in Figures 10c and 10d. In these tests, an increase in dilution meant that the area of the added cross-section material decreased, (see Figure 10). This implies that the increase in dilution was caused either by the additive material not being “caught” by the process or by the powder material not reaching the melt pool. In Figure 11b can be seen to what extent the laser can “dig” inside the substrate material when the cladding parameter combination is in an unstable region and the additive material cannot reach the melt pool properly.

This situation may be contrasted with Figure 11a, where cladding parameters have resulted in stable powder cloud behavior and the additive material can sufficiently enter the melt pool.

Both Figures 11a and 11b depict excessive melting of substrate material close to the edges of the clad bead. This is due to excessive energy input caused by the dwell time in the oscillating scanning mirror. This could be avoided by tuning the power adjustment settings so that laser power would be lower at this region.

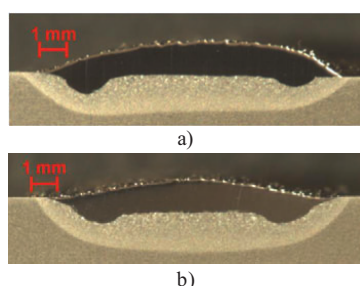


Figure 11. Cross-section of clad beads. 11a. Frequency 100 Hz, gas flow 3 l/min and 60° powder feeding angle. 11b. Frequency 150 Hz, gas flow 3 l/min and 70° powder feeding angle.

Discussion

Powder cloud behavior and powder cloud emission

In certain cases, a powder cloud may absorb energy from the laser beam to the extent that visible light from the powder cloud is emitted, and then the powder starts to vaporize. This vapor creates a plume-like formation on top of the melt pool similar to that which Katayama et al. [28] have reported from keyhole welding research. A forming plume can increase lasers absorption to powder cloud. Our spectrometer measurements together with video from the powder cloud indicate that when the vapor plume was formed, a powder cloud emission of visible light increased significantly in the wavelength range of 450-650nm. This indicates that the vapor formation increased the absorption of laser energy by the powder cloud /plume. The increased light emission means that there must have been a related increase in the absorption of energy by the powder cloud /plume.

This type of vapor absorption behavior can be self-reinforcing. When vapor forms in a suitable spot, absorption of energy by the powder cloud/vapor plume increases, which can triggers an uncontrollable

vaporization of the powder material. This type of behavior was noticed via video imaging of the powder cloud, e.g. cladding at 80 Hz scanning amplitude, 3 l/min carrying gas flow and a 70 degree feeding angle (see Figure 8). In this case, the powder cloud was calm at first, but when the direction of the vapor movement changed, powder cloud vaporization increased to such a degree that a virtually explosive- type phenomenon was noticed. This is a good example for demonstrating that when vapor moves away from the melt pool, it does not represent a such a problem for stability, but if vapor stays on top of the melt pool, it can create instability through the increased energy absorption by the plume to the powder cloud. Figure 12 depicts an example of how light intensity emitted by powder clouds / plumes changes when the powder cloud behaves as described above. Every peak in Figure 12 represents one scan, and the higher peaks were formed when the process was at an unstable stage due to increased energy absorption by the plume. The lower peaks were formed when vapor flowed away from the powder cloud such that absorption did not increase due to the lack of plume formation in the powder cloud, and thus less light emission occurred.

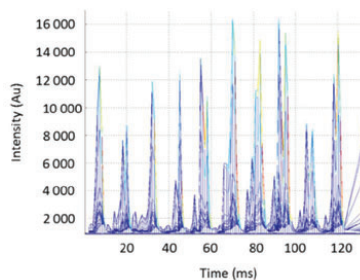


Figure 12. Spectrometer intensity measurements by time and intensity. From an 80 Hz test frequency, 70° powder feeding angle and 6 l/min powder feeding gas flow.

As Figure 9 shows, with a higher feeding gas flow rate, powder cloud behavior was more likely to be calmer, and less vaporization occurred. This was the result of the higher gas flow, which blew the forming vapor away from the powder cloud. When vapor doesn't form a standing plume, which would otherwise accelerate lasers absorption to the powder cloud, powder cloud behavior stabilizes.

The spectrometer can then be used for monitoring powder material stability during the process. By measuring the intensity of light emitted by the powder cloud at a wavelength range of 450-650 nm process stability can be monitored and any vaporisation caused problem areas can be identified. Thus clad bead quality

management can be ensured by spectrometer monitoring.

Effect of scanning frequency

The vaporization of powder material comes from the interaction of a scanned laser beam with the powder material. This is due to the dual character of the scanned beams. When laser energy input is viewed over a short time period, the scanned laser beam has a relatively high power density. When a certain parameter combination is employed, powder can be vaporized when the scanned laser beam hits it, for example when the beam moves at a low velocity (i.e., low scanning frequency). This dual characteristic of the scanned beam is highlighted when the effects of different scanned amplitudes on the powder cloud are compared. 150 Hz scanning frequency produced the most-likely-to-be-stable process, whereas 80 Hz produced the most-likely-to-be-unstable process (see Figure 9). In terms of stability, cladding using a 100 Hz scanning frequency naturally placed between these two. When scanning frequency increases, interaction time between the powder particle and laser beam conversely decreases, and in turn the energy input into a single powder particle decreases. From the standpoint of stability, it is better to use higher scanning frequencies if possible, because with these, the beam interaction with a single particle decreases, and alongside this, probability of unstable powder cloud behavior also decreases.

Dilution

Dilution is highly dependent on the behavior of the powder cloud, as even slight vaporization seems to increase dilution. This is due to the eruption of vapor disturbing the powder flow. When this occurs, the powder does not necessarily land in the melt pool, but rather the vapor forces the powder off course and the powder particle hits the solid, cold substrate material. This can thus lead to solid-solid interaction between the powder particle and substrate, which in turn leads to the powder particle ricocheting away, as J. Lin [20] stated in his study. These powder particles are then lost. When the amount of additive materials in the melt pool decreases but the laser energy level remains constant, melting of substrate materials increases, and thus dilution increases.

Our best results in terms of dilution occurred when there was no vaporization and the powder feeding angle was steep, set at 60°. With steeper feeding angles, the powder seemed to more likely to hit the melt pool, thus increasing the volume of the clad bead, (Figures 10c and 10d). It is also worth acknowledging that even though in these tests, dilution rates were

relatively high, in the best cases around 15%, these results can be compared with each other to illustrate to what extent process stability affects dilution. Clearly, even a small disturbance in the powder cloud results in higher dilution rates. Dilution rates could be easily reduced, for example by decreasing laser power or by increasing the additive powder mass flow; i.e., by adjusting the energy-mass balance.

Powder feeding angle and stability

Finding the optimum powder feeding angle for cladding is crucial for ensuring good clad bead quality. Too high of a powder feeding angle can expose the powder cloud to risk of vaporization. Respectively, too low of a powder feeding angle can increase dilution due to the decrease of powder efficiency. Figures 10c and 10d depict how much less clad bead growth was at 40° compared to that at 60°. The correct powder feeding angle ensures stable powder cloud behavior and good powder efficiency.

With steep powder feeding angles, process seem to be more easily unstable, e.g. with a 70° powder feeding angle, no fully stable powder cloud behavior was observed. This phenomenon has two possible explanations. First, when powder is fed closer to a perpendicular angle, the powder cloud height is higher in relation to the laser beam. The laser beam must go longer distance inside the powder cloud, increasing energy absorption by the powder cloud and possibly causing instability in the powder cloud. Secondly, when a defocused laser beam and a steep powder feeding angle are used, the powder is feeding point inside the laser is closer to the focal point. This is why at the powder entry point to the laser beam, the laser actually has higher power intensities than at the substrate surface level. These two things can increase probability for vaporization in the powder cloud.

One question that remains unanswered in this study is why powder material acts more unstable at a 50° powder feeding angle but more stable at a 60° one. Logically, a 60° powder feeding angle should create a thicker powder cloud in relation to the laser beam than a 50° one, which in turn should make powder cloud behavior more stable at a 50° feeding angle than at a 60° one. When moving from 70° towards 40° powder feeding angles, powder cloud behavior should calm down because of the decrease of powder cloud height in relation to the laser beam. However, as this study has shown, the 50° powder feeding angle is on sort discontinuity point in the results. We cannot give a conclusive answer to the question of why the powder cloud acted so unstable at a 50° feeding angle. Powder particle velocity under the laser light does not explain

the difference in behavior, because even though particle velocity is higher at a 60° feeding angle than at a 50° one, the amount of time under the laser light was virtually the same. In the end, the period of time the powder particle remains under the laser light defines how much powder particle receives energy from the laser. One hypothesis for the discrepancy with the 50° powder feeding angle is that the powder diverges from or ricochets off the surface of the substrate in such a way that some powder particles drift into parts of the beam where they can vaporize and discharge vaporization, due to the vapor-caused absorption increase in the powder region. However, based on our results, this cannot be stated conclusively, and the matter requires further research.

Conclusions

Spectrometer data together with high speed video showed that when powder material starts to vaporize, it forms a kind of plume, and the powder cloud / plume starts to emit visible light. When this happens, vapor material in the plume enhances absorption of laser energy by the powder cloud, which in turn increases vapor formation. During vapor plume formation, visible light is emitted from the powder cloud within a wavelength range of 450 – 650 nm.

The powder feeding angle has a significant effect on the process stability of the cladding process. If near perpendicular powder feeding angles are used along with scanning optics, the powder cloud is exposed to vaporization. Thus, so that process stability is ensured, it is recommendable to use slightly less steeper powder feeding angles. In this study, the 60° powder feeding angle ensured well process stability.

The importance of powder feeding gas flows concerning process stability was noted to be significant. When the higher gas flow of 6 l/min was used, the process stabilized as compared to the use of the lower gas flow of 3 l/min. This was due to the effect of the higher gas flow pushing forming vapor away from the powder cloud. Thus forming vapor did not have change to accelerate absorption to the powder cloud, which would have caused increasing amount of vaporization and instability.

Also crucial is the effect of scanning frequency on powder cloud behavior. If the scanned beam moves too slowly; i.e., the scanning frequency is set too low, the powder material can begin to vaporize in the powder cloud. In this study, 100 Hz was determined to be a sufficient scanning frequency for ensuring stable process conditions.

If the powder material starts to vaporize in the powder cloud, then powder delivery into the melt pool is disrupted, causing an increase in dilution. When the additive material does not reach the melt pool, a greater proportion of laser energy goes towards melting the substrate material, increasing dilution.

Acknowledgements

The authors wish to express their gratitude to the Finnish Metals and Engineering Competence Cluster (FIMECC)'s Innovation and Network program, Regional Council of Päijät-Häme, Tekes and the European Regional Development Fund for funding the research

Meet the Authors

Joonas Pekkarinen M.Sc. (Tech.), Research scientist and PhD student at LUT. **Antti Salminen** D.Sc. (Tech.), Professor of Laser Materials Processing at LUT. **Veli Kujanpää** D.Sc. (Tech.), Research Professor at VTT Technical Research Centre of Finland. **Jarmo Ilonen** D.Sc. (Tech.), Post-doctoral Researcher at LUT. **Lasse Lensu** D.Sc. (Tech.), Assistant Professor at LUT. **Heikki Kälviäinen** D.Sc. (Tech.), Professor of Computer Science at LUT.

References

- [1] Toyserkani, E., Khajepour, A. & Corbin, S. (2005) Laser Cladding. CRC Press. 280 pp.
- [2] Weerasinghe, V.M. & Steen, W.M. (1987) Laser Cladding with Pneumatic Powder Delivery, Applied Laser Tooling, 183-211
- [3] Ion, J. C. (2005) Laser Processing of Engineering Materials: Principles, procedure and industrial applications. Oxford, Elsevier, 556pp.
- [4] Hammeke, A. W. (1987) Laser spray nozzle and method. US Patent, No. 4724299, Apr 15,
- [5] Schneider, M. (1998) LASER CLADDING WITH POWDER - effect of some machining parameters on clad properties. Doctoral thesis, Thesis University of Twente, Enschede, Netherlands. 177pp.
- [6]] Huang, Y-L., Liang, G-Y., Su, J-Y. & Li, J-G. (2005) Interaction between laser beam and powder stream in the process of laser cladding with powder feeding. Modelling and Simulation in Materials Science and Engineering, vol. 13 no. 1, 47-56.
- [7] Fu, Y., Loreda, A., Martin, B. & Vannes, A.B. (2002) A theoretical model for laser and powder

- particles interaction during laser cladding. *Journal of materials processing technology*, vol. 128, iss. 1-3, 106-112
- [8] Picasso, M., Marsden, C.F., Wagnière, J.-D., Frenk, A. & Rappaz, M. (1994) A simple but realistic model for laser cladding. *Metallurgical and materials transactions B*, vol. 25B no. 2, 281-291.
- [9] Pekkarinen, J., Kujanpää, V. & Salminen, A. (2012) Laser cladding with scanning optics: Effect of power adjustment. *Journal of Laser Applications*, Vol. 24, Iss. 3, 7 pp.
- [10] Pekkarinen, I.J., Kujanpää, V. & Salminen, A. (2012) Laser cladding using scanning optics. *Journal of Laser Applications*, Vol. 24, Iss. 5, 9 pp.
- [11] Tuominen, J., Näkki, J., Pajukoski, H., Peltola, T., Vuoristo, P., Kuznetsov, M. & Turichin, G. (2011) Laser cladding with 15 kW fiber laser. *Proceedings of the 13th NOLAMP Conference*. Trondheim University of Technology, Trondheim, 27-29 June, 12 pp.
- [12] Tuominen, J., Näkki, J., Pajukoski, H., Peltola, T. & Vuoristo, P. (2012) Recent developments in high power laser cladding technologies. In: *Proceedings of 31st International Congress on Applications of Lasers & Electro-Optics ICALEO*, Anaheim, USA, September 23-27.
- [13] Klocke, F., Brecher, C., Heinen, D., Rosen C-J. & Breitbach, T. (2010) Flexible scanner-based laser surface treatment. *Proceedings of the LANE Conference*, Physics Procedia, Vol. 5, Part 1, 2010, 467-475.
- [14] Neto, O.O.D. & Vilar, R.M.S. (1998) Interaction between the laser beam and the powder jet in blown powder laser alloying and cladding. *Proceedings of the International Congress on Applications of Lasers & Electro-Optics ICALEO*, Part 2, November 16-19, Sheraton World Resort Hotel, Orlando, FL. 180-189.
- [15] Liy, C-Y. & Lin, J. (2003) Thermal processes of a powder particle in coaxial laser cladding. *Optics & Laser Technology*, vol. 35, iss.2, 81-86.
- [16] Lin, J. (1999) Temperature analysis of powder streams in coaxial laser cladding. *Optics & Laser Technology*. vol. 31, iss. 8, 565-570
- [17] Diniz Neto, O.O. & Vilar, R. (2002) Physical-computational model to describe the interaction between a laser beam and a powder jet in laser surface processing. *Journal of Laser Applications*, vol. 14, no. 1, 46-51
- [18] Toyserkani, E., Khajepour, A. & Corbin, S. (2003) Three-dimensional finite element modeling of laser cladding by powder injection: effects of powder federate and traveling speed on the process. *Journal of Laser Applications*, vol. 15, no 3, 153-160.
- [19] Hoadley, A.F.A. & Rappaz, M. (1992) A thermal model of laser cladding by powder injection. *Metallurgical transactions B*, vol. 23, no. 5, 631-642
- [20] Lin, J. (1999) A Simple model of powder catchment in coaxial laser cladding. *Optics & Laser Technology*, Vol. 31, Iss. 3, 233-238
- [21] Pelletier, J.M., Sahour, M.C., Pilloz, M. & Vannes, A.B. (1993) Influence of processing conditions on geometrical features of laser claddings obtained by powder injection. *Journal of material science*, vol. 28 no.19, 5184-5188
- [22] de Oliveira, U. Ocelik, V. & De Hosson, J.Th.M. (2005) Analysis of coaxial laser cladding processing conditions. *Surface and Coatings Technology*, Vol.197, Iss. 2-3, 127-136
- [23] Hoadley, A.F.A. & Rappaz, M. (1992) A thermal model of laser cladding by powder injection. *Metallurgical transactions B*, vol. 23, no. 5, 631-642
- [24] Huang, Y. (2011) Characterization of dilution action in laser-induction hybrid cladding. *Optics & Laser Technology*, vol.43, iss. 5, 965-973
- [25] Han, L., Phatak, K.M. & Liou, F.W. (2004) Modeling of laser cladding with powder injection. *Metallurgical and Materials Transactions B*, Vol. 35, Iss. 6, 1139-1150
- [26] De Castro, E. & Morandi, C. (1987) Registration of Translated and Rotated Images Using Finite Fourier Transforms, *IEEE Transactions on pattern analysis and machine intelligence*
- [27] Simon, D. (2006) *Optimal State Estimation*. John Wiley & Sons
- [28] Kawahito, Y., Kinoshita, K., Katayama, S., Thubota, S. & Ishide, T. (2005) Visualization on interaction between laser beam and YAG-laser-induced plume. *Proceedings of the laser materials processing conference ICALEO Laser Institute of America*, Miami, Florida USA, Oct. 31-Nov. 3.

ACTA UNIVERSITATIS LAPPEENRANTAENSIS

542. PERFILEV, DANIIL. Methodology for wind turbine blade geometry optimization. 2013. Diss.
543. STROKINA, NATALIYA. Machine vision methods for process measurements in pulping. 2013. Diss.
544. MARTTONEN, SALLA. Modelling flexible asset management in industrial maintenance companies and networks. 2013. Diss.
545. HAKKARAINEN, JANNE. On state and parameter estimation in chaotic systems. 2013. Diss.
546. HYYPIÄ, MIRVA. Roles of leadership in complex environments
Enhancing knowledge flows in organisational constellations through practice-based innovation processes. 2013. Diss.
547. HAAKANA, JUHA. Impact of reliability of supply on long-term development approaches to electricity distribution networks. 2013. Diss.
548. TUOMINEN, TERHI. Accumulation of financial and social capital as means to achieve a sustained competitive advantage of consumer co-operatives. 2013. Diss.
549. VOLCHEK, DARIA. Internationalization of small and medium-sized enterprises and impact of institutions on international entrepreneurship in emerging economies: the case of Russia. 2013. Diss.
550. PEKKARINEN, OLLI. Industrial solution business – transition from product to solution offering. 2013. Diss.
551. KINNUNEN, JYRI. Risk-return trade-off and autocorrelation. 2013. Diss.
552. YLÄTALO, JAAKKO. Model based analysis of the post-combustion calcium looping process for carbon dioxide capture. 2013. Diss.
553. LEHTOVAARA, MATTI. Commercialization of modern renewable energy. 2013. Diss.
554. VIROLAINEN, SAMI. Hydrometallurgical recovery of valuable metals from secondary raw materials. 2013. Diss.
555. HEINONEN, JARI. Chromatographic recovery of chemicals from acidic biomass hydrolysates. 2013. Diss.
556. HELLSTÉN, SANNA. Recovery of biomass-derived valuable compounds using chromatographic and membrane separations. 2013. Diss.
557. PINOMAA, ANTTI. Power-line-communication-based data transmission concept for an LVDC electricity distribution network – analysis and implementation. 2013. Diss.
558. TAMMINEN, JUSSI. Variable speed drive in fan system monitoring. 2013. Diss.
559. GRÖNMAN, KAISA. Importance of considering food waste in the development of sustainable food packaging systems. 2013. Diss.
560. HOLOPAINEN, SANNA. Ion mobility spectrometry in liquid analysis. 2013. Diss.
561. NISULA, ANNA-MAIJA. Building organizational creativity – a multitheory and multilevel approach for understanding and stimulating organizational creativity. 2013. Diss.
562. HAMAGUCHI, MARCELO. Additional revenue opportunities in pulp mills and their impacts on the kraft process. 2013. Diss.

563. MARTIKKA, OSSU. Impact of mineral fillers on the properties of extruded wood-polypropylene composites. 2013. Diss.
564. AUVINEN, SAMI. Computational modeling of the properties of TiO₂ nanoparticles. 2013. Diss.
565. RAHIALA, SIRPA. Particle model for simulating limestone reactions in novel fluidised bed energy applications. 2013. Diss.
566. VIHOLAINEN, JUHA. Energy-efficient control strategies for variable speed controlled parallel pumping systems based on pump operation point monitoring with frequency converters. 2014. Diss.
567. VÄISÄNEN, SANNI. Greenhouse gas emissions from peat and biomass-derived fuels, electricity and heat – Estimation of various production chains by using LCA methodology. 2014. Diss.
568. SEMYONOV, DENIS. Computational studies for the design of process equipment with complex geometries. 2014. Diss.
569. KARPPINEN, HENRI. Reframing the relationship between service design and operations: a service engineering approach. 2014. Diss.
570. KALLIO, SAMULI. Modeling and parameter estimation of double-star permanent magnet synchronous machines. 2014. Diss.
571. SALMELA, ERNO. Kysyntä-toimitusketjun synkronointi epävarman kysynnän ja tarjonnan toimintaympäristössä. 2014. Diss.
572. RIUNGU-KALLIOSAARI, LEAH. Empirical study on the adoption, use and effects of cloud-based testing. 2014. Diss.
573. KINNARINEN, TEEMU. Pressure filtration characteristics of enzymatically hydrolyzed biomass suspensions. 2014. Diss.
574. LAMMASSAARI, TIMO. Muutos kuntaorganisaatiossa – tapaustutkimus erään kunnan teknisestä toimialasta. 2014. Diss.
575. KALWAR, SANTOSH KUMAR. Conceptualizing and measuring human anxiety on the Internet. 2014. Diss.
576. LANKINEN, JUKKA. Local features in image and video processing – object class matching and video shot detection. 2014. Diss.
577. AL-SAEDI, MAZIN. Flexible multibody dynamics and intelligent control of a hydraulically driven hybrid redundant robot machine. 2014. Diss.
578. TYSTER, JUHO. Power semiconductor nonlinearities in active du/dt output filtering. 2014. Diss.
579. KERÄNEN, JOONA. Customer value assessment in business markets. 2014. Diss.
580. ALEXANDROVA, YULIA. Wind turbine direct-drive permanent-magnet generator with direct liquid cooling for mass reduction. 2014. Diss.
581. HUHTALA, MERJA. PDM system functions and utilizations analysis to improve the efficiency of sheet metal product design and manufacturing. 2014. Diss.
582. SAUNILA, MINNA. Performance management through innovation capability in SMEs. 2014. Diss.
583. LANA, ANDREY. LVDC power distribution system: computational modelling. 2014. Diss.

